ABSTRACT

MOU, GANG. Modeling and Control of a Magnetostrictive System for High Precision Actuation at a Particular Frequency. (Under the direction of Dr. Paul I. Ro.)

A magnetostrictive actuator made of Terfenol-D alloy can generate high mechanical strains with broadband response and provide accurate positioning. These characteristics have been employed as controllers and vibration absorbers in industrial and heavy structural applications, such as fast tool servo systems and precision micropositioners. Full utilization of magnetostrictive transducers in these applications requires a suitable controller as well as quantification of the transducer dynamics in response to various inputs.

However, at moderate to high drive levels, the output from a magnetostrictive actuator is highly nonlinear and contains significant magnetic and magnetomechanical hysteresis. The control of this nonlinear system is a challenge. In order to simplify this problem, 50Hz is chosen as the working frequency for the actuator in the experiments since it shows near linear property at 50Hz and the approach used at 50Hz could be extended to a broader frequency range in the applications.

First, with an optical sensor, the dynamics of the actuator are measured under voltage inputs at different frequencies and amplitudes. Using SAS System V8, a second order dynamic model is obtained at one frequency (50Hz). This model matches the open loop behavior very well. A PID controller is then developed. The control command signal generated through the DSP board is directed to the actuator. A close loop control system is thus formed.

As a nonlinear control approach, sliding mode control can offer some ideal properties, such as insensitivity to parameter variations or uncertainties, external disturbance rejection, and fast dynamic response. In order to obtain better tracking performance and robustness, a sliding mode control algorithm is introduced into the system.

The experiment results from the sliding mode controller are compared with those from the open loop and PID control. The comparison shows improvement in the displacement tracking performance at this frequency. Further work will involve the modification of the sliding mode controller using a time-varying switching gain and improvement in modeling of the actuator over a broader frequency range.

Modeling and Control of a Magnetostrictive System for High Precision Actuation at a Particular Frequency

By

Gang Mou

A thesis submitted to the Graduate Faculty of
North Carolina State University
In partial fulfillment of the requirements for the Degree of
Master of Science

Mechanical Engineering

Raleigh
2002

Approved By:

Chair of Advisory Committee

BIOGRAPHY

Gang Mou was born in China in October 1971. He received his BS and MS degrees in Mechanical Engineering from Sichuan Institute of Technology at Chengdu, China, in 1992 and 1995 respectively. After his graduation, he worked as an Engineer and Department Manager at Chengdu Keguang Company, Chinese Academy of Sciences. In August 1999, he came to North Carolina State University (NCSU) and joined the Precision Engineering Center (PEC) in the Mechanical and Aerospace Engineering Department at NCSU, to work on developing a dynamic model and control algorithms for a high precision magnetostrictive actuation system.

ACKNOWLEDGEMENTS

I would like to express my first words of gratitude to my advisor Dr. Paul I. Ro. Without his guidance, support and encouragement this thesis would have never been materialized. Apart from advising me on the research matters, he has always been a superb mentor and supporter. His respectable attitude towards scientific work and goal for excellence would be my guide for ever. I wish to thank thesis committee members Dr. Gregory D. Buckner and Dr. Fen Wu for taking the time to give advice for my research and to review this thesis. Due to their help, lots of significant technical bugs were identified and subsequently corrected. I also wish to acknowledge and thank Mr. Ken Garrard at the Precision Engineering Center (PEC) for his help on the program in this project. Without his generosity, *Chapter V* would not have turned out as it did. My heartful appreciation goes to Mrs. Nancy McAllister for her great help to review my thesis word by word. Thus, numerous grammar and syntax errors in my thesis were marked out and have been corrected.

I want to thank Dr. Tom Dow for his leadership at the PEC, making it an ideal place for research and study. Thanks go to Mr. Alex for his help in setting up the experiment's instruments. My fellows at the PEC were a great source of knowledge when I started my research project there. They are Markus, Byoung, David Gill, and Matias. When I approached the lab equipment and instruments, they always accommodated me without hesitation. Additionally, they gave me aid when I was faced with the problems that came

with the experimental work. I wish to acknowledge the financial support for this project, provided by a grant from the National Science Foundation (NSF).

No words could express my grateful feeling for all the supports from my wife QIU Xiaoxia, my parents and my whole family. They have made great efforts and given me unconditional help to make it possible for me to pursue and finish this work. I hope this thesis is worthy of their love and kindness.

TABLE OF CONTENTS

LIST OF FIGURES

Chapter I Page

Chapter II

Chapter III

Chapter IV

Chapter V

Chapter I

Introduction

1.1 Introduction to Magnetostriction

In mechanical and manufacturing industries, smart materials have been widely used to obtain high precision actuation and controlled response trajectory. Over the past decades, with advances in material sciences and actuation technologies for high precision purposes, the demand for the design and control of high precision actuators of smart structures, such as piezoelectric, electrostatic and magnetostrictive actuators, has grown quite noticeably.

The smart structure materials show interesting behavior and performance. Among those characteristics, one common nature is that they react mechanically to external stimuli. And the actuators or transducers made of smart materials have the same characteristic. As shown in *Figure 1.1*, the fundamental principle of a typical smart structure actuator is to transform the various inputs of physical energy, in the form of power energy or control energy, into mechanical work, i.e. the desired actuation displacement, velocity, or acceleration. This property is ideal for actuators or transducers.

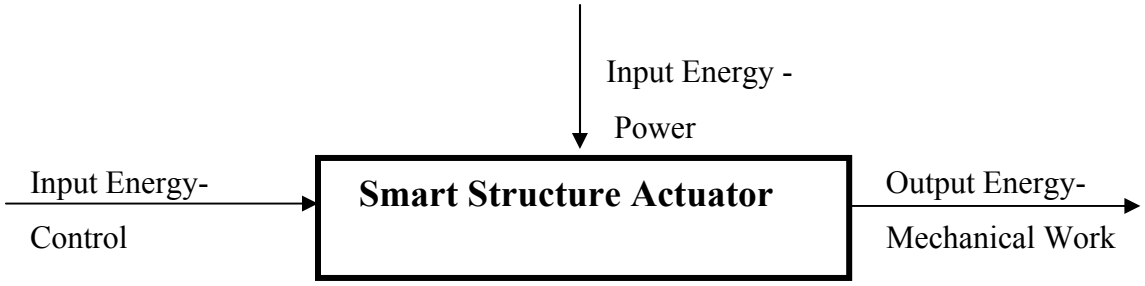

Figure 1.1: Fundamental Principle of a Smart Structure Actuator

Among these smart materials, piezoelectric material is known for providing some ideal properties. For instance, it can generate actuation with very high resolution and operates under high frequency range and low voltage. Therefore, piezoelectric actuators (PZT) have been applied widely in industry. However, in the circumstances of low frequency range and higher loading bearing, piezoelectric material does not show those consistent performances. Traditional actuators, such as hydraulic and piezoelectric actuators are usually not suitable to control the motion of cutting tools due to the limitation of either the bandwidth or the actuating force. Magnetostrictive material exhibits high force at nearly instantaneous speed; and actuators made of these materials occupy a small volume and require relatively low voltage input. Magnetostrictive material has great potential to perform better than piezoelectric devices and hydraulic systems in machining applications. It next emerged as an ideal material for high precision actuation and sensing. And, with the progress in the development of magnetostrictive materials and alloys, magnetostrictive actuators have even broader applications.

Magnetostrictive material is a compositive alloy containing terbium (T_b) and dysprosium (D_y) with iron (F_e). Terbium (T_b) generates strains; dysprosium (D_y)

minimizes the field strengths required to generate the strains; iron (F_e) allows the alloy's exceptional transduction properties to be used at or above room temperature. Terfenol-D is the best known alloy with the typical composition $T_{b0.3}D_{y0.7}F_{e1.95.}$ The name Terfenol-D comes from its metallic elements: TER ~ terbium, FE ~ iron, NOL ~ Naval Ordinance Labs (now NOWC), where the material was first developed, and D ~ dysprosium. While the Terfenol-D devices require low voltage level input, Terfenol-D can produce "giant" magnetostriction, a strain greater than most available commercial smart materials.

There exist two types of magnetostriction. The first one is called spontaneous magnetostriction. If a magnetostrictive material is cooled from Curie points, the magnetostrictive material will go through a transition from state of paramagnetism to the state of ferromagnetism. The procedure forms spontaneous magnetostriction. The second type is field-induced bulk magnetostriction. It is described as a property encountered in magnetic materials where the material changes its shape upon the application of a magnetic field. The magnetostriction discussed in this thesis refers to the field-induced bulk magnetostriction. Magnetostrictive materials have the ability to convert magnetic energy into mechanical energy and vice versa. As a magnetostrictive material is magnetized, it strains or exhibits a fractional change in length accompanied by an inverse change in girth. Conversely, if an external force is applied to cause a strain, the magnetic state of the material changes. This magnetostriction is quantifiable and often defined using the following equation:

$$\lambda = \frac{\Delta \boldsymbol{L}}{\boldsymbol{L}} \qquad (1.1)$$

where ΔL represents the changes measured in length, L is the constrained length of the magnetostrictive rod of the actuator. For a Terfenol-D actuator, the value of λ is often at the range of 1500-2000 parts per million (ppm). In contrast, the value of λ is only 20 ppm for iron. Therefore, the value of λ is the indicator of the level of magnetostriction. Apparently, λ is of the same unit with strain ε. For magnetostrictive actuators, the total strain ε consists of λ and the elastic deformation.

This coupling process between magnetic and mechanical energies is the transduction capability that allows a magnetostrictive material to be used in both actuation and sensing devices.

1.2 Magnetostrictive Materials

Magnetostrictive materials have been studied for a long time. In 1842, James Joule identified the very first magnetostrictive effect when he observed that a sample of nickel changed in length while being magnetized. Subsequently, cobalt, iron and alloys of these materials were found to show a significant magnetostrictive effect with strains of about 50ppm.

One of the first practical applications of magnetostriction was in SONAR devices in echo location during the World War II. Another early application was torque sensing. The material used in those devices was made of nickel alloys and had saturation magnetostriction values of only 50ppm. The strain is quite low so the material had limited applications.

In the 1960s, the rare-earth elements terbium (T_b) and dysprosium (D_y) were found to have between 100 and 10,000 times the magnetostrictive strains found in nickel alloys. However, these properties only exist at very low temperature. Desired actuation applications operating at ambient temperature and above were almost impossible.

Since then, researchers have looked for a material that would operate at a high temperature and have a large magnetostrictive strain, but would require only a low magnetic field. It is found that the addition of iron to T_b and D_y to form the compounds T_bF_{e2} and $DyFe_2$ brought the magnetostrictive properties to room temperature. These materials also required very large magnetic fields to generate large strains. By alloying the two compounds, the magnetic field required to produce saturated strains was considerably reduced. The resulting alloy $T_{b.27}$ $D_{y.73}$ $F_{e1.95}$, commercially known as Terfenol-D, is at present the most widely used magnetostrictive material. Terfenol-D is capable of having strains as high as 2000-3000 ppm [1]. And since the 1980s, it has been a commercially available material for application in many areas.

1.3 Magnetostrictive Devices

Concerning the classification of magnetostrictive devices, there are various categories, either based on the operating frequency or applications. For convenience, magnetostrictive devices are grouped into five main categories:

1. Mechanical magnetostrictive actuators

Within this category, the magnetostrictive actuators are applied to generate accurate actuation at a given force varying over a range of operating frequencies. Linear

and rotational actuators are two main sub-categories, based on the type of motion the actuators provide.

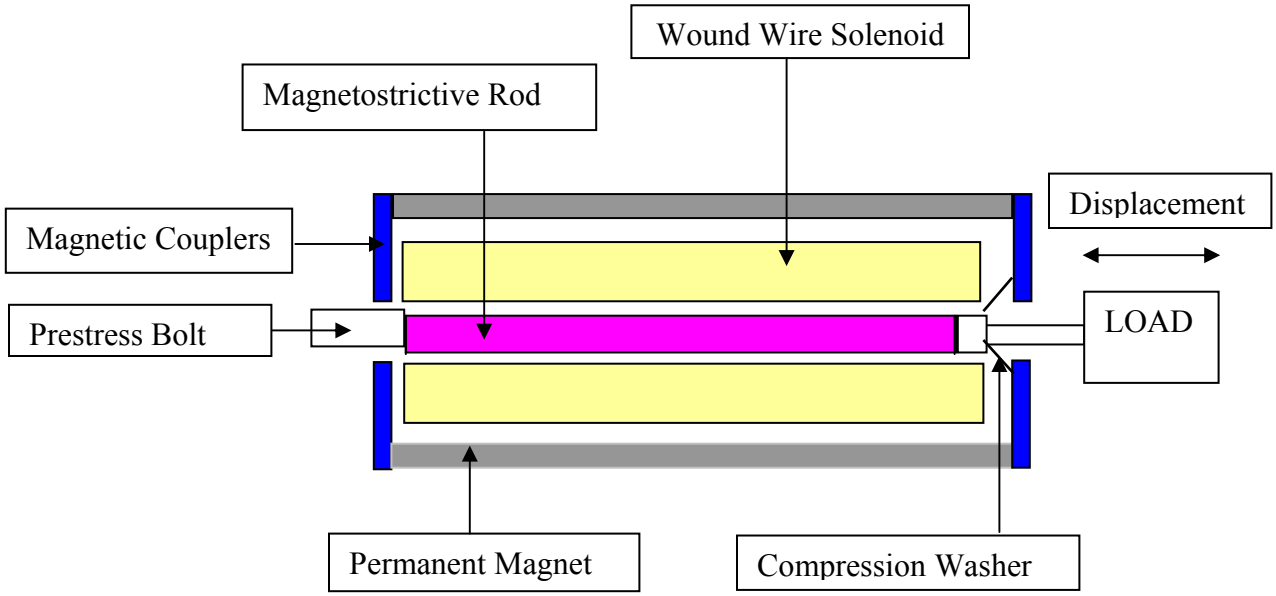

Figure 1.2: **Structure of a Linear Magnetostrictive Actuator**

Figure 1.2 shows the structure of a linear actuator. With the proper control algorithm, this actuator could be applied as a fast tool servo driven system, which is specifically designed for turning non-round parts. For example, Active Machining System (AMS), made by Etrema Inc., is such a computer controlled system that utilizes the power and fast response of a magnetostrictive actuator to precisely position the cutting tool in synchrony with a machine tool spindle. The actuator, applied as a fast tool servo, is mounted on the cross-slide of a lathe and controls the position of the cutting tool, according to control commands from the computer.

2. Sonar devices at low frequency

Magnetostrictive actuators are often operated at low frequency in this category. One typical application is the underwater acoustic sonar. Terfenol-D has been proven very attractive for underwater sound projection given its output strain, force and impedence-matching characteristics. Searching for more powerful sonar units forced researchers to increase either the size of the radiating surface or the vibration amplitude of the devices. On the other hand, the volume and weight constraints typically limit the allowable size of the device. Therefore, the research was focused on improving the vibration amplitudes. This demand led to the reviving of the flextensional transducer. Magnetostrictive flextensional transducers provide high power at low frequencies. The power output of the magnetostrictive flextensional transducers is about 25 times greater than that of PZT flextensional transducers. This occurs because its dynamics strain is approximately five times larger, and the power output is approximately proportional to the square of the strain.

3. Shock and vibration isolation devices

In conventional vibration isolation systems, spring and damper are often not effective in low frequency range and large mass cases. With the introduction of magnetostrictive actuators, active and passive vibration cancellation methods become very appealing. A feedback control system is often employed with suitable transducers to sense displacement, velocity and acceleration. Thus it can reduce the shock or vibration effectively.

4. Ultrasonic magnetostrictive actuators

Although piezoelectric actuators are sometimes preferred for ultrasonic or even megahertz range ultrasonic, the ruggedness and durability of magnetostrictive devices constitute a very appealing characteristic. In addition, magnetostrictive materials do not need to be repolarized when accidently heated beyond the Curie temperature point, whereas the piezoelectric actuators require this.

The ultrasonic magnetostrictive actuators are used in the fields of sonochemistry, ultrasonic welding, food processing, waste material conversion and ultrasonic machining.

Chemical processes such as polymerization can be commercialized using Terfenol-D ultrasonics. Several processes for ultrasonic destruction of environmentally damaging materials are in final stages of development. Since Terfenol-D is a low voltage, current driven magnetostrictive material, hand tools can be made safer. The high energy density of Terfenol-D also makes hand tools smaller in size.

5. Miscellaneous applications

From design and performance consideration, there are some differences among the above four categories. However, they have strong commonalities as well. First, it is often desirable to achieve linearity in the performance. To this end, it is common practice to operate magnetostrictive actuators under a bias condition, which consists of applying both a mechanical and a magnetic bias to the driver. As previously indicated, the magnetic bias is supplied with permanent magnets, located in series or parallel with the drive motor, or alternatively with DC currents.

Secondly, magnetostriction is a property that causes certain ferromagnetic materials to change shape in a magnetic field. The magnetic domain in the crystal will rotate when a magnetic field is applied. This provides a proportional, positive and repeatable expansion in microseconds, which is desired for actuation.

Lastly, the magnetostriction effect arises from an alignment of the magnetic domains. The crystal's magnetic anisotropy couples the magnetic field with the lattice distortion and consequently produces strain. The magnetostrictive effect is very sensitive to composition and manufacturing.

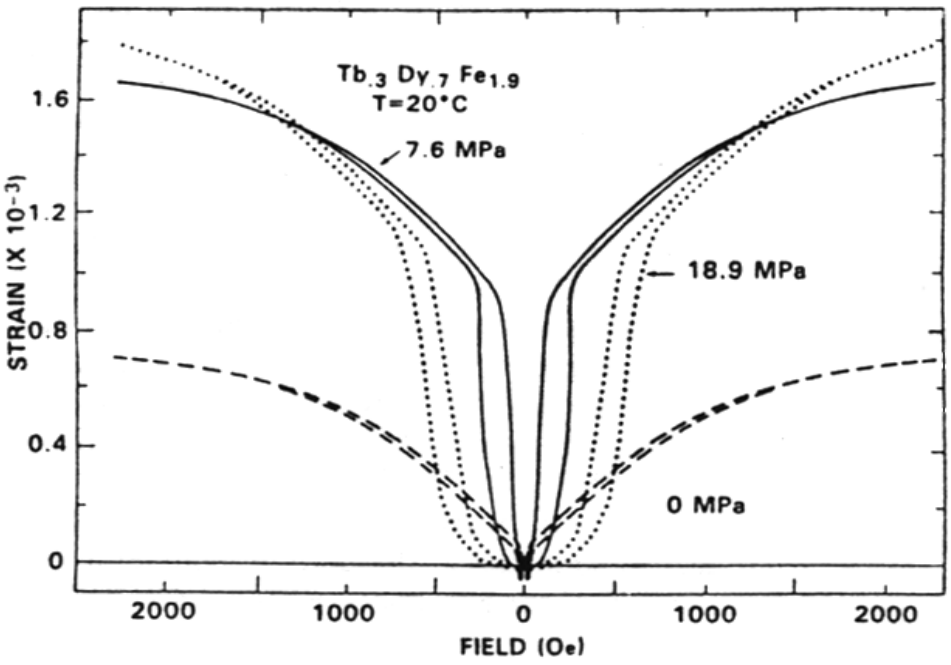

Figure 1.3: Micro-strain vs. Applied Magnetic Field

The strain produced by a magnetostrictive actuator is a nonlinear function of the applied magnetic field. The magnitude of the magneto-mechanical coupling and the material stiffness are strong functions of the material prestress. In *Figure 1.3*, the strain is

plotted as a function of the applied magnetic field. In addition to the highly nonlinear property, it exhibits hysteric responses. Given the nonlinearities, using a linear feedback control scheme is not practical. Therefore, it's a challenge to implement real-time control for the magnetostrictive actuator.

1.4 Origin of the Research Project

Magnetostrictive actuators have various applications in mechanical area. The typical applications of the magnetostrictive actuation include a fast tool servo system for tool positioning and control in the manufacturing industry—an example is, the smart machine tools with actuators to compensate for structural vibrations under variable loads; combustion engine fuel injections in the internal combustion industry; pumps and valves in the hydraulic industry; high precision positioning in the defense and aerospace industry—an example is the smart fixed wings with actuators that alter airfoil shape to accommodate changing drag or lift conditions.

As seen above, magnetostrictive materials have some desirable properties for actuation. However, they also show a very nonlinear property. In addition, a so-called non-affine property exists within a magnetostrictive system. These properties are the main limitations for its application in industry.

How to establish a proper model and use this model in real-time control is the main interest. Since variable structure control is known to be an effective approach for such a

nonlinear system, motivated by this, modeling and control of a magnetostrictive actuation system is chosen as the subject for this project.

The main equipment used in this research includes a Magnetostrictive Actuator (Model#: AA-140J) manufactured by Etrema Products Inc., IA; a PWM AC SERVO AMPLIFIER (Model#: 16A20ACT Brush Type) manufactured by Advanced Motion Controls, CA; an Angstrom Resolver (Model 101) assembled by Opto Acoustic Sensors at Raleigh, NC; an IBM-compatible personal computer; and a DT2823 ISA-bus DSP-board marketed by Data Translation Inc. at Marlboro, MA. The actuator and the amplifier were donated by Lord Corporation located at Cary, NC. This research project obtained its main financial support from the National Science Foundation (NSF). The research work related with this project was physically done at the Precision Engineering Center (PEC), Mechanical and Aerospace Engineering Department, North Carolina State University at Raleigh, NC.

1.5 Project Objectives

Since modeling and control for the magnetostrictive system is the objective of this project, the following related procedures, which also make up the main contents of this thesis, were necessary for the research.

Chapter I gives an overall introduction of the fundamental principle of the magnetostrictive actuator and this research project.

Chapter II includes main contents on design and structure of the magnetostrictive actuator. It also covers the application of magnetostrictive actuators. And, it presents the characteristics of the magnetostrictive materials and the actuator, especially on the nonlinear property and hysteresis phenomenon.

In *Chapter III*, the system identification problem is addressed. Using Least Square Technique (LST) and SAS System V8 program, a time-delay and dynamic model is established by matching the data series gathered from the input and output signal on the actuator. It's a so-called Black Box Model.

Chapter IV illustrates the controller design issue. PID control and sliding mode control (SMC) are two main control techniques being demonstrated. Matlab simulations are done first in order to verify the validation of the established model. The proposed controllers will demonstrate their tracking performances, respectively.

Chapter V provides the implementation of the control experiments and results analysis. Incorporated with a data acquisition board and computer, the experiments are conducted. The close loop performance of the proposed controller is to be verified by the experiments. Both results from open loop and close loop control experiments are compared and discussed.

Finally, in *Chapter VI*, overall discussion and future work are presented.

References:

1. A P Dorey and J H Moore, “Advances in Actuators,” IOP Publishing Ltd 1995.
2. Ralph C. Smith, “A Nonlinear Model-Based Control Method for Magnetostrictive actuators”, Proceedings of the 36th Conference on Decision & Control, December 1997.
3. Ralph C. Smith, “Inverse Compensation for Ferromagnetic Hysteresis,” Proceedings of the 38th Conference on Decision & Control, December 1999.
4. M. E. H. Benbouzid, “Artificial Neural Networks for Finite Element Modeling of Giant Magnetostrictive Devices,” IEEE Transaction On Magnetics, Vol. 34, No. 6, November 1998.
5. L. Gros, G. Reyne, C Body and G. Meunier, “Strong Coupling Magneto Mechanical Methods Applied to Model Heavy Magnetostrictive Actuators,” IEEE Transaction On Magnetics, Vol. 34, No. 5, September 1998.
6. R. Venkataraman, “Modeling and Adaptive Control of Magnetostrictive Actuators,” Ph.D Dissertation, University of Maryland, College Park, 1999.
7. Ralph C. Smith, “A Nonlinear Physic-Based Optimal Control Method for Magnetostrictive Actuators,” ICASE Report No. 98-4.
8. R D Greenough, “Actuation with Terfenol-D,” IEEE Transaction on Magnetics, Vol. 27, No. 6, November 1991.
9. Gutierrez, H. M. and Ro, P. I., "Sliding-mode control of a nonlinear-input system: application to a magnetically levitated fast-tool servo", IEEE Trans. on Ind. Elec., vol.45, no.6, pp. 921-927, 1998.
10. J.-J. E. Slotine and W. Li, Applied Nonlinear Control, Prentice Hall, 1991.

Chapter II

Magnetostrictive Actuation System

2.1 The Magnetostrictive Actuation System

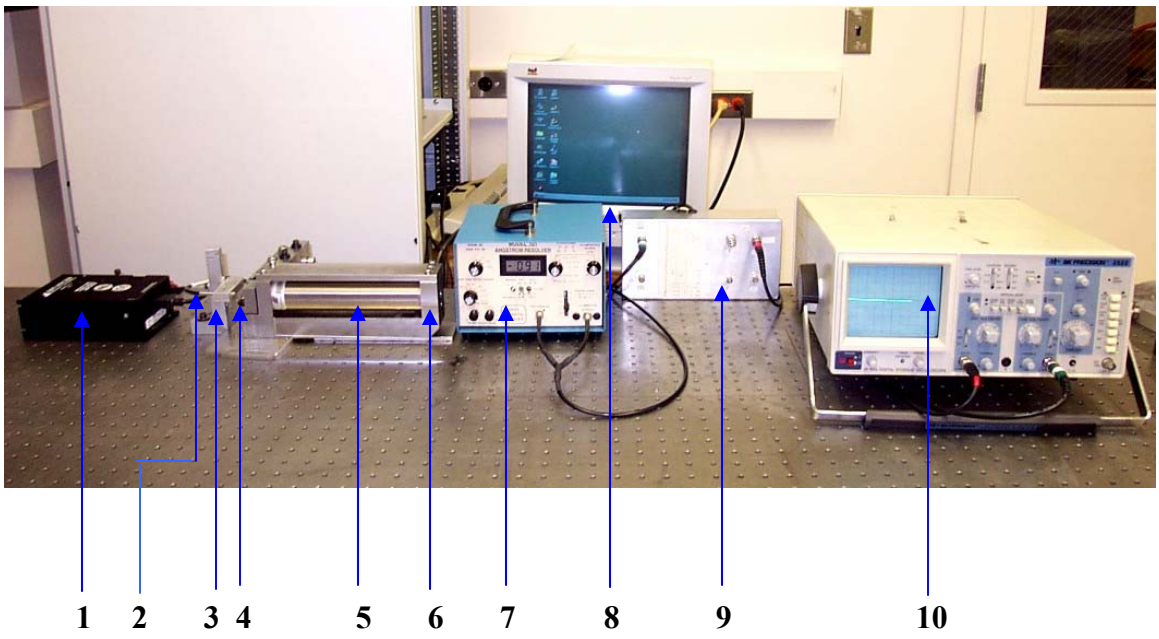

Figure 2.1: The Main Components of the Magnetostrictive Actuation System

As demonstrated in *Figure 2.1*, the magnetostrictive actuation system in this research project is made of the following components:

1. *Brush type PWM servo amplifier*, manufactured by Advanced Motion Controls, Camarillo, CA. Pulse width modulation (PWM) is the most efficient and cost-effective approach for amplifying the electric signals in a precision motion control application. The amplifier translates the low-energy reference signals from the controller into a high-

energy signal. This PWM amplifier has several operation modes to select from: current mode, voltage mode, IR compensation mode, and tachometer mode. Since a DT2823 DSP board is employed in this system and its output is a voltage signal, the voltage mode is selected as the operation mode.

2. *Optical sensor*, produced by Opto Acoustic Sensors, Cary, NC

3. *Fixture,* used to hold the Optical sensor probe.

4. *Cutting tool,* mounted on the actuator clamp, provided by Lord Corporation, Cary, NC.

5. *Magnetostrictive actuator*, manufactured by Etrema Products Inc. in Ames, IA.

6. *Angstrom Resolver*, with filter and signal processing circuits inside for receiving the signal from the optical sensor.

7. *Personal Computer*, to execute the control program and store collected data.

8. AD/DA converter board and its interface box, made by Data Translation Inc. at Marlboro, MA—used to collect data and generate control commands.

9. *Fixture, clamp plates and attached structure*, machined by Lord Corporation, Cary, NC. In order to get higher precision and keep the actuator from free vibration movement caused by the actuation, the actuator itself needs to be fixed on the desktop table.

10. *Oscilloscope,* used to observe the signals in and out from the actuator.

This magnetostrictive actuator, incorporated with the other components, is also a fast tool servo system, capable of generating high precision actuation movement. A typical application is cutting work pieces with irregular shaped profiles. For instance, with a proper controller, the actuator can be mounted on a diamond turning machine (DTM) to turn non-round or ecliptic work pieces with high precision.

2.2 Structure of the Magnetostrictive Actuator

The actuator model in this research project is an AA–140J013ES1 magnetostrictive Terfenol-D actuator manufactured by Etrema Products Inc. in Ames, IA. It's a linear actuator with an actuation range up to 200 micrometers. *Figure 2.2* illustrates the main structures of this magnetostrictive actuator along its cross-section. The following components comprise the magnetostrictive actuator:

1. A rod made of a smart material alloy named Terfenol-D, which converts electrical inputs (current or voltage) into mechanical outputs.
2. A nonlinear preload spring, which provides the prestress. An optimized prestress system will optimize the output and efficiency of the actuator, especially for low load applications. The prestress is determined by the selected compliance and time constant of the springs.
3. A cylindrical permanent magnet. This component provides a magnetic field bias H_b for the actuator that is able to reduce power consumption, minimize the need for DC bias current, and minimize heat generation. In addition, magnetic bias is necessary in order to get approximate linear response in its displacement.
4. A wound wire solenoid (coils), with current or voltage input, provides the actuation power through magnetic flux.
5. A stainless steel push rod, the main moving part within the actuator. It is the executive mechanism of the actuation for the linear axial displacement.
6. A non-magnetic outer housing, which is often made from aluminum. This part functions as a shield for the magnetic components inside the actuator.

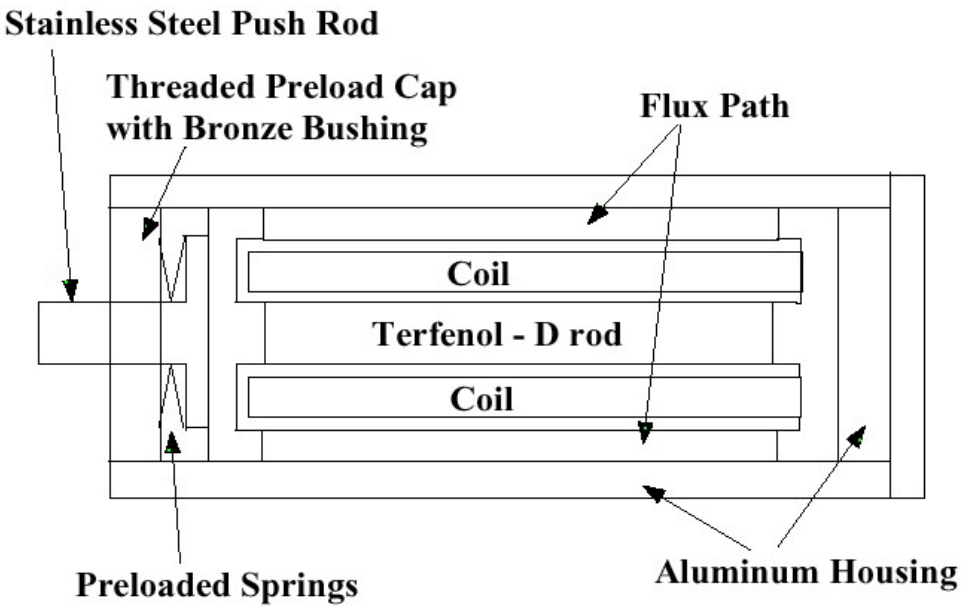

Figure 2.2: Cross Section of the Magnetostrictive Actuator

If a magnetic field is applied (the deformation of the actuator in response to external stimulus as a change in the applied magnetic field) the result is a motion of the push rod with respect to the outer casing. This motion is along its axial direction and is utilized for high precision actuation purposes.

This actuator incorporates a permanent magnet bias and preloaded springs for prestress. The unit length is 22.0 cm and the unit diameter is 4.7 cm. The housing is made of aluminum while the push rod, i.e. the moving unit, is made of stainless steel. The prestress is adjustable from 0 to 1 KSI (kilopounds per square inch, 1 KSI = 6.9 MPa). While the permanent magnet bias is approx. 500 Oe (Oersted, unit of intensity of the magnetic field, 1 Oe = 79.577 Amp/m). Its rated load is 1740 N.

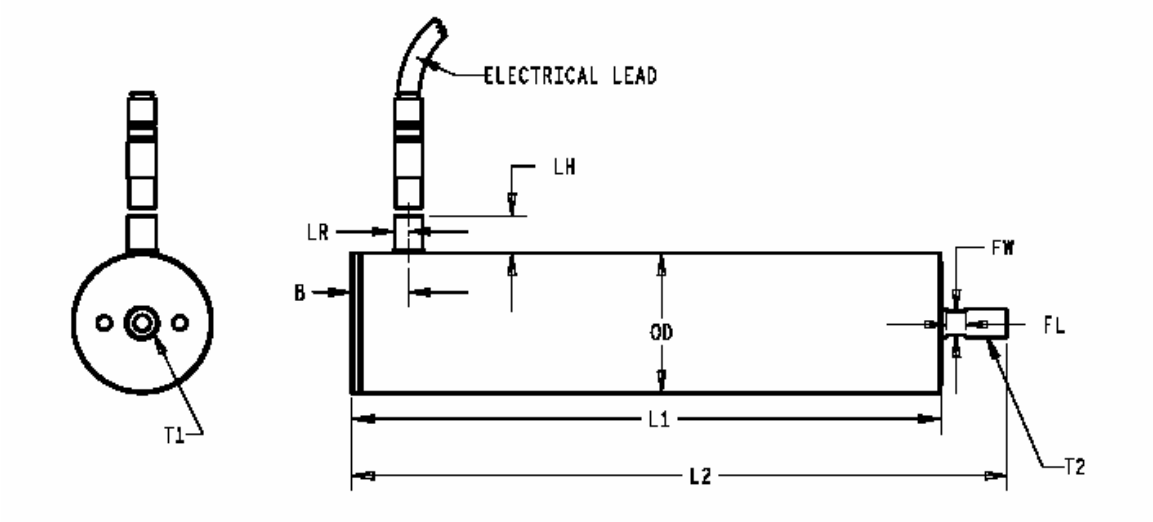

Figure 2.3: Cross Section of the TERFENOL-D Rod

(Courtesy of ETREMA Products, Inc)

Figure 2.3 gives the dimension and size of the Terfenol-D rod in the actuator. The following table lists the dimension parameters of the magnetostrictive actuator.

Model#: AA-140J013
Diameter D: 47.0 mm (1.85")
Length L1: 198 mm (7.80")
Length L2: 220 mm (8.68")
Connector Center B: 19 mm (0.76")
Flat Width FW: 7.9 mm (0.31")
Flat Length FL: 6.4 mm (0.25")
Thread T1 and T2 in English: 3/8-24 UN 2B 0.53 Deep; 3/8-24 UN 2A 0.50 Long
Thread T1 and T2 in Metric: M8 x 1.25-11 mm Deep; M8 x 1.25-12 mm Long
Unit Weight: 2.3 kg (5.07 lb)

Table 2.1 Dimension parameters of Magnetostrictive Actuator (AA-140J013)

2.3 Characteristics of the Magnetostrictive Actuator

As illustrated in *Figure 2.2*, the magnetostrictive rod made of Terfenol-D material is the main component of a magnetostrictive actuator. Magnetostrictive material provides many desirable properties for the magnetostrictive actuator. The most important characteristics are:

1. Larger displacement

For accurate positioning of mechanical loads, with unsurpassed force and speed, Terfenol-D shows outstanding capabilities among the various solid-state actuators. For the voltage signal input under the same amplitude and frequency, magnetostrictive material performs a longer displacement than most of the other commercial smart materials such as piezoceramics or nickel alloys. This property is especially appealing for the application of long-range actuation.

2. Frequency response

The magnetostrictive actuator could operate over a large frequecy range from DC to 20 KHz. This brings a broad application from low-frequency range to ultrasonic range. As seen in *Figure 2.4*, the near linear range is about 20Hz to 200Hz.

The frequency response of an actuator is determined not only by the inherent properties, for instance, inductance and speed, of the magnetostrictive material, but is strongly influenced by the mechanics of the system, namely, the physical construction of the device and its Q factor and the inertial effect of the whole system. The design of the outer housing structure also has an influence. Due to the existence of macroscopic eddy currents, the frequency range of the actuator is inherently limited. However, this

limitation can be minimized by laminating the Terfenol-D material. Its working frequency range thus could be extended to 80 kHz range if the thickness of lamination is in 1 mm range, as predicted by Etrema Products Inc.

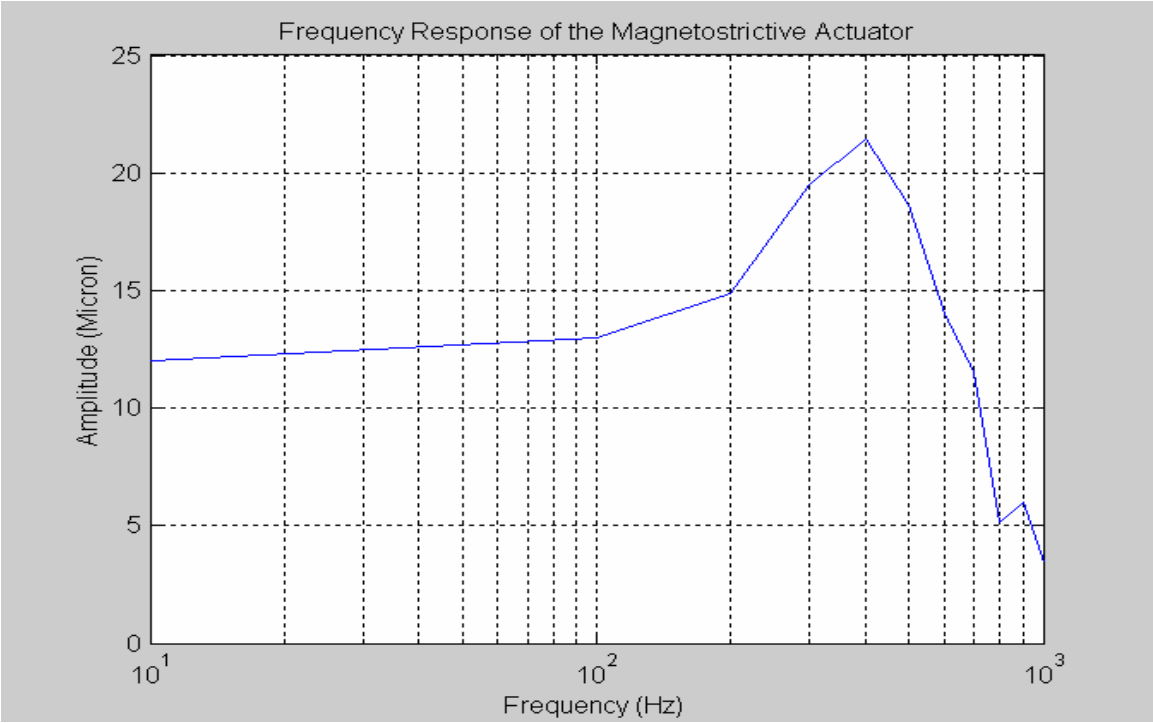

Figure 2.4: Frequency Response of AA-140J013 Magnetostrictive Actuator

3. High strain

For actuators, high strain means larger actuation movement and bigger load. With the development of the magnetostrictive materials, the strain goes up steadily to 2000-3000 ppm range, much higher than those of other commercial smart materials.

4. Precision control

For a magnetostrictive actuator, the concept of precision is related to its actuation range and repeatability. A magnetostrictive actuator can provide repeatable displacement with high accuracy, ideal for high precision purpose acutation. A Terfenol-D rod with 10cm length and 5 cm^2 could have a minimum step of the change in length of 0.01 nm within its linear displacement of 100 micrometers [10].

5. *Operating under low voltages*

Compared with other smart structure actuators, such as piezoelectric crystals, which require higher voltages (200-300 Volts) to produce desired mechanical deformations, magnetostrictive materials readily respond to significantly lower voltages, often around 10-50 Volts. A DSP board can provide the input signal in this range with a moderate amplifier.

6. *Fast response*

The mechanical response time of a magnetostrictive actuator is within several microseconds due to the molecular level of the magnetostrictive strain. For example, under a 20Hz AC signal, the response time is about 0.3 microseconds. Fast response is crucial for high precision actuation, since it will reduce the tracking error within a short time period. And fast response is particularly good for the implementation of a real-time controller.

7. *Operating over a wide temperature range*

Although a magnetostrictive actuator is senstive to temperature variation, it can operate over a wide temperature range from 40 to 200 °F. In order to get ideal performance with maximum strain, room temperature is required. Strain under other temperature conditions will cause a strain decrease.

2.3.1 Magnetostriction Hysteresis

In addition to the ideal properties, magnetostrictive material shows strong hysteresis. The magnetostrictive actuator shows a strong hysteretic relationship between the current or voltage input and its actuation displacement.

Hysteresis, in Greek, means *lag behind*. Apparently, this hysteresis phenomenon is partly due to the lag of the response between the input and output. In view of energy, this magnetostrictive hysteresis phenomenon is caused by the energy dissipation within the system.

Figure 2.5 describes the association of quasi-static strain and applied magnetic field H. A very small linear part around the origin point, the apparent different paths in *Figure 2.6*, also exhibit the magnetostrictive hysteresis and complex nonlinear responses.

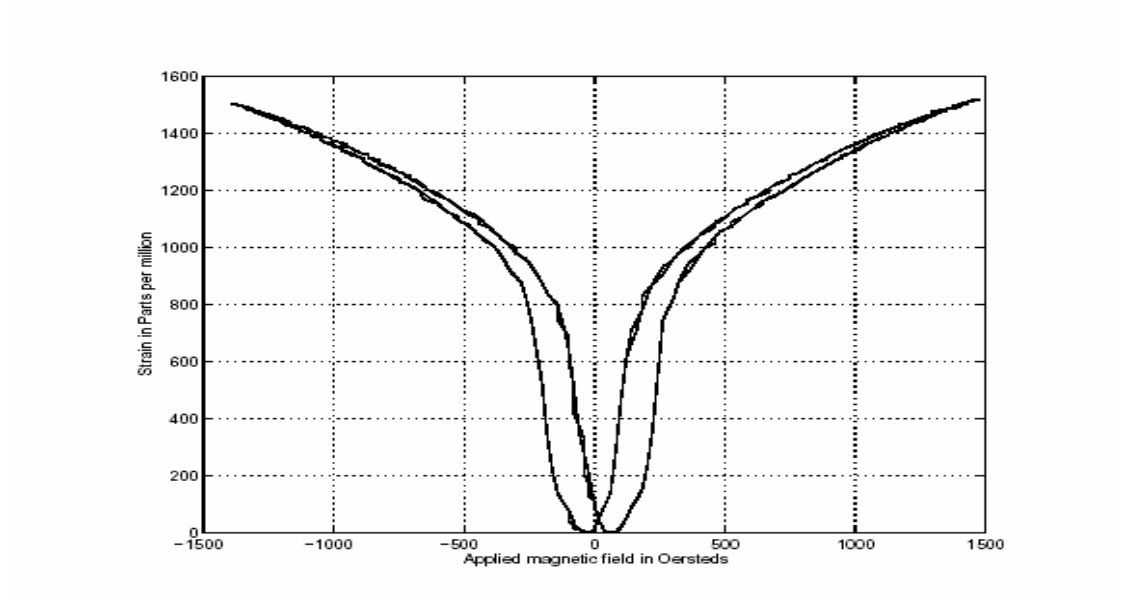

Figure 2.5: Quasi-Static Strain vs. Applied Magnetic Field H for an TERFNOL-D Actuator (Courtesy of ETREMA Products, Inc)

The values of each point in *Figure 2.6* are obtained by inputing the DC voltage to the acuator and measuring the corresponding displacement. The input voltage goes up gradually from -11V to 11V, inceremented by 1V each step. Then voltage input goes down from 11V, step by step, and back to -11V DC again. The waiting time between two consecutive voltage inputs is about 1 minute. Apparently, even when the input voltages are the same at the up and down procedure, respectively, the corresponding displacements of the actuator are different. This difference in amplitudes in *Figure 2.6* can reach as large as 100 micrometers. This property is called magnetostrictive hysteresis or hysteresis.

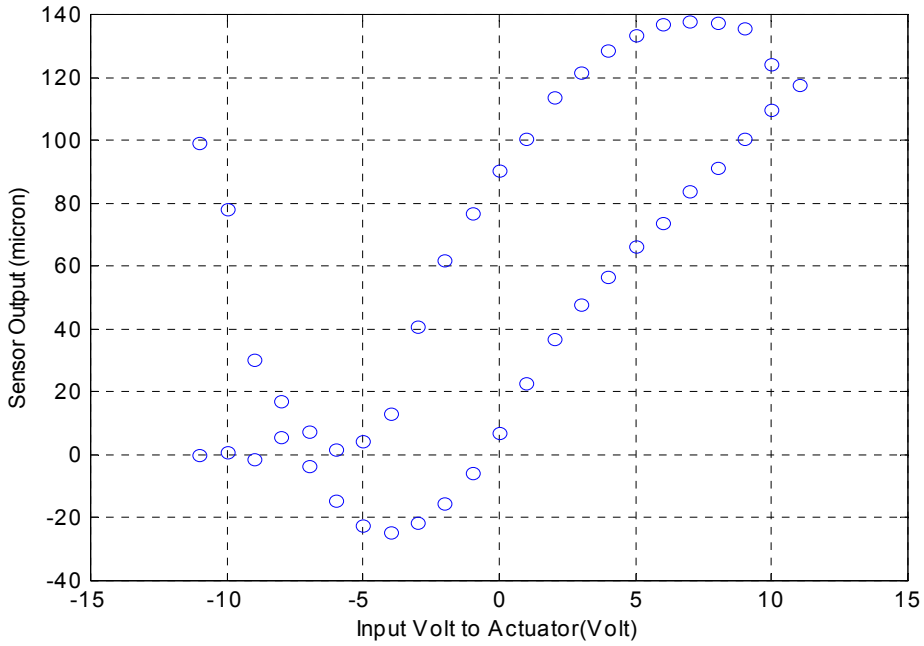

Figure 2.6: Magnetostrictive Hysteresis under DC Voltage Inputs

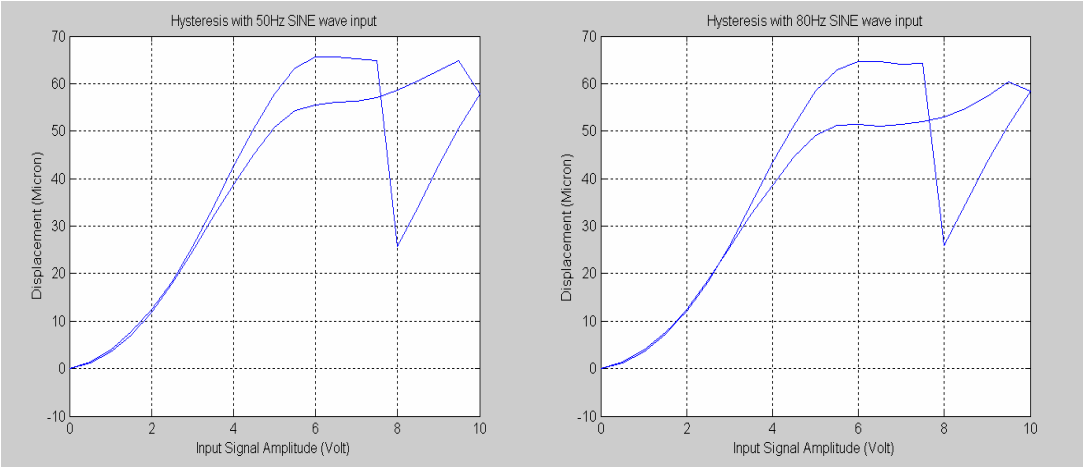

Figure 2.7: Magnetostrictive Hysteresis under AC Signal Input

Hysteresis is an important property of the magnetostrictive actuator. Likewise, under the inputs of an AC voltage signal, the magnetostrictive actuator shows hysteresis, although it's somewhat different. The above *Figure 2.7* shows the magnetostrictive hysteresis. Obviously, under AC signal inputs, the energy loss is larger than those under

DC signal inputs. Roughly, the amplitude of the displacement of the actuator on the upward path is proportional to the amplitude of the input signal, whereas the downward path is not. Instead, it shows a steep jump midway in its path back to the origin point.

2.3.2 Nonlinearities and Non-affine Property

In most cases, a linear range is required for actuation application. However, the magnetostrictive material shows strong nonlinearities. The behavior of a magnetostrictive actuator is nonlinear in every aspect. First, with an applied magnetic field, the magnetostrictive core will be magnetized nonlinearly. In other words, the magnetostriction is not proportional to the magnetization. The prestress mechanism inside the magnetostrictive actuator causes nonlinearities as well. Washers are usually used in this prestress mechanism against the magnetostrictive core. When compressed to some extent, they produce nonlinearities and thus bring mechanical hysteresis to the actuator. If the control input is coupled nonlinearly with states and can't be decoupled through analytical methods, this system is called a non-affine system.

Due to the existence of nonlinearities, the actuation displacement is expected to be not proportional to the amplitude of the input signal. A proper controller is essential for its application in manufacturing.

2.3.3 Temperature effects

Temperature has a strong impact on the performance of the magnetostrictive actuator. Strain change, thermal expansion, and resistance change are three consequences

caused by changing temperature. The thermal expansion ratio of the magnetostrictive core is about $12 \text{ X } 10^{-6} /^{\circ} \boldsymbol{C}$. Roughly, when heated from room temperature ($20^{\circ} \boldsymbol{C}$) to $100^{\circ} \boldsymbol{C}$, the thermal expansion could reach 1.5% of the whole length of the Terfenol-D rod. That's up to 0.003m, which is not an allowable elongation for a 0.2m long actuator. However, the displacement of the actuation motion will be smaller, since the strain of the magnetostrictive core will decrease dramatically as the temperature increases. As a result, the total changing in the displacement is the combination of these factors.

Therefore, maintaining a controlled room temperature is critical in applications. Certain cooling methods are necessary for the operation. For instance, in order to cool off the magnetostrictive actuator in operation, a certain time waiting (at least 15 minutes) is kept between two consecutive experiments. In high precision applications, heat sink and cooling fluid are required to maintain the required temperature.

2.4 Open Loop Performance of the Magnetostrictive Actuator

In the experiments, voltage signals with different frequencies and different amplitudes are imposed on the magnetostrictive actuator in order to see how the actuator behaves. Thus, raw data are being collected for modeling purposes. Some of the experimental results are shown in *Figure 2.8* through *Figure 2.14*.

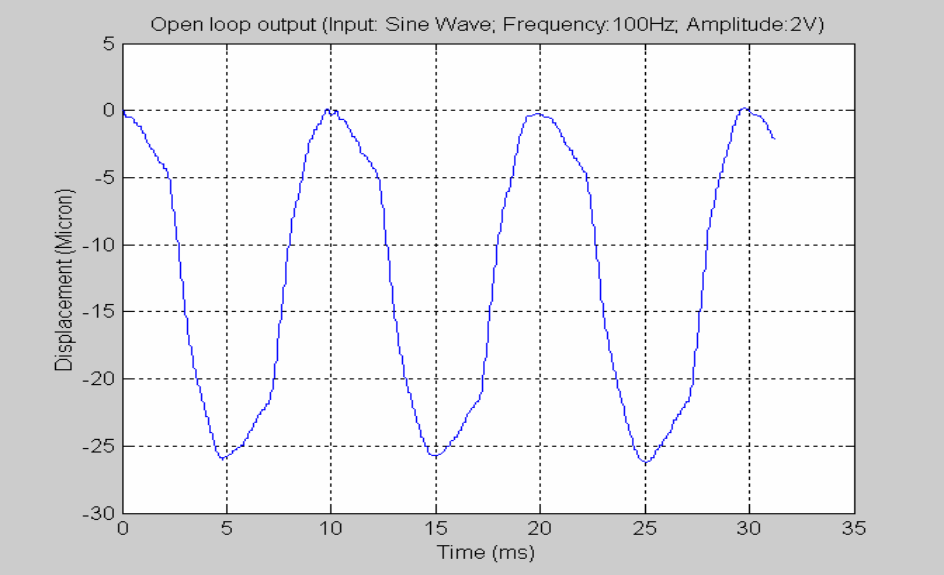

Figure 2.8: Open Loop performance with Sine Wave Input (Frequency: 100Hz, Amplitude: 2V)

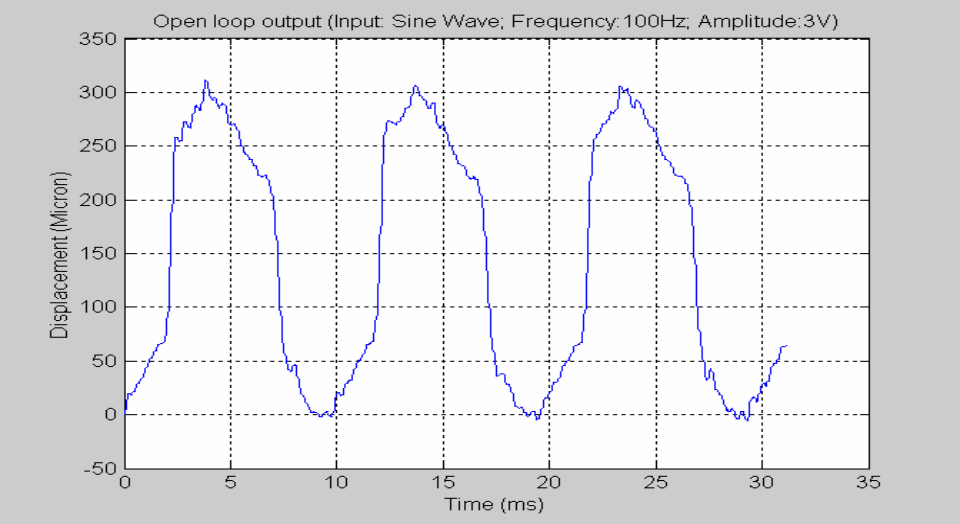

Figure 2.9: Open Loop performance with Sine Wave Input (Frequency: 100Hz, Amplitude: 3V)

In *Figure 2.8* and *Figure 2.9*, the input wave frequencies are the same, but the amplitudes are different. *Figure 2.8* shows the position output of the magnetostrictive

actuator with input frequency of 100Hz. From *Figure 2.8* to *Figure 2.9*, the amplitude increases from 2 volts to 3 volts. The actuation displacement then increases from 25 microns to 150 microns, roughly. And the displacement trajectory with 2V is smoother than those with 3V amplitude. Obviously, the actuation displacement is not proportional to the amplitude of the input signal. In other words, it's a nonlinear system.

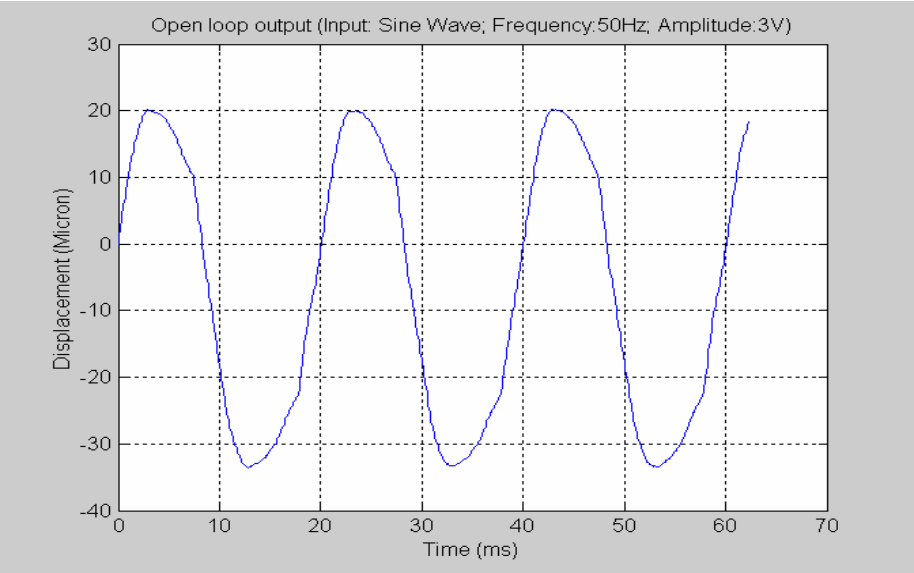

Figure 2.10: Open Loop Performance with Sine Wave Input

(Frequency: 50Hz, Amplitude: 3V)

A trend that can be observed from these figures is, with lower frequency or amplitude input, the displacement trajectory is smoother than those with higher frequency or amplitude input. In other words, the higher the operating frequency is, the more nonlinear performance it will show.

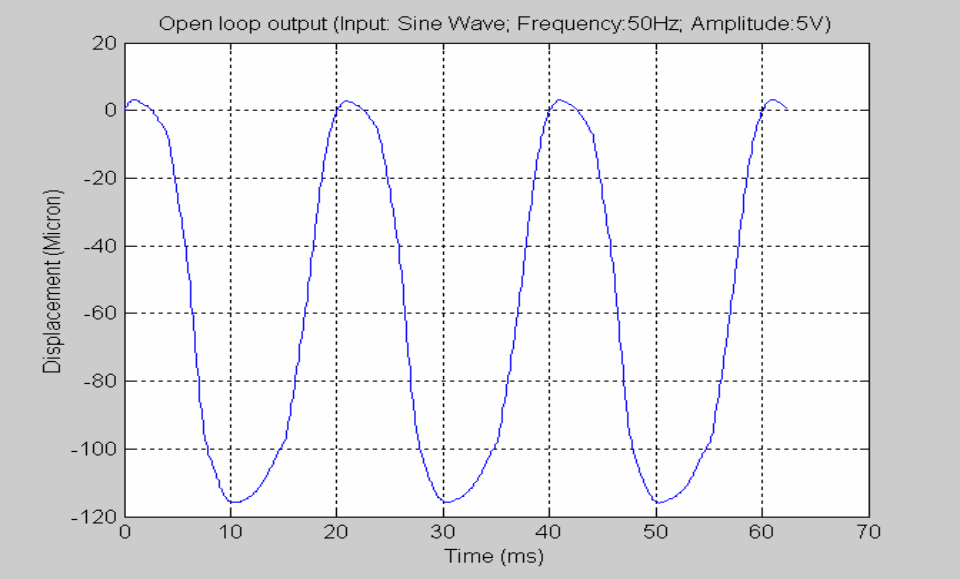

Figure 2.11: Open Loop Performance with Sine Wave Input

(Frequency: 50Hz, Amplitude: 5V)

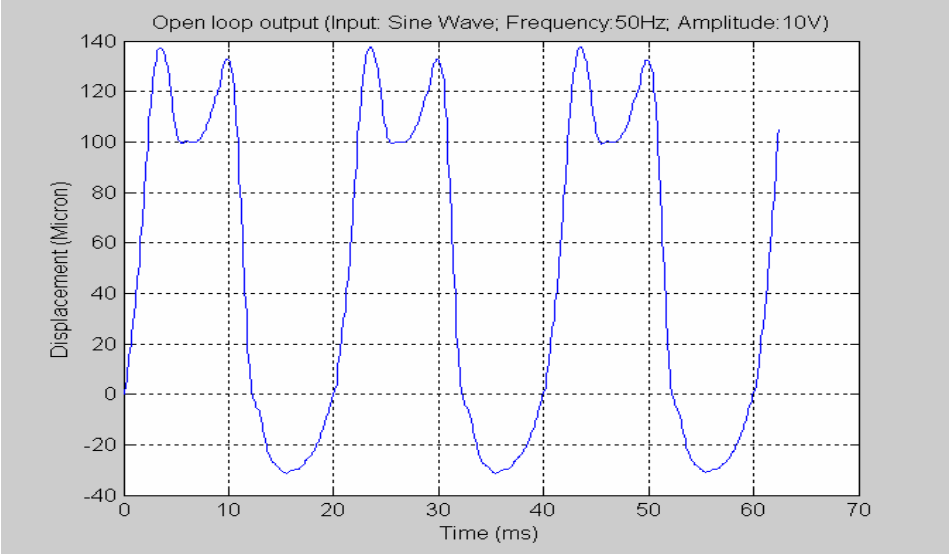

Figure 2.12: Open Loop Performance with Sine Wave Input

(Frequency: 50Hz, Amplitude: 10V)

Figure 2.10 through *Figure 2.12* also show the open loop performance under the sinusoid signal input with the same operating frequency of 50Hz but different amplitudes. The frequency of the output from the actuator follows the input signal in each figure.

Here, however, the displacement is not proportional to the magnitude of the input voltage; i.e., it is very nonlinear. This phenomenon is quite obvious, especially under high drive level (high frequency or amplitude). Around the peaks and valleys of the output sinusoid wave, the nonlinearity is very prominent. If the amplitude or frequency of the input signal increases to some degree, the nonlinearity will prevail in the performance. If no proper controller is introduced, this property will definitely limit the application of the magnetostrictive actuator.

The following *Figure 2.13* and *Figure 2.14* show another open loop output under the input of a triangular wave signal. These results verify the fact that the magnetostrictive actuator is a very nonlinear system under various types of inputs.

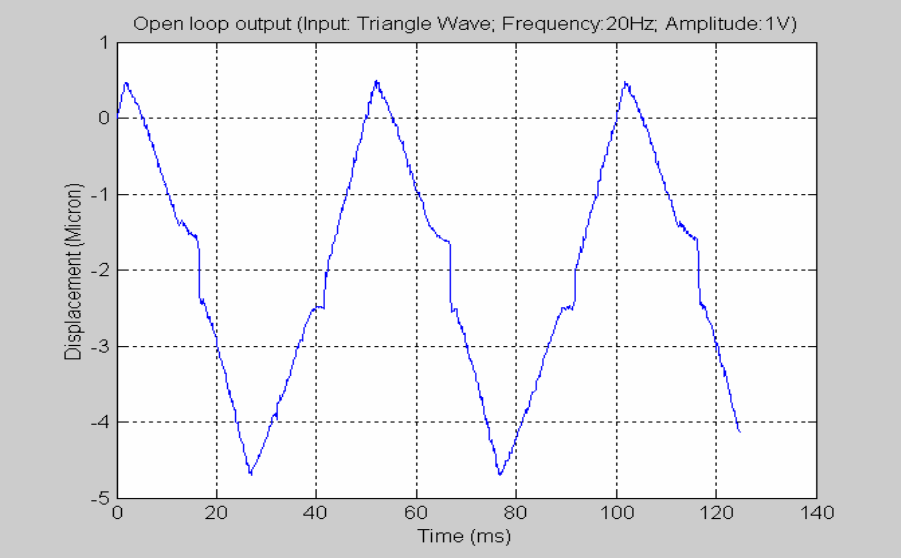

Figure 2.13: Open loop response with triangle wave input

(Frequency: 20Hz, Amplitude: 1V)

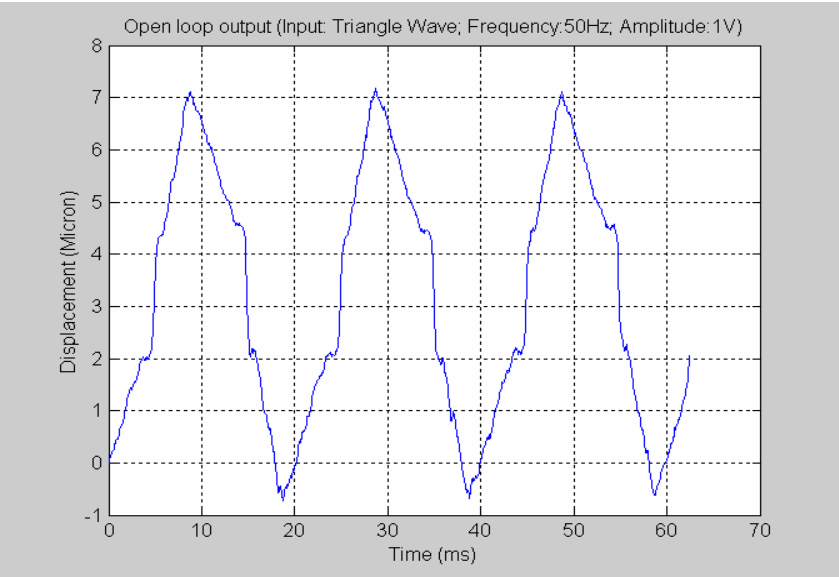

Figure 2.14: Open loop response with triangle wave input

(Frequency: 50Hz, Amplitude: 1V)

The control of this actuation system is the main interest, and then not only the modeling of the actuator itself, but also the associated components of the actuator are concerned. This modeling procedure is fraught with uncertain knowledge of the system that might change with temperature and time. Without knowing the uncertainties precisely, it's still possible to use techniques of adaptive and robust control if a rough knowledge of the uncertainty can be obtained. Hence, this actuation system including the magnetostrictive actuator itself along with the associated prestress, magnetic path, and the PWM amplifier will be modeled as a whole black box system, which is the topic of the next chapter.

References:

1. A P Dorey and J H Moore, “Advances in Actuators,” IOP Publishing Ltd 1995.
2. Marcelo J. Dapino, "Nonlinear and Hysteretic Magnetomechanical Model for Magnetostrictive Transducers," PhD Dissertation, Iowa State University, 1996.
3. Ralph C. Smith, “A Nonlinear Model-Based Control Method for Magnetostrictive actuators,” Proceedings of the 36th Conference on Decision & Control, 1997.
4. Ralph C. Smith, “Inverse Compensation for Ferromagnetic Hysteresis,” Proceedings of the 38th Conference on Decision & Control, December 1999.
5. M. E. H. Benbouzid, “Artificial Neural Networks for Finite Element Modeling of Giant Magnetostrictive Devices,” IEEE Transaction On Magnetics, Vol. 34, No. 6, November 1998.
6. L. Gros, G. Reyne, C Body and G. Meunier, “Strong Coupling Magneto Mechanical Methods Applied to Model Heavy Magnetostrictive Actuators,” IEEE Transaction On Magnetics, Vol. 34, No. 5, September 1998.
7. R. Venkataraman, “Modeling and Adaptive Control of Magnetostrictive Actuators,” Ph.D Dissertation, University of Maryland, College Park, 1999.
8. Ralph C. Smith, “A Nonlinear Physic-Based Optimal Control Method for Magnetostrictive Actuators,” ICASE Report No. 98-4.
9. R D Greenough, “Actuation with Terfenol-D,” IEEE Transaction On Magnetics, Vol. 27, No. 6, November 1991.
10. Sergey F. Tsodikov, Vadim I. Rakhovsky, “Magnetostrictive Force Actuators For Superprecise Positioning,” IEEE 18th Int. Symp. On Discharges and Electrical Insulation in Vaqcum-Eindhoven, 1998.

Chapter III

System Identification

3.1 Modeling of the Magnetostrictive Actuation System

Due to the existence of the magnetostriction, hysteresis, and nonlinearities, modeling of a magnetostrictive actuator is a challenging work. Researchers have tried various methods to model magnetostrictive actuators. Most of the models for magnetostrictive actuators are based on the H-M curve [1]; i.e. the relationship between the magnetostriction M and the applied magnetic field H as shown in *Figure 3.1*. There are two main categories in the modeling techniques for the magnetostrictive hysteresis—the Preisach approach [3, 4] and the quasi-macroscopic models. The Preisach model provides an observed characterization of the relations between the input and output of the magnetostrictive materials, but ignores some unmodeled physical mechanisms. It's a universal approach, in a sense. The model requires the estimation of many numerical parameters, but does not try to include the physical dynamics of the material. The second or quasi-macroscopic model is a physical-based model, which is also called the domain wall approach. It concerns both the reversible and irreversible domain wall movements in the material. And the approach uses parameters related to the magnetic characterization of the input magnetic field. This second modeling method is formed by extending Jiles and Atherton's ferromagnetic hysteresis model to magnetostrictive actuators [5, 6].

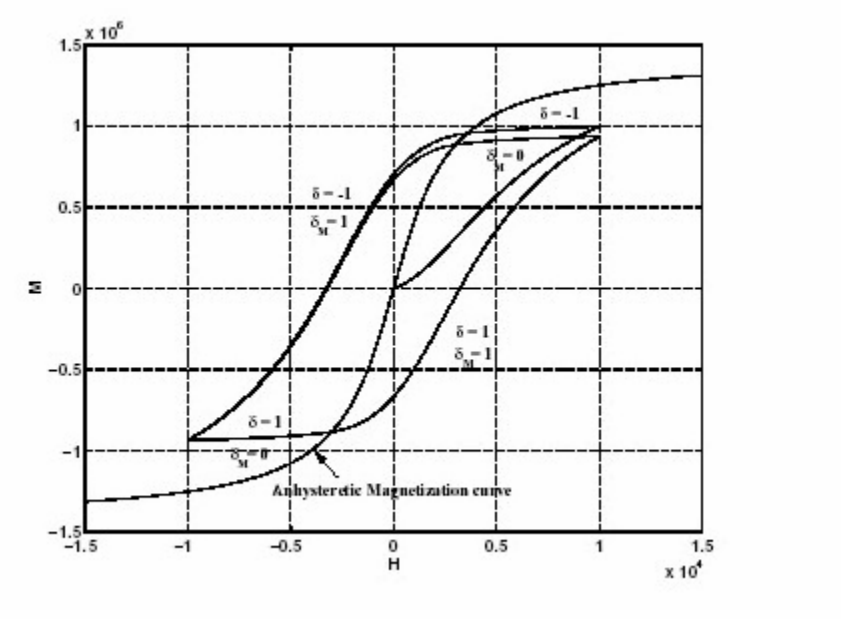

Figure 3.1 Magnetostriction M vs. Applied Magnetic Field H

In 1983, Jiles and Atherton [5, 6] proposed a model for ferromagnetic hysteresis with phenomenological and thermodynamic considerations. This model is very appealing from the control point of view because it describes hysteresis as the solution of four differential equations. Some researchers proposed a model using finite element analysis methods. Others developed low dimensional models using the energy balance principle [4]. Other modeling approaches concerned the development of a physics-based model for magnetostrictive material that captures hysteretic phenomena and can be subject to rigorous mathematical analysis towards control design [5].

The behavior of a magnetostrictive actuator, and thus its application in engineering, depends not only on the energy type (electromagnetic, elastic, or thermal) supplied to it, but also on how this energy is applied. In particular, the sequence of these energies applied to the magnetostrictive actuator also has an impact upon its performance. This

indicates the complexity of magnetostrictive behavior and the existence of coupling between energy regimes. In order to fully utilize the desirable features of Terfenol-D, it is necessary to characterize the electric, magnetic elastic, and thermal regimes, as well as the interactions among them.

A proper mathematic model can accurately predict the performance of a transducer in the form of a mathematical formulation that provides some numerical output in response to a numerical input. Depending on the degree of accuracy, models can simulate actuator performance or even predict it precisely. Mathematical performance simulations are highly useful, for predicting actuator behavior is ultimately desirable.

Predictive modeling is relevant to the use of magnetostrictive actuators in three ways. First, well-posed models provide the ability to scale results in a way that experiments often do not. For instance, although the magnetostrictive actuator model developed in this thesis is dependent on the actuator size and model, it is still able to provide a modeling approach for a common magnetostrictive actuator.

Second, predictive modeling allows the actuator designer to understand and analyze actuator behavior before any prototype is developed. Thus, time and cost to design are reduced efficiently.

Finally, in control applications, modeling can enable the knowledge of how much change in the voltage input that is necessary to obtain a desired change in the output for displacement.

The next question is how to predict the actuator behavior. The simplest and perhaps most common model of magnetostrictive performance is the linear piezomagnetic equations [6]. These equations represent the magnetic-elastic bi-directional energy transduction in a form amenable to performance modeling, material property characterization, electric circuit analogue representations, and control implementation. The value, however, of this model is limited. The linear piezomagnetic equations provide insight on the actuator performance at the low signal level, where the performance of the magnetostrictive actuator is quasi-linear. Magnetostrictive transduction is an intrinsically nonlinear and hysteretic process; thus, the modeling procedure should address the nonlinear regimes properly found in applications.

Therefore, a new approach to modeling a magnetostrictive actuator will be proposed based on statistical principle using a SAS System program. In this approach, first, the magnetostrictive actuator system is treated as a single input-single output (SISO) system. The voltage is the only input and the displacement is the only output. With this assumption, two time series—voltage input and displacement output—are obtained from experiments. The first time series consists of the output from the A/D converter board. In fact, it's the input signal to the magnetostrictive actuator. The second time series is made of the displacement values from the actuator. This series of values is obtained from the

optical sensor, i.e., the output voltage signal from the actuator. A calibration factor, or sensor gain, exists between the voltage and the displacement value.

First, the relationship between the values of the two time series is observed. Since this is a very nonlinear system, a higher order polynomial structure is suggested as one possible mathematic model. Then 3rd and 4th order models were tried and tested using the SAS program. However, the comparison between the simulation and experimental results indicated that the polynomial model is not suitable for the actuator at all.

Considering that the system shows strong hysteresis, it definitely has time delay property. Thus a time-delay structure model is proposed to model the magnetostrictive system. This time-delay model is assumed to have the following structure:

$$y(t) = a_1 x(t) + a_2 x(t-1) + a_2 x(t-2) + \ldots + a_n x(t-n) + b \qquad (3.1)$$

where *y(t)* denotes the current output from the actuator, *x(t)* is the current input to the actuator, *x(t-n)* is the backward *n* steps input. $a_1, \ldots a_n$ are the parameters to be determined by the algorithm, and b is the intercept or so-called translation constant.

3.2 Least Squares Technique

The approach employed here to identify the system dynamics is called Least Squares Technique (LST). It is a basic technique for parameter estimation problems in system identification. Assuming the mathematical model can be written in the form:

$$\mathrm{Y(t)} = X_1(t)\ K1\ + \ \ldots + X_n(t)\ Kn\ = X(t)K \qquad (3.2)$$

where Y is the observed variable, $K_1, K_2, \ldots K_n$ are unknown parameters to be determined, and $X_1, X_2, \ldots X_n$ are inputs, which are known, at different time.

The variables in the model are indexed by t, which often denotes time. t is assumed to be a discrete set which could be the result of sampling in an experiment. The pairs ($Y(i), X(i)$), i= 1, 2, …, t are obtained from experiments.

The problem here is to determine the parameters K_1 through K_n in such a way that the outputs computed from the model in Equation (3.2) agree as closely as possible with the measured variables $y(i)$ in the sense of least squares.

Let

$$\mathrm{Y}(t) = [y(1) \;\; y(2) \ldots y(t)]^{\mathrm{T}}$$

$$\mathrm{X}(t) = [x(1)\, x(2) \ldots \; x(t)]^{\mathrm{T}}$$

$$\mathrm{E}(t) = [e(1) \;\; e(2) \ldots e(t)]^{\mathrm{T}}$$

where the residuals e(i) are defined by:

$$e = y(i) - \hat{y}(i) = y(i) - X(t)^T K \tag{3.3}$$

The least square error is defined by

$$\mathrm{V(K, t)} = \frac{1}{2}\sum_{i=1}^{t}(y(i) - x(t)^T k)^2 = \frac{1}{2}E^T E = \frac{1}{2}\left\|E\right\|^2 \tag{3.4}$$

where $E = Y - \hat{Y}$

The solution to the least-squares problem is given by the following theorem:

Theorem:

The function of Equation (3.4) is minimal for parameters $\hat{K}$ such that

$$X^T X\hat{K} = X^T Y \tag{3.5}$$

If the matrix $(X^T X)$ is nonsingular, the minimum is unique and given by

$$\hat{K} = (X^T X)^{-1} X^T Y \tag{3.6}$$

3.3 Time Delay Model for the Magnetostrictive Actuator Model

The ARMA model is a typical structure type for a time delay system. The definitions for the ARIMA and ARMA models are:

ARIMA— *Auto-Regressive Integrated Moving-Average (ARIMA) model*.

ARMA—*Autoregressive moving-average (ARMA) model*.

Using three time series obtained from the experiments:

#1: Time series (sec)	#2: Input series (volt)	#3 Output series (volt)
0.000	0.000	*0.000*
...	i_1	y_1
…	....	...
0.100	i_n	y_n

In order to test the response, the input signal to the actuator consists of two sinusoid waves at different frequencies and amplitudes, which is expressed by:

$$X(t) = 2V * \text{Sin}(2*PI*40t) + 1V * \text{Sin}(2*PI*60t + 1/3*PI) \tag{3.7}$$

Raw data including two time series (input and output) is collected from open loop experiments illustrated in *Chapter II*. After being processed using the regression algorithm of SAS System V8, a time delay model for the magnetostrictive actuator is obtained:

$$Y(n) = 2.88980 * X(n) + 6.156454 * X(n-4) \quad (3.8)$$

Figure 3.2 demonstrates simulated output using the time delay model and the actual output from the experiment. *Figure 3.3* uses a different input signal, which also consists of two different sinusoid waves in the *Figure 3.2*. The modeling results are very similar in *Figure 3.2* and *Figure 3.3*.

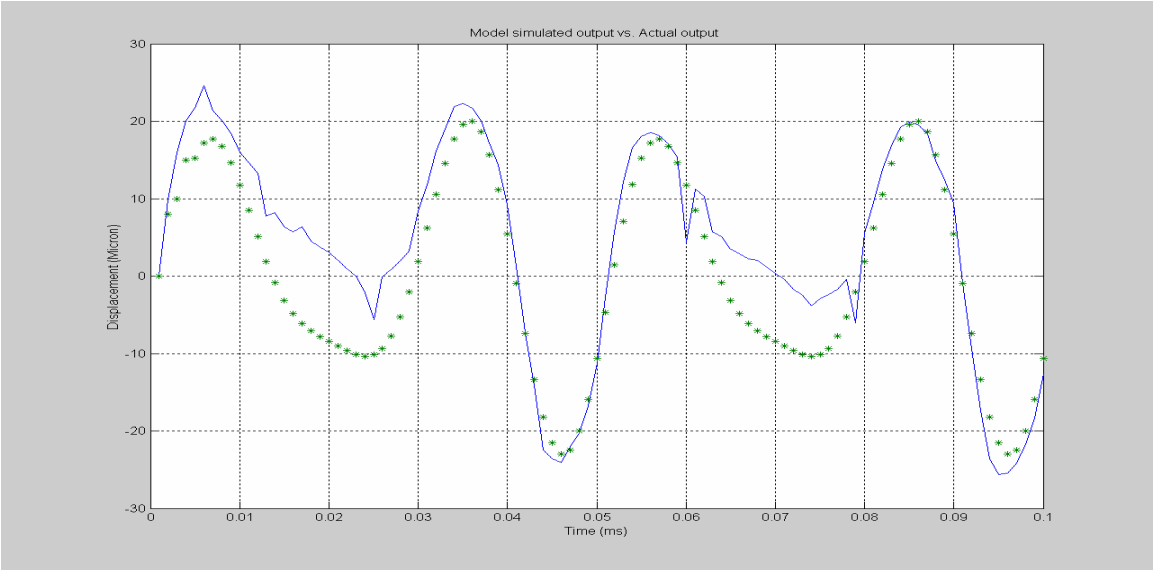

Figure 3.2: Model simulated output vs. Actual output
series 1(-) – output series 2 (*)– model simulated output value
Y(n) = 2.88980*X(n) +6.156454 *X(n-4)
X(t) = 2V*Sin(2*PI*40*t)+1V*Sin(2*PI*60*t+ 1/3*PI)

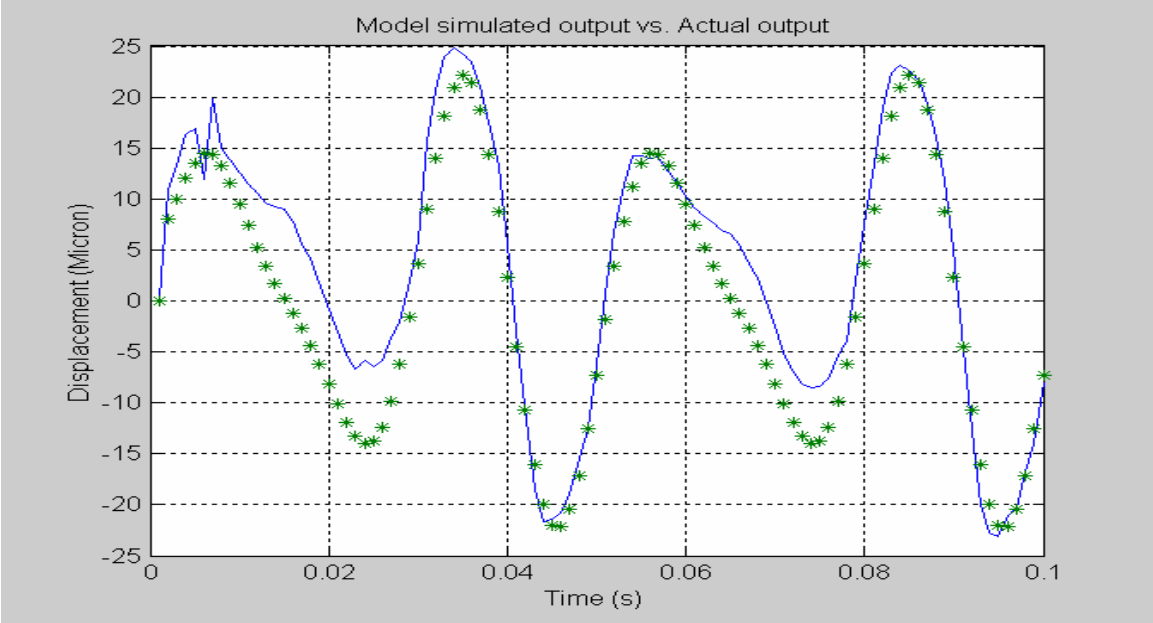

Figure 3.3: Model simulated output vs. Actual output
series 1(-) – output; series 2 (*)– model simulated output value
Y(n) = 2.86289*X(n) +6.23818 *X(n-4)
X(t) = 2V*Sin(2*PI*40*t)+1V*Sin(2*PI*60*t+ ½*PI)

3.4 Second Order Dynamic Model

For control purposes, this time delay model will use as many as four steps of previously stored values to predict the current output. This will increase the difficulty of implementing the controller since real-time control is required to achieve high precision. And, it may cause instability in some situations. So, this time delay model is not practical for real-time control.

Considering that the magnetostrictive actuation system is a very nonlinear plant, a higher order dynamic model is necessary to describe its behavior. Using SAS System V8, a second order dynamic model is obtained. The ARIMA or ARMA is the auto regression moving average models [11, 12]. An ARIMA model predicts a value in a response time series as a linear combination of its own past values, past errors (also called shocks or

innovations), and current and past values of other time series. The program code is showed below:

SAS System V8 Program Code:

```
proc arima data=work.raw;

   /*--- Look at the input process -------------------*/
   identify var=x nlag=10;
   run;

   /*--- Fit a model for the input -------------------*/
   estimate p=3;
   run;

   /*--- Crosscorrelation of prewhitened series ------*/
   identify var=output crosscorr=(input) nlag=10;
   run;

   /*--- Fit transfer function - look at residuals ---*/
   estimate input=( 3$ (1,2)/(1,2) x ) plot;
   run;

   /*--- Estimate full model -------------------------*/
   estimate p=1 input=( 3$ (1)/(1,2) x );
   run;
quit;
```

Assuming that, the model structure in transfer function form is:

$$Y(t) = \text{intercept} + (\text{num}/\text{den})^{*}X(t) \qquad (3.9)$$

The values of the numerator and the denominator are then obtained from SAS System program, when the driving signal is sine wave with frequency of 50Hz and amplitude of 3 volts :

num = [1 -1.2872 0.29768];

den = [7.56088 -7.5816 0.2708];

intercept = 0.901033

Rewriting the dynamic model using State Space Representation:

$$\dot{\boldsymbol{X}} = \boldsymbol{AX} + \boldsymbol{Bu}$$

$$\boldsymbol{Y} = \boldsymbol{CX} + \boldsymbol{Du}$$

where matrices A, B, C and D are:

$$\boldsymbol{A} = \begin{bmatrix} 1.2972 & -0.2977 \\ 1 & 0 \end{bmatrix} \qquad \mathbf{B} = \begin{bmatrix} \mathbf{1} \\ \mathbf{0} \end{bmatrix}$$

$$\boldsymbol{C} = \begin{bmatrix} 2.1628 & -1.9827 \end{bmatrix} \qquad \boldsymbol{D} = 7.5615$$

respectively. Then eigenvalues λ of matrix A is being checked.

$$\lambda > 0$$

So, this plant is unstable. Then the controllability and observability of the A matrix are checked. The result indicates it is controllable and observable.

Rearranging the matrix form into differential equations, the plant becomes:

$$\dot{x}_1 = 1.2972x_1 - 0.2977x_2 + u$$

$$\dot{x}_2 = x_1$$

$$y = 2.1628x_1 - 1.9827x_2 + 7.5615u \qquad (3.10)$$

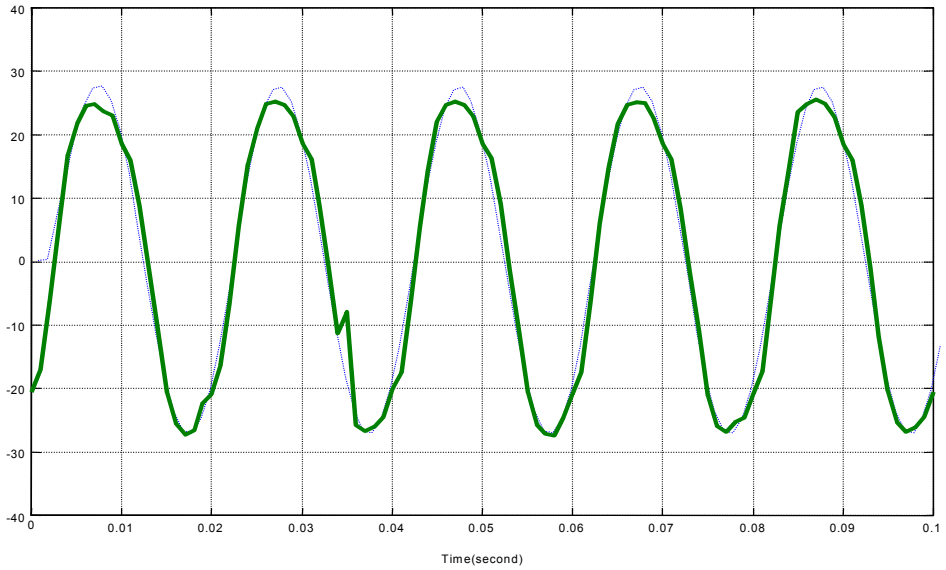

Figure 3.4: Model Simulated Output (dashed line) vs. Actual Output (bold line)
X axis – time (sec); Y axis – displacement (micron)
Reference input: Sine wave; Amplitude: 3V; Frequency: 50Hz

Figure 3.4 shows the comparison between the model simulated output and the actual measured output. The model simulated output matches the actual output very well. The tracking error is acceptable if it is compared with the amplitude of the output signal. Therefore, this second order dynamic model is more accurate from the simulation results. This model will be applied in the controller design and experiments implementation in *Chapter IV* and *Chapter V*, to verify the validity of the model in practical applications.

Reference:

1. R. Venkataraman, P.S Krishnaprasad, “A Model for a Thin Magnetostrictive Actuator,” Technical Research Report, University of Maryland, College Park, 1998.

2. R. Venkataraman, P.S Krishnaprasad, “Characterization of an ETREMA MP 50/6 Magnetostrictive Actuator,” Technical Research Report, University of Maryland, College Park, 1998.

3. A.Adly, I. Mayergoyz and A. Bergqvist, “Preisach modeling of magnetostrictive hysteresis,” Journal of Applied Physics, 69(8), pp.5777-79, 1991.

4. J. B. Restorff, H.T. Savage, A.E. Clark and M. Wunfogle, “Preisach modeling of hysteresis in Terfonol,” J. Appl. Phys., 67(9), pp 5016-18, 1996.

5. D. Jiles and D. Atherton, “Ferromagnetic hysteresis," IEEE Transactions on Magnetics, vol. MAG-19, pp. 2183{2185, September 1983.

6. D. Jiles and D. Atherton, “Theory of ferromagnetic hysteresis," Journal of Magnetism and Magnetic Materials, vol. 61, pp. 48, 1986.

7. V. Basso and G. Bertotti, “Hysteresis models for the description of domain wall motion,” IEEE Trans. Magn. 32(5), pp.4210-12, 1996.

8. Ralph C. Smith, “A Nonlinear Optimal Control Method for A Magnetostrictive Actuators, Journal of Intelligent Material System and Structures,” Vol.9, pp. 468-486, June 1998.

9. Gutierrez, H. M. and Ro, P. I., "Sliding-mode control of a nonlinear-input system: application to a magnetically levitated fast-tool servo," IEEE Trans. on Ind. Elec., vol.45, no.6, pp. 921-927, 1998.

10. J.-J. E. Slotine and W. Li, “Applied Nonlinear Control,” Prentice Hall, 1991.

11. SAS/ETS Software: “Applications Guide 1,” SAS Institute, 1985.

12. SAS/ETS V8 User's GUIDE: “PROC ARIMA CHAPTER,” SAS Institute, 1985.

13. W. Gao and J.C. Hung, “Variable Structure Control of Nonlinear System: A New Approach,” IEEE Trans. Ind. Electronics, pp.45-55, vol.40, 1993.

Chapter IV

Controller Design for the Magnetostrictive Actuation System

4.1 Introduction

As depicted in *Chapter I*, the alloy Terfenol-D inherently owns some exceptional magnetomechanical properties and provides a great potential for a variety of transducer and actuator applications. That potential is now being implemented with the development of linear and rotary actuators. However, such devices usually require advanced instrumentation to implement servo-controlled loops, for example, in the case of linear micropositioning and active vibration control [1]. The performance of a magnetostrictive actuator is very nonlinear at modest or high drive level and its open loop actuation performance is not satisfactory if high precision is the interest [2]. Therefore, it's necessary to develop a proper controller to reduce the tracking error and obtain better close-loop actuation performance. In *Chapter III,* a time-delay model and a second order dynamic model have been established. These two models will be applied in the close-loop control.

Researchers had modeled the magnetostrictive actuator using the Finite Element Analysis approach [3]. Another model proposed by R. Venkataraman and P.S.

Krishnaprassad is a bulk and low dimensional model [6]. This model accounts for magnetic hysteresis, eddy current effects, magneto-elastic effects, inertial effects, and mechanical damping. From the viewpoint of control, nonlinear model-based control and optimal control methods have been tried [2, 7]. R D Greenough gave a variable structure control approach for the magnetostrictive actuator system [8]. J. M. Nealis and R. C. Smith developed a model reference adaptive control (MARC) for magnetostrictive transducers operating at fixed, high frequency condition [15, 20]. Due to the existence of the nonlinearities and saturations in the magnetostrictive actuator, the experimental results from these approaches are not very satisfactory so far. In this project, a new modeling method and control approach will be proposed and verified through experiments.

Figure 4.1 shows the block diagram for implementing close-loop control. The optical sensor incorporated with the Angstrom Resolver will observe the actuation displacement driven by the voltage signal from the PWM signal amplifier. Then the signal from the Angstrom Resolver is directed to the data acquisition board (DSP board), which communicates with the computer. The DSP board will convert the analog signal into the digital value used by the computer. The computer then generates a digital control command obtained from the control algorithm to the D/A part of the DSP board. This command will be output to the PWM amplifier in analog form, i.e. in voltage. Thus, all the components in *Figure 4.1* form a close-loop control system for the magnetostrictive actuator.

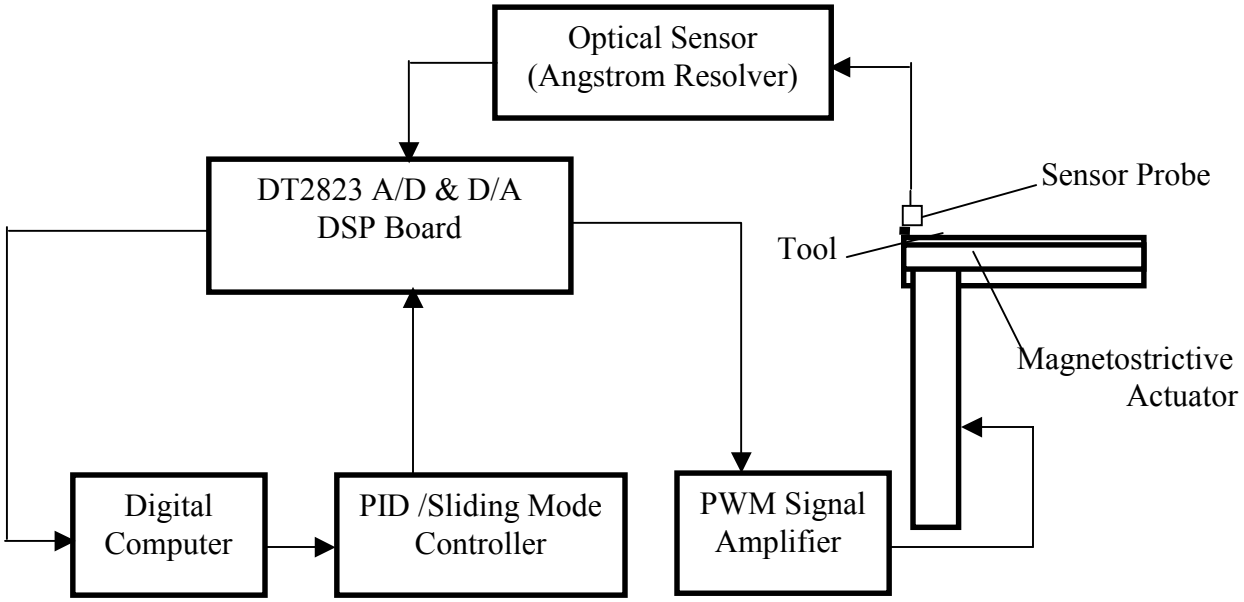

Figure 4.1 Close-loop Control Experiment Block Diagram

In order to simplify the modeling and control problem, 50Hz is chosen as the working frequency for the actuator since the actuator shows quasi-linear property at this frequency and 50Hz is often used in applications such as machining.

4.2 PID Controller Design

PID is a classic control algorithm in industry. PID control, namely, proportional, integral and derivative control, is a traditional and effective close-loop controller for many mechanical and electrical systems. The main advantage of PID control is that it can be done without having a very accurate model of the controlled system itself. Instead, tuning the control gain is a trial and error procedure. Since the model of a

magnetostrictive actuation system is neither perfectly known nor accurate, the PID controller is tested first to obtain close-loop performance without having an accurate model.

PID control is an error driven control approach. The ideal PID controller written in the continuous time domain form is:

$$u(t) = Kp + Ki\int_0^t e(t)dt + Kd\frac{de(t)}{dt} + u_0 \qquad (4.1)$$

Where *Kp, Ki* and *Kd* are the proportional, integral, and derivative control gain, respectively, e(t) is the error, defined as the difference between the desired displacement and the measured displacement at a specific time t, and $\boldsymbol{u}_0$ is the initial value of the control input. With $\boldsymbol{u}(\boldsymbol{t})$ as the current control input. *Kp, Ki* and *Kd* can be tuned properly to get optimized close-loop performance. *Table 4.1* illustrates the correlation among parameters *Ki, Kp* and *Kd* and the control performance.

Close-loop Response	***Rise Time***	***Overshoot***	***Setting Time***	***Steady State Error***
Kp	Decrease	Increase	Small Change	Decrease
Ki	Decrease	Increase	Increase	Eliminate
Kd	Small Change	Decrease	Decrease	Small Change

Table 4.1: Correlation between PID Parameters and Performance

Because *Kp*, *Ki*, and *Kd* are dependent of each other, these correlations may not be exactly as listed above. In fact, changing one of these variables will change the effect of the other two. For this reason, Table 4.1 is only a reference when the values of *Ki*, *Kp*, and *Kd* are determined.

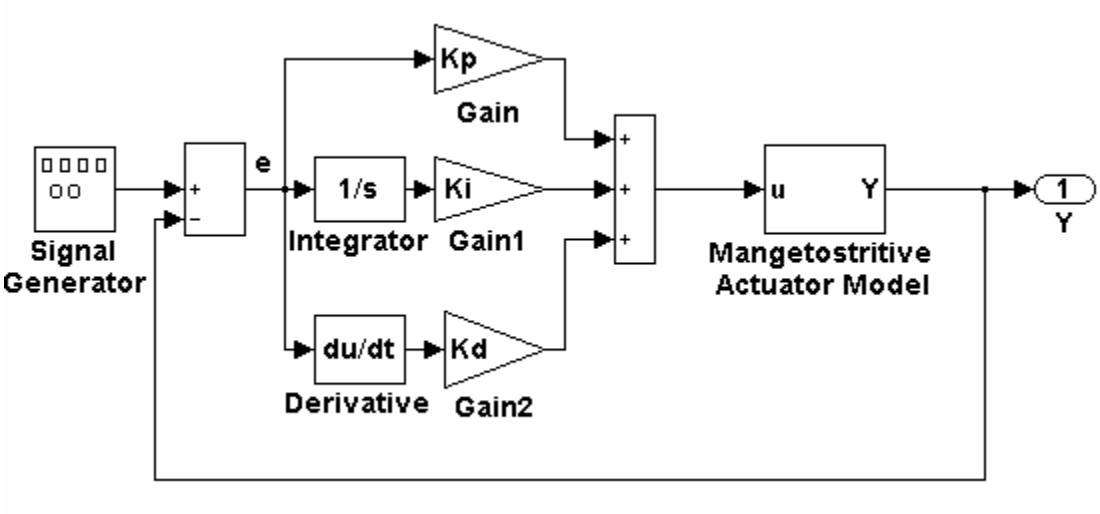

Figure 4.2: Structure of the PID Controller

Figure 4.2 illustrates the structure of this PID controller. In order to implement the PID controller for the magnetostrictive actuator with a DSP board, it needs to be discretized. This is to approximate the integral and the derivative terms to the format suitable for computation by a digital computer. From a numerical point of view, the error is defined as:

$$e(t) = Yd - Ym \tag{4.2}$$

Where *e(t)* is the error between the value of the desired displacement, *Yd* and the displacement value measure *Ym*. The output of PID controllers will change in response to a change in the measured displacement.

Integral control

With integral action, the controller output is proportional to the amount of time the error is present. Integral action eliminates offset. The response is somewhat oscillatory and can be stabilized somewhat by adding derivative action.

Integral action gives the controller a large gain at low frequencies that results in eliminating offset and "beating down" load disturbances. The controller phase starts out at -90 degrees and increases to near 0 degrees at the break frequency. Derivative action adds phase lead and is used to compensate for the lag introduced by integral action.

Derivative control

With derivative action, the controller output is proportional to the rate of change of the measurement or error. The controller output is calculated by the rate of change of the measurement with time.

Derivative action can compensate for a change in measurement. Thus, derivative action inhibits more rapid changes of the measurement than proportional action. When a load or set-point change occurs, the derivative action causes the controller gain to move in the wrong direction when the measurement gets near the set-point. Hence, derivative action is often used to avoid overshooting.

In addition, derivative action can stabilize loops since it adds phase lead. Generally, if derivative action is applied, more controller gain and reset can be used. With a PID controller the amplitude ratio now has a dip near the center of the frequency response. Integral action gives the controller high gain at low frequencies, and derivative action causes the gain to start rising after the "dip." At higher frequencies the filter on derivative action limits the derivative action. If the controller had no filter the controller amplitude ratio would steadily increase at high frequencies up to the Nyquist frequency, which is equal to half the sampling frequency. The controller phase now has a hump due to the derivative lead action and filtering. The time response is less oscillatory than with the PI controller. Derivative action has helped stabilize the closed control loop.

4.2.1 PID control using time-delay model

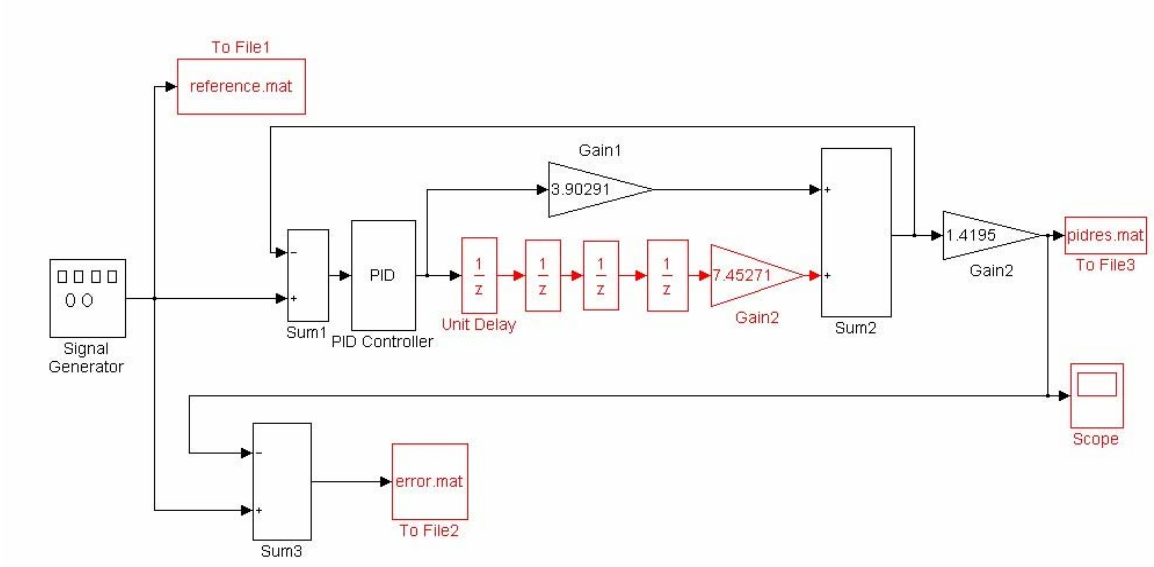

Figure 4.3: PID Control Simulated Diagram Using Time-Delay Model

Figure 4.3 illustrates the PID control layout using the time-delay model. In the simulation program, the time-delay model is included because a controlled object or plant is a necessity. But when the actual experiment is conducted, the model part does not exist.

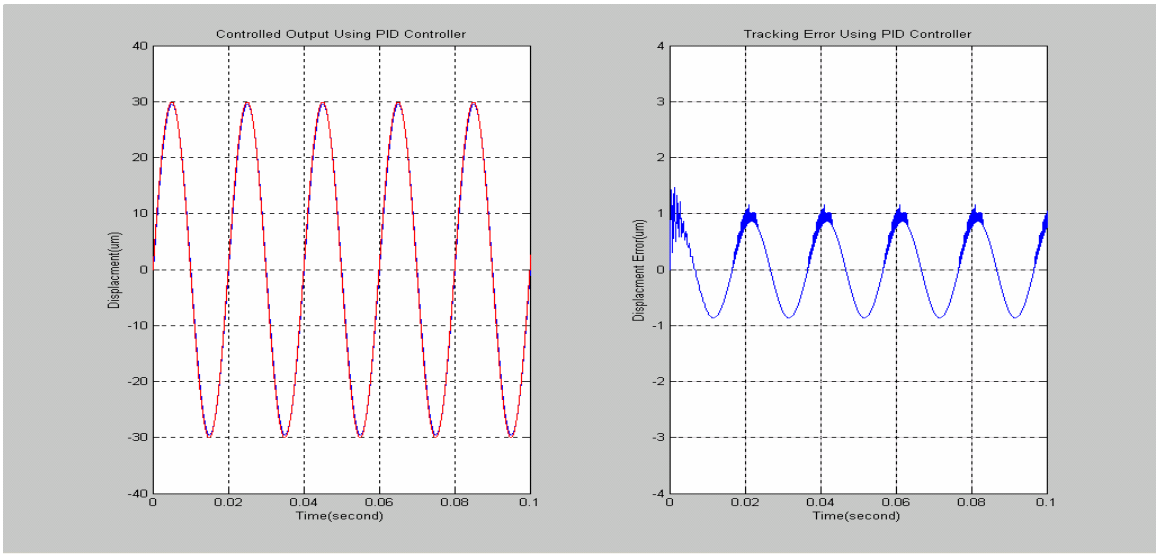

Figure 4.4: Simulated Results using PID Controller
Desired Trajectory: Amplitude: 30 microns; Frequency: 50Hz
$Kp = 0.2$, $Ki = 0.010$, $Kd = 0.0$

Figure 4.3 above demonstrates the simulated results using PID control. The desired trajectory is a sinusoid wave with amplitude of 30 microns and frequency at 50Hz. The right plot in *Figure 4.3* shows the tracking error. There is an overshooting at first. Then the tracking error keeps oscillating in a sinusoid wave shape with the same frequency as the desired trajectory. And its amplitude stays at about 1 micron level. The error accounts for up to 3% of the amplitude of the desired trajectory. It is not a negligible error. Therefore, the PID controller gains need to be adjusted gradually by trial and error.

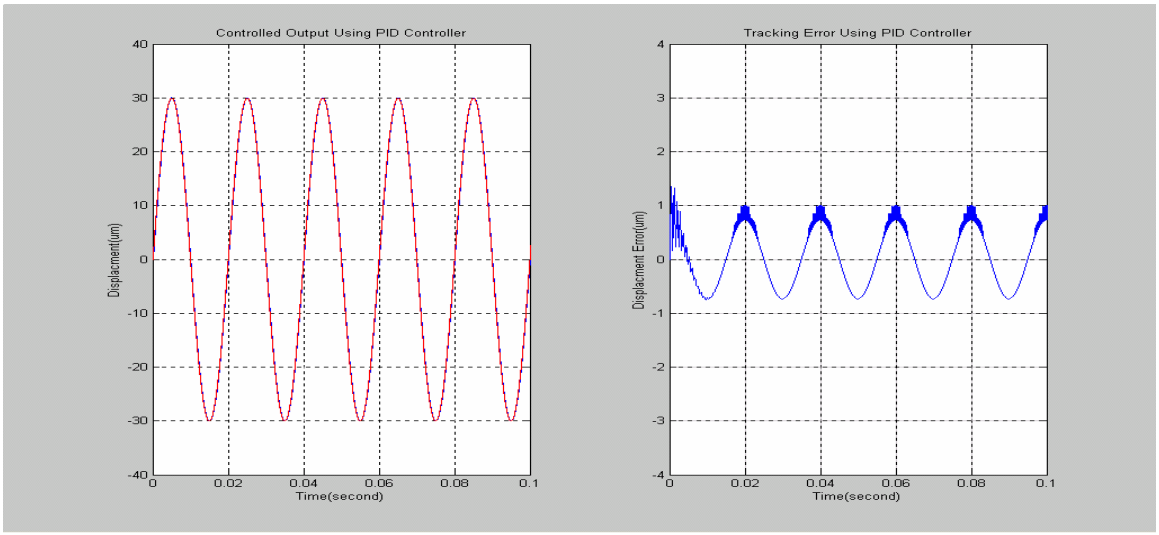

Figure 4.5: Simulated Tracking Performance Using PID Controller
Desired Trajectory: Amplitude: 30 microns; Frequency: 50Hz
Kp = 0.21, Ki = 0.0, Kd = 0.0

In *Figure 4.5*, *Ki* and *Kd* are set to 0. Then the PID control becomes a simple P (proportional) control. But the simulated results are very similar. The tracking error is as large as 0.9 micron, and a noise signal appears prominently at the peak part of the sinusoid wave.

After adjusting the PID parameters for many trials, the tracking performance using the time-delay model didn't show much improvement. The main reason is that this model is not accurate enough and its structure is too simple. It doesn't include any nonlinearity. This implies that the nonlinear magnetostrictive actuation system requires a more complicated model. In addition, advanced control strategies other than PID control are in consideration in order to obtain robustness.

4.2.2 PID control using second order dynamic model

In this section, the second order dynamic model is applied in the control simulation program. *Figure 4.6* outlines the PID control for the magnetostrictive actuator. The actuator model is simplified as a subsystem (plant) in *Figure 4.6*, and its structure is shown in *Figure 4.7*.

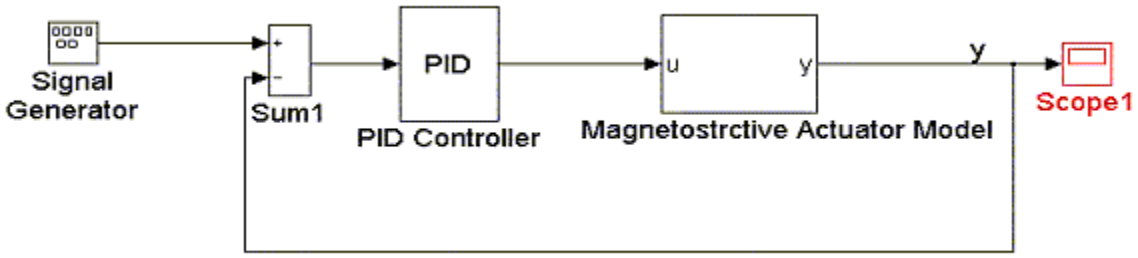

Figure 4.6: PID Control Simulation Diagram Using Second Order Dynamic Model

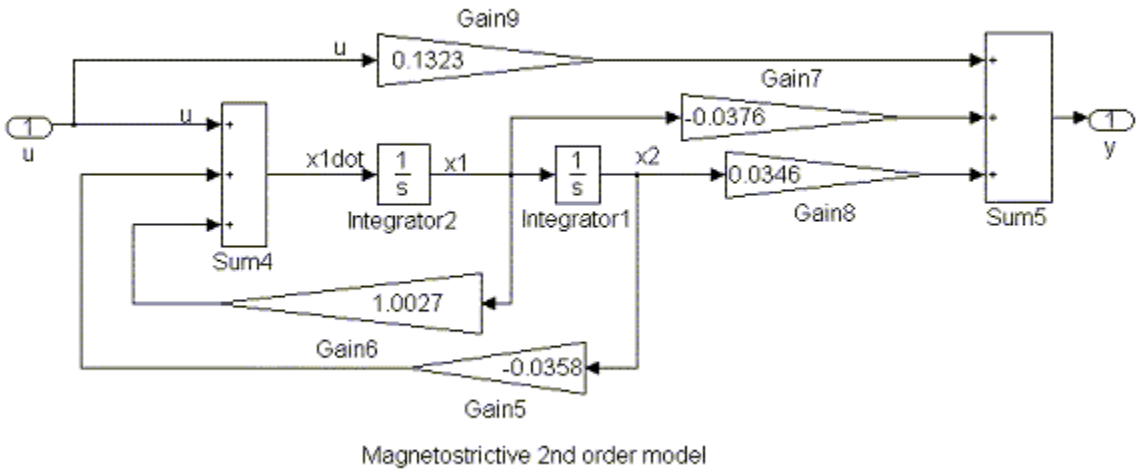

Figure 4.7: Structure of the Second Order Dynamic Model

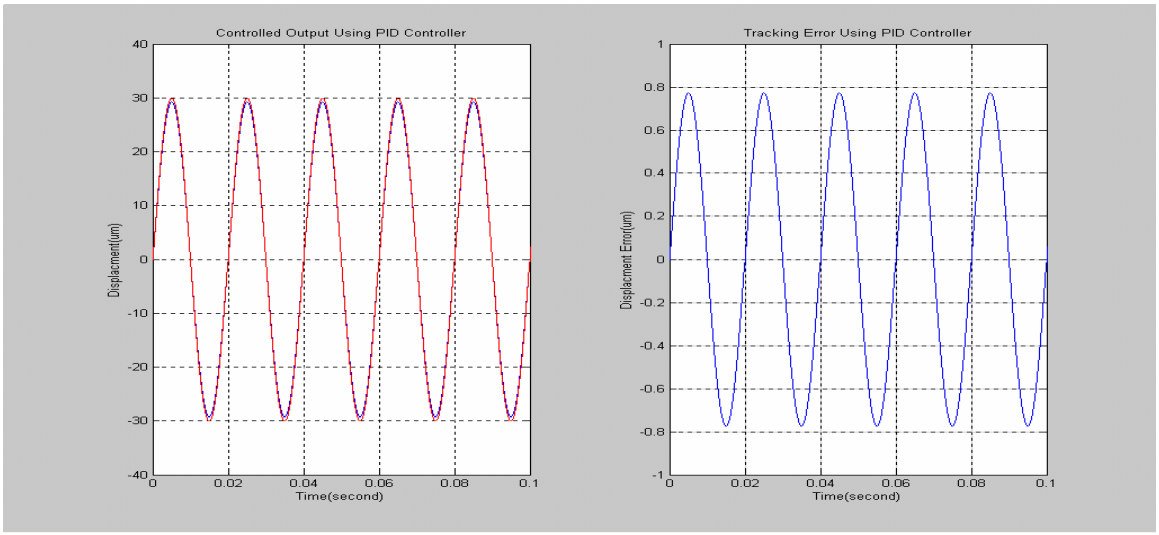

Figure 4.8: Simulated Tracking Performance Using PID Controller
Desired Trajectory: Amplitude: 30 microns; Frequency: 50Hz
Kp = 5.0, Ki = 0.0, Kd = 0.00001

If compared with simulated results from *Figure 4.4* or *Figure 4.5*, it is noticed that the amplitude of the tracking error in *Figure 4.8* has been reduced roughly from 1 to 0.8 micron range. By further adjusting *Kp,* the tracking error becomes even smaller in *Figure*

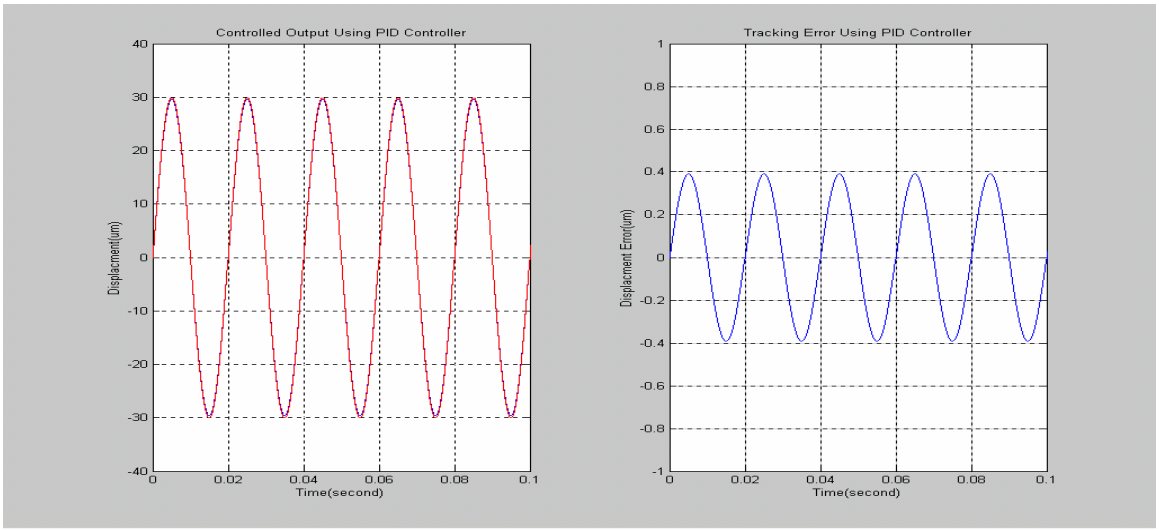

Figure 4.9: Simulated Tracking Performance Using PID Controller
Desired Trajectory: Amplitude: 30 microns; Frequency: 50Hz
Kp = 10.0, Ki = 0.0, Kd = 0.0001

4.9 and *Figure 4.10*. In addition, overshooting disappears and the tracking trajectory becomes very smooth. Certainly, different models will yield different tracking performances for the same system, even using the same control technique.

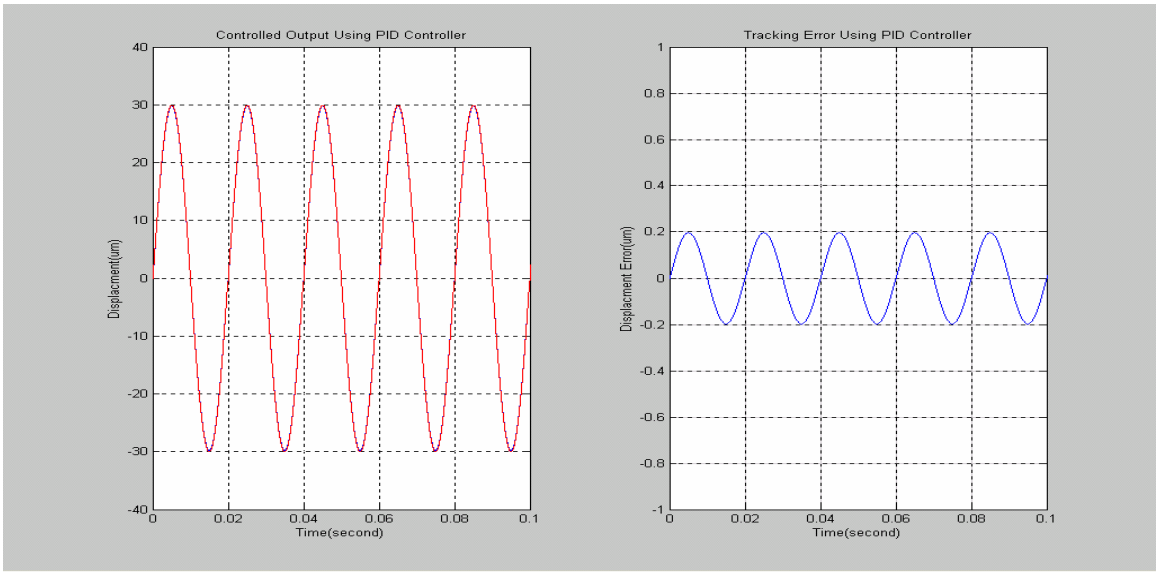

Figure 4.10: Simulated Tracking Performance Using PID Controller
Desired Trajectory: Amplitude: 30 microns; Frequency: 50Hz
Kp = 20.0, Ki = 0.0, Kd = 0.0001

By more trial and error, the tracking error using PID control can be reduced to 0.01 micron as shown in *Figure 4.10*. This error takes up to 0.067% of the amplitude of the desired displacement. Hence, the tracking performance is fairly acceptable.

Generally, the tracking errors using the second order dynamic are much smaller compared with those using the time-delay model. Since tracking error is one main index to assess modeling performance, this second order dynamic model is a more accurate and effective model, compared with the time-delay model.

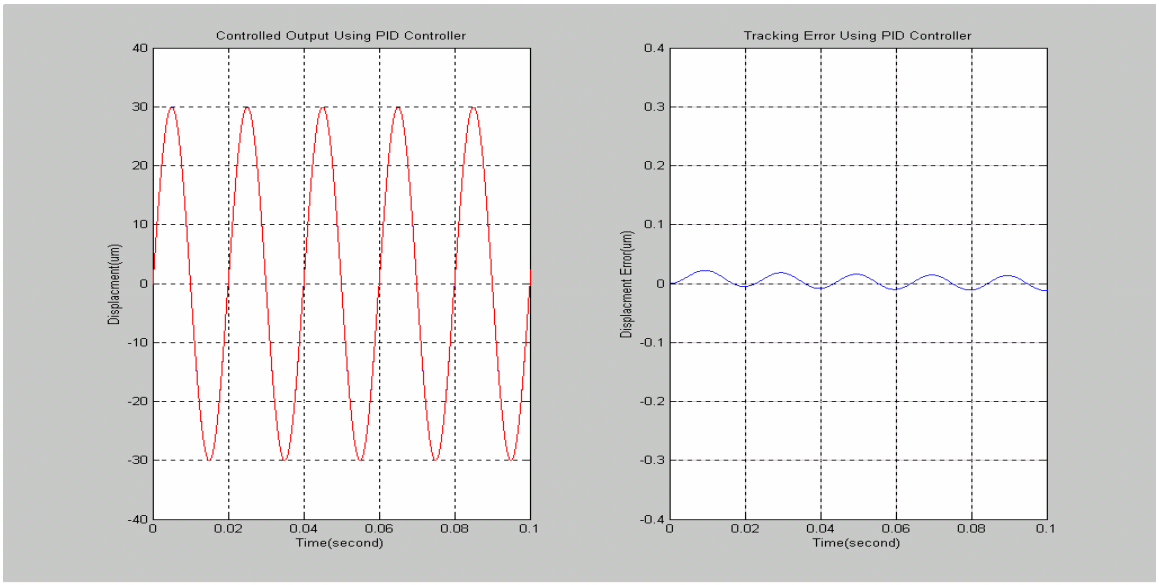

Figure 4.11: Simulated Tracking Performance Using PID Controller
Kp = 25.0, Ki = 5.0, Kd = 1.0

The tracking error does not, however, converge to zero due to the limitation of the PID control algorithm. In general, PID control is more applicable in a linear system. For this nonlinear magnetostrictive actuation system, a more advanced and robust control technique is very necessary. For this reason, the sliding mode controller is then presented in the next section.

4.3 Observer Design

The dynamic model obtained here has two states and both states are not measurable. In order to apply this model in sliding mode control, a states observer is constructed to approximate the two states.

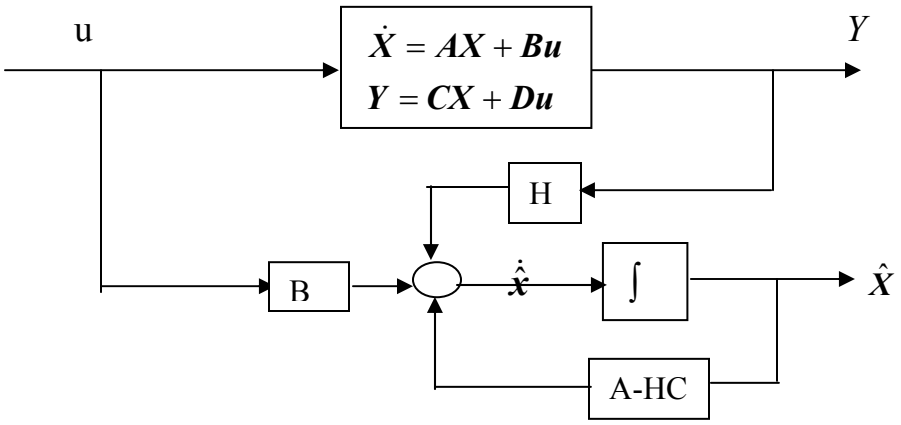

Figure 4.12: Block Diagram for the States Observer

Assume the states of the original system are not measurable and the output Y is measurable. This is the situation in the dynamic model for the magnetostrictive system. In *Figure 4.12*, the structure of the states observer is shown. With a feedback matrix gain H, the output Y combined with matrix B and (A-HC), forms the basic scheme of this states observer. The output $\hat{X}$ from this second order states observer then approximates the dynamics of the two states in the original system [17].

For the observer, its eigenvalues are set to some negative values to guarantee stability. For example, if:

$$\lambda_1 = \lambda_2 = -5$$

Then:

$$|\lambda I - (A - HC)| = |\lambda I - A + HC|$$

$$= \left| \begin{vmatrix} \lambda & 0 \\ 0 & \lambda \end{vmatrix} - \begin{bmatrix} 1.2872 & -0.2977 \\ 1.0 & 0 \end{bmatrix} + \begin{bmatrix} 2.1628h_1 & -1.9827h_1 \\ 2.1628h_2 & -1.9827h_2 \end{bmatrix} \right|$$

$$= \begin{vmatrix} \lambda - 1.2872 + 2.1628h_1 & 0.2977 - 1.9827h_1 \\ -1 + 2.1628h_2 & \lambda - 1.9827h_2 \end{vmatrix}$$

$$= \lambda^2 + (2.1628\boldsymbol{h}_1 - 1.9827\boldsymbol{h}_2 - 1.2872)\lambda + (2.5521\boldsymbol{h}_2 - 0.6439\boldsymbol{h}_2 - 1.9827\boldsymbol{h}_1 + 0.2977)$$

$$(2.1628h_1 - 1.9827h_2 - 1.2872) = 10$$

$$(2.5521\boldsymbol{h}_2 - 0.6439\boldsymbol{h}_2 - 1.9827\boldsymbol{h}_1 + 0.2977) = 25$$

$$\boldsymbol{h}_1 = 386.86$$

$$\boldsymbol{h}_2 = 359.86$$

$$\hat{A} = A - HC = \begin{bmatrix} -777.018 & 713.1923 \\ -835.70 & 767.027 \end{bmatrix}$$

Eigenvalues of matrix $\hat{\boldsymbol{A}}$ are being checked. Both eigenvalues are negative. So the observer plant is stable.

The states observer is expressed as:

$$\dot{\hat{X}} = (A - HC)\hat{X} + HY + Bu \tag{4.3}$$

or in matrix form:

$$\begin{bmatrix} \dot{\hat{\boldsymbol{x}}}_1 \\ \dot{\hat{\boldsymbol{x}}}_2 \end{bmatrix} = \begin{bmatrix} -777.018 & 713.1923 \\ -835.70 & 767.027 \end{bmatrix} \begin{bmatrix} \hat{\boldsymbol{x}}_1 \\ \hat{\boldsymbol{x}}_2 \end{bmatrix} + \begin{bmatrix} 359.86 \\ 386.86 \end{bmatrix} \boldsymbol{y} + \begin{bmatrix} 1 \\ 0 \end{bmatrix} \boldsymbol{u} \tag{4.4}$$

The structure of this states observer is provided in *Figure 4.13*. If the output *Y* and control input *u* in the original system are known, the two states of the observer can be obtained. The observer has the same error dynamics of the original plant. These two states will be used in the sliding mode controller design to approximate the two states. So the states are also named virtual states of the original control plant.

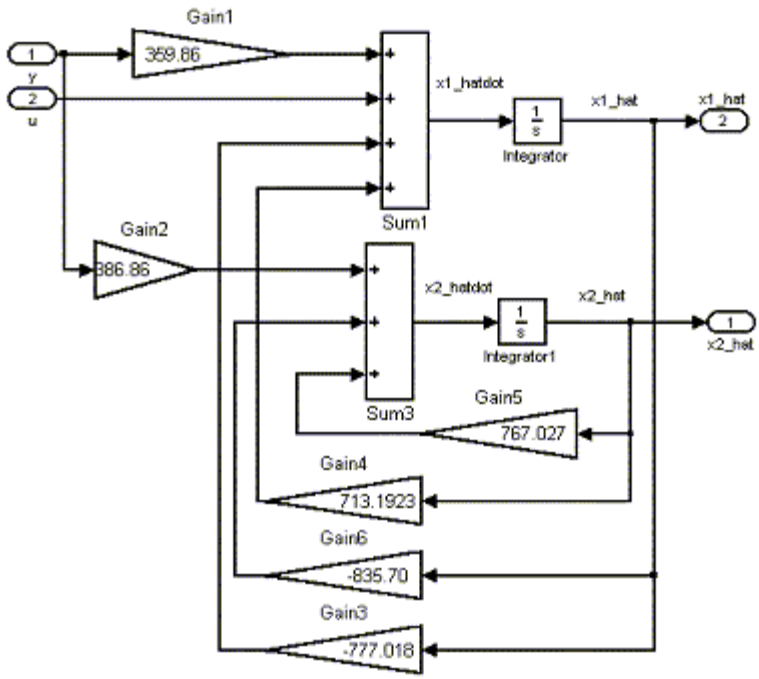

Figure 4.13 Structure of the States Observer

4.4 Sliding Mode Controller Design

Considering that the existence of nonlinearities and hysteresis in the magnetostrictive actuation system and that the PID control is proved not good enough, a robust control approach needs to be developed. Sliding mode control (SMC) is often served as a design tool for the robust control of linear and nonlinear systems [19]. There are three main advantages to using SMC. First, the dynamic structure of the plant is simplified and its order is reduced by the introduction of the switching function. Second, the closed-loop response becomes totally insensitive to system uncertainties and disturbances. This property makes SMC very attractive for robust control. It provides inherent order reduction, which often leads to decoupling and simplification of the design procedure and

direct incorporation of robustness. The third advantage to using SMC is that it makes possible the design of a high performance control system at a relatively low cost.

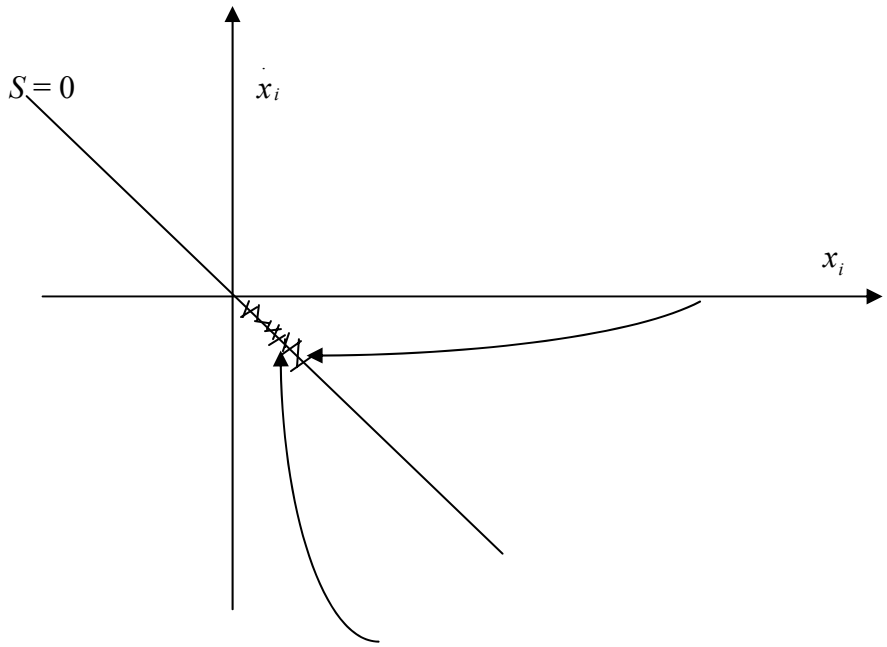

Figure 4.14: The Concept of Sliding Model Control Approach

Figure 4.14 illustrates the concept of sliding model control. Where *S* stands for the sliding surface, x_i is the state of the control plant. As shown in *Figure 4.14*, the chattering caused by the high rate switching activities is a typical issue in the sliding mode control approach.

This magnetostrictive actuator system has a second order dynamic model, demonstrated in *Chapter III*. As a conventional sliding mode control approach,

equivalent control is often applied in simple nonlinear control applications [18]. The sliding surface S is, actually, the equivalent first order system. S represents the performance of the feedback control. For example, if the magnetostrictive actuator keeps moving along the desired trajectory, then

$$S = 0 \tag{4.7}$$

is the perfect situation. However, in a real system, the existence of noise, disturbance, and model inaccuracy will cause tracking error.

Tracking error *e(t)* in sliding mode control is often defined as the difference between the desired state trajectory and the actual trajectory at time t. Also *e(t)* will be converged to zero if S is forced to keep on $S = 0$ surface. This is true in the case of a perfect situation. When the actuation trajectory is moving beyond the desired surface, the sliding surface S falls off the surface $S = 0$. The sliding mode control law is computed again based on the new value of S. The inverse control law with a restricted stability condition is given in such a way that S returns to the desired surface $S = 0$. Hence, this second order system still keeps its stability.

In the presence of modeling uncertainties, the inverting control law method has to be discontinuous. Specifically, the control law will reverse the sign as the sliding surface rides over zero. Even though the sliding surface returns back to the switching surface $S = 0$, it may not be constantly kept on the surface $S = 0$ in that the value of the control law is not known precisely. The value of S term could fall to the other side of surface $S = 0$. In which case, the control law is reevaluated. As a result, a good tracking performance of

sliding mode control will be compensated for by the high control activities. Therefore, sliding mode control often requires a fast pace operating system for the purpose of implementation. The fundamental conception on the conventional sliding mode control with a fixed switching gain is given by Slotine and Li [3].

For this magnetostrictive actuation system, the sliding switching surface *S* is defined as:

$$\boldsymbol{S} = \left(\frac{\boldsymbol{d}}{\boldsymbol{dt}} + 2\lambda + \lambda^2 \int \boldsymbol{dt} \right)^{\boldsymbol{n}-1} \boldsymbol{e} \tag{4.8}$$

where λ is a positive constant, n is a positive integer number, and e is the tracking error:

$$\boldsymbol{e} = \boldsymbol{x}_d - \boldsymbol{x}$$

where x_d and x are the desired state value and actual state value. *n* is 2 for this plant. Then Equation (4.8) changes into:

$$\begin{aligned} \boldsymbol{S} &= \left(\frac{\boldsymbol{d}}{\boldsymbol{dt}} + 2\lambda + \lambda^2 \int \boldsymbol{dt} \right) \boldsymbol{e} \\ &= \dot{\boldsymbol{e}} + 2\lambda \boldsymbol{e} + \lambda^2 \int \boldsymbol{e}\, \boldsymbol{dt} \end{aligned} \tag{4.9}$$

S has a second order error dynamic as represented in Equation (4.9).

Then, the states observer in *Section 4.2.1* is applied here since both states of this model are not measurable.

From Equation (4.4), equivalent control term *Ueq* is obtained:

$$\boldsymbol{y} = 2.1628\boldsymbol{x}_1 - 1.9827\boldsymbol{x}_2 + 7.5615\boldsymbol{u} \tag{4.10}$$

$$Ueq = (\boldsymbol{y} - 2.1628\boldsymbol{x}_1 + 1.9827\boldsymbol{x}_2) / 7.5615 \tag{4.11}$$

As pointed out by Slotine, a fixed-gain sliding mode control approach may not assure stability in the presence of parametric uncertainties and unmodeled nonlinear dynamics [8].

In order to guarantee the bounded sliding surface, the switching gain K needs to satisfy the stability condition

$$\frac{1}{2}\frac{d}{dt}S^2 = S\dot{S} \le 0 \tag{4.12}$$

To maintain S at zero, such that the actuator tracks the desired trajectory, the equivalent control law U_{eq} is introduced. The equivalent control law U_{eq} is estimated to achieve the condition

$$S = 0 \qquad \text{and} \qquad \dot{S} = 0 \tag{4.13}$$

The derivative of S is given as

$$\dot{S} = \ddot{e} + 2\lambda\dot{e} + \lambda^2 e \tag{4.14}$$

where

$$\dot{e} = \dot{x}_d - \dot{x} \qquad \text{and} \qquad \ddot{e} = \ddot{x}_d - \ddot{x}$$

then

$$U = U_{eq} + K\,\mathrm{sgn}(S) \tag{4.15}$$

where K is the switching gain, an arbitrary positive number that guarantees $S = 0$.

In experimental implementations, the measured data can be stored at each sampling period. Then the second derivative can be obtained by:

$$\ddot{x}(k) = \frac{\dot{x}(k) - \dot{x}(k-1)}{T} \tag{4.16}$$

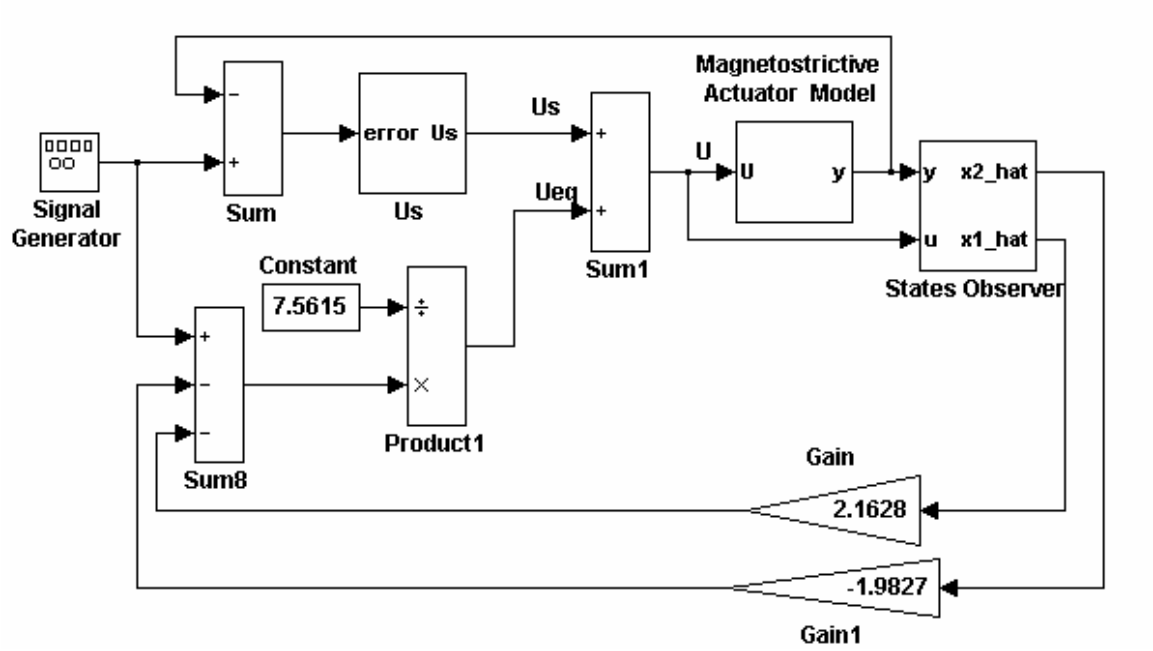

Figure 4.15: Sliding Mode Controller Block Diagram

Figure 4.15 shows the structure of this sliding mode controller.

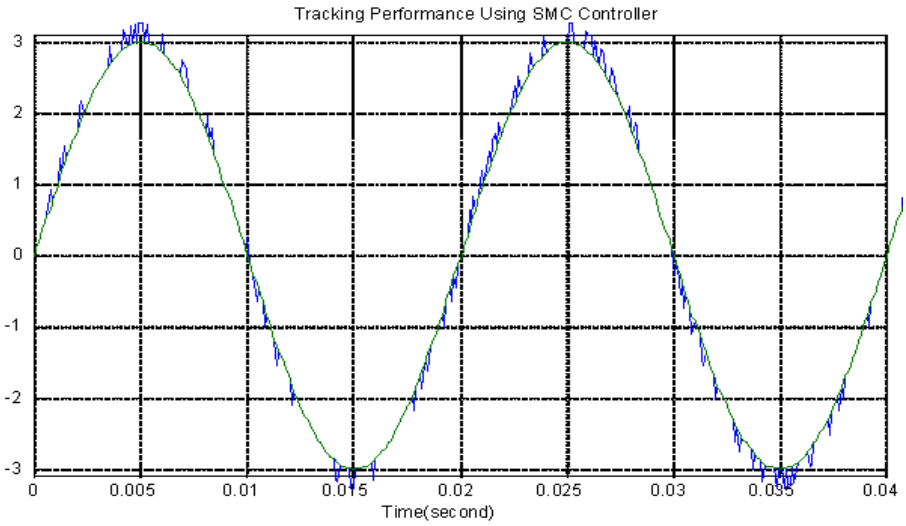

Figure 4.16: Tracking Performance Using Sliding Mode Controller and Second Order Dynamic Model, Switching Gain $K = 2$

In *Figure 4.16*, the simulated output using SMC follows the desired trajectory quite well. Obviously, chattering error always accompanies the simulated output trajectory at very high frequency. It inherently results from the sliding mode control algorithm itself or the finite switching frequency. The dynamic model is presumed perfectly accurate to represent the actual system. So, in the simulation program, there is no modeling error. The sliding mode control law will drive the trajectory oscillating up and down along the desired trajectory with high frequency switching activity.

As expected, the tracking performance using the sliding mode controller is much better compared with those results from the PID controller. *Figure 4.17* is one of the plots for the tracking error trajectory.

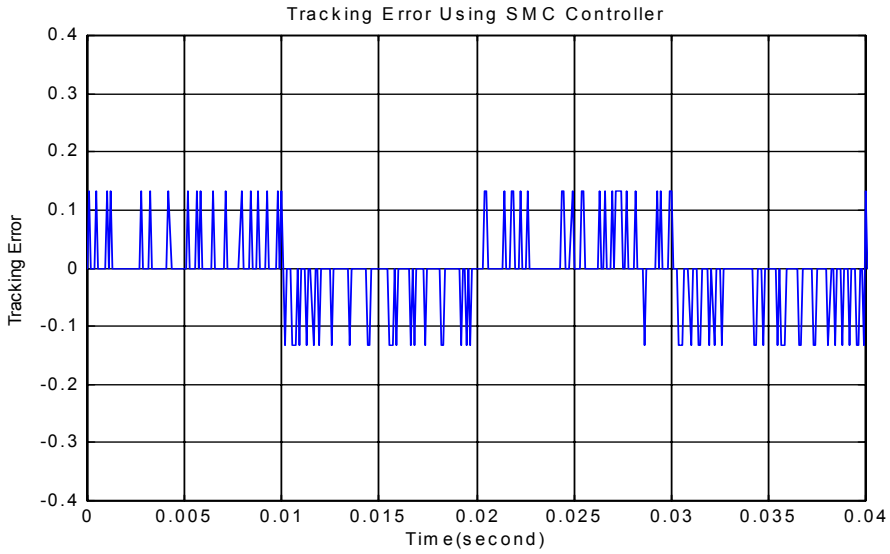

Figure 4.17: Tracking Error Using Sliding Mode Control and Second Order Dynamic Model

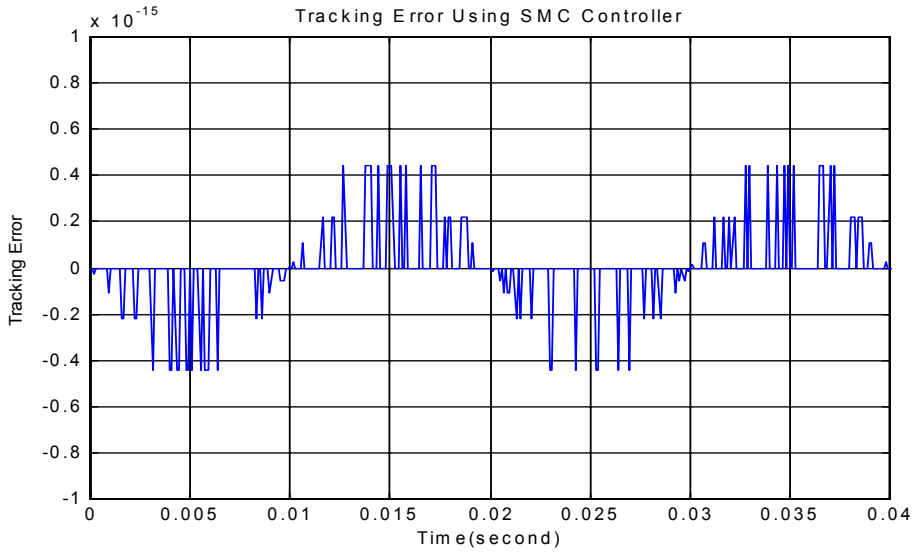

Figure 4.18: Tracking Error Using Pure Equivalent Control (K = 0.0)

Figure 4.18 shows the situation when a pure equivalent control term *Ueq* is applied in sliding mode control. This tracking error can be neglected. It is virtually zero. Tracking performance is improved since there is no disturbance or noise in this simulation program. However, in a real control application, the model is not known perfectly, and there exist many uncertain factors that will affect the results of control implementation.

4.4 Sliding Mode Control with Variable Switching Gain

A fixed switching gain may not be very practical due to strong nonlinearities of the magnetostrictive actuation system; a sliding mode control algorithm with variable switching gain is a possible solution. For the magnetostrictive actuation problem, where the actuator follows the desired trajectory x_d, the SMC approach is of interest. Displacement error e is given by

$$e(t) = x_d(t) - x(t) \tag{4.17}$$

The equivalent 1st order system, the surface S, is expressed in terms of an arbitrary constant λ and the tracking error e [8].

$$S = \left(\frac{d}{dt} + 2\lambda + \lambda^2 \int dt \right)^{n-1} e \tag{4.18}$$

Consequently, when the feedback algorithm is used to drive the actuator on the desired trajectory, the sliding surface S is retained at zero. If the actuator tip is off track, then the surface S takes on a value other than zero. As a result, sliding surface S represents the performance of feedback tracking motion control [5]. To maintain S at zero, such that the actuator tracks the desired trajectory, the equivalent control law U_{eq} is introduced. The equivalent control law U_{eq} is estimated to achieve the condition

$$S = 0 \qquad \text{and} \qquad \dot{S} = 0 \tag{4.19}$$

The derivative of S is given as

$$\dot{S} = \ddot{e} + 2\lambda\dot{e} + \lambda^2 e \tag{4.20}$$

where

$$\dot{e} = \dot{x}_d - \dot{x} \qquad \text{and} \qquad \ddot{e} = \ddot{x}_d - \ddot{x}$$

then

$$U = U_{eq} + K\,\mathrm{sgn}(S) \tag{4.21}$$

where K is the fixed switching gain; an arbitrary positive number that guarantees $S = 0$.

Equation (4.21) represents the control command in conventional sliding mode control. In order to apply a varying switching gain in sliding mode control, K must be a

variable varying with time, or *K (t)*. On the other hand, to guarantee the bounded sliding surface, the variable switching gain *K* must satisfy the stability condition [8].

$$\frac{1}{2}\frac{d}{dt}S^2 = S\dot{S} \le 0 \tag{4.22}$$

In practical implementations, the measured data can be stored at each sampling period, so the second derivative term can be expressed by

$$\ddot{x}(k) = \frac{\dot{x}(k) - \dot{x}(k-1)}{T} \tag{4.23}$$

Where *T* is a sampling period.

Suppose the nominal plant has the same structure as the established model without any disturbance, so that a nominal control term U_m can be obtained. Then the variable switching gain is chosen as:

$$\boldsymbol{K(t)} \ \geq \ \left|\boldsymbol{U} - \boldsymbol{U_m}\right| \tag{4.24}$$

The *Equation (4.24)* is rearranged as

$$\boldsymbol{K(t)} \ = \ \boldsymbol{a}\left|\boldsymbol{U} - \boldsymbol{U_m}\right| \tag{4.25}$$

where *a* is an arbitrary positive constant, $a \geq 1$, [2].

Thus, the modified sliding control law *U* is expressed as:

$$U(t) = U_{eq}(t) + K(t)\,\mathrm{sgn}\big(S(t)\big) \tag{4.26}$$

In discretized time domain, it can be implemented in the digital control environment as

$$U(k) = U_{eq}(k) + a\left|U(k-1) - U_m(k)\right|\mathrm{sgn}\big(S(k)\big) \tag{4.27}$$

where variable switching gain K is obtained from the difference of the preceding control law $U(k-1)$ and the nominal $U_m(k)$ to prevent an algebraic loop. This calculation should be performed at a high frequency to decrease side effects from delay.

Sliding mode control with variable switching gain expects to show the capability of compensating for the uncertainties and imprecise parameters of the dynamic model for the magnetostrictive actuation system.

Although a sliding mode controller incorporated with the dynamic model shows good tracking performance in simulation programs, in real implementation, noise and disturbance always occur and often affect or attenuate the actual performance. In addition the finite sampling frequency will cause chattering as expected. In order to verify the modeling validity and the close-loop controller performance, the sliding mode controller needs to be tested in experiment implementation. This topic and related contents will be discussed in the next chapter.

References:

1. Reenough R.D., Jenner A. G., and Wikinson A. J., “Machine, Actuators & Control,” pp67, ImechE. Seminar series, 1993.
2. W. Shim, and P. Ro, “Robust Friction Compensation of Submicron Positioning and Tracking for a Ball-screw Driven Slide System,” Precision Engineering, J. Int. Soc. Precision Eng. and Nanotech., vol. 24, no. 2, pp.160-173, April 2000.
3. Gutierrez, H. M. and Ro, P. I., "Sliding-mode control of a nonlinear-input system: application to a magnetically levitated fast-tool servo," IEEE Trans. on Ind. Elec., vol.45, no.6, pp. 921-927, 1998.
4. Slotine, “Sliding Controller Design for Non-linear Systems,” Int. J. Control, vol. 40, no. 2, pp.421-434, 1984.
5. M. Dunnigan et al., “Position Control of a Vector Controlled Induction machine using Slotine’s Sliding Mode Control Approach,” IEE Proc.: Elec. Power Appl., vol. 145, no. 3, pp.231-238, May 1998.
6. P. Korondi et al., “Sliding Mode based Disturbance Observer for Motion Control,” Proc. IEEE Conf. Decision and Contr., vol. 2, pp. 1926-1927, 1998.
7. A. Phillips, and M. Tomizuka, “Robust Wide-Range Controller using Multirate Estimation and Control for Velocity Reguation and Tracking,” Adv. Info. Storage and Proc. Sys. Amer. Soc. of Mech. Eng., vol. 1, pp 189-196, 1995.
8. J. Slotine, and L. Weiping, “Applied Nonlinear Control,” Prentice Hall, 1991.
9. S. Mitra, “Digital Signal Processing A Computer-Based Approach,” McGraw Hill Inc., 1998.

10. C.-L. Hwang, "Sliding mode control using time-varying switching gain and boundary layer for electrohydraulic position and differential control," IEE Proc.-Control Theory Appl. Vol. 143, No. 4, July 1996.
11. Kuo-kai Shyu, et al., "A Modified Variable Structure Controller," Automatica, Vol. 28, No. 6 pp. 1209-1213, 1992.
12. S.S.GE, et al., "Adaptive Control of non-affine Nonlinear Systems Using Neural Networks," Proceedings of the 15th IEEE International Symposium on Intelligent Control (ISIC 2000), July 2000.
13. G. Monsees, et al., "Adaptive Switching Gain for a Discrete-Time Sliding Mode Controller," Proceedings of the American Control Conference, Chicago, Illinois, June 2000.
14. Sarah Spurgeon and Raymond Davis, "A nonlinear Design Approach for Sliding Mode Control Systems," Proceedings of the 32nd Conference on Decision and Control, San Antonio, Texas, December 1993.
15. Ralph C. Smith, "A Nonlinear Model-Based Control Method for Magnetostrictive Actuators," Proceedings of the 36th Conference on Decision and Control, San Diego, California, USA, December 1997.
16. Ralph C. Smith, "Partial and Full Inverse Compensation for Hysteresis in Smart Material Systems," Proceedings of the American Control Conference, Chicago, Illinois, June 2000.
17. Brogan, "Modern Control Theory," Prentice Hall, 1991.
18 V. I. Utkin, "Sliding Modes in Control Optimization," Springer-Verlag, 1992.

19 K. David Young, V. I. Utkin, Umit Ozguner, “A Control Engineer’s Guide to Sliding Mode Control,” 1996 IEEE Workshop on Variable Structure Systems, 1996.

20 J. M. Nealis and R. C. Smith, “An Adaptive Control Method for Magnetostrictive Transducers with Hysteresis,” pp. 4260-65, Proceedings of the 40th IEEE Conference on Decision and Control, Orlando, Florida USA, December 2001.

Chapter V

Experiments and Analysis

5.1 Experiment Setup and Sensor Calibration

5.1.1 Selection of Sensor

The experiments conducted in this chapter aim to explore the features of the magnetostrictive actuator, such as hysteresis and nonlinearities. And, the open loop and close-loop control performance using PID and sliding mode controllers are investigated. Researchers have used LVDT as the sensor to measure the displacement of the magnetostrictive actuator [1]. The actuation displacements of the actuator, in the order of microns, are measured with an optical sensor here. This optical sensor, though, is extremely sensitive and difficult to calibrate. For this reason, the calibration of the optical sensor based measurement system is done first.

The instrument used here for experiments is called the Angstrom Resolver, manufactured by Opto Acoustic Sensors at Cary, NC. The Angstrom Resolver is an optical fiber based, non-contacting with high frequency and high resolution surface motion, electric-optical transducer measuring system. The main features of this optical sensor that make it attractive for measuring the magnetostrictive actuation displacement are:

1. **Frictionless Measurement**

There is no physical contact between the sensor tip and the actuator surface. This is very desirable when vibration exists. Because it is non-contacting, there is no wear or change in performance after the experiments have been run for a long time.

2. High resolution and repeatability

The minimal displacement this optical sensor can detect is as small as one nano-inch, or 2.54 x 10^{-11} meter.

3. High bandwidth

The bandwidth of the optical sensor is from DC signal to 1 MHz level. It fully covers the actuator operation frequency range.

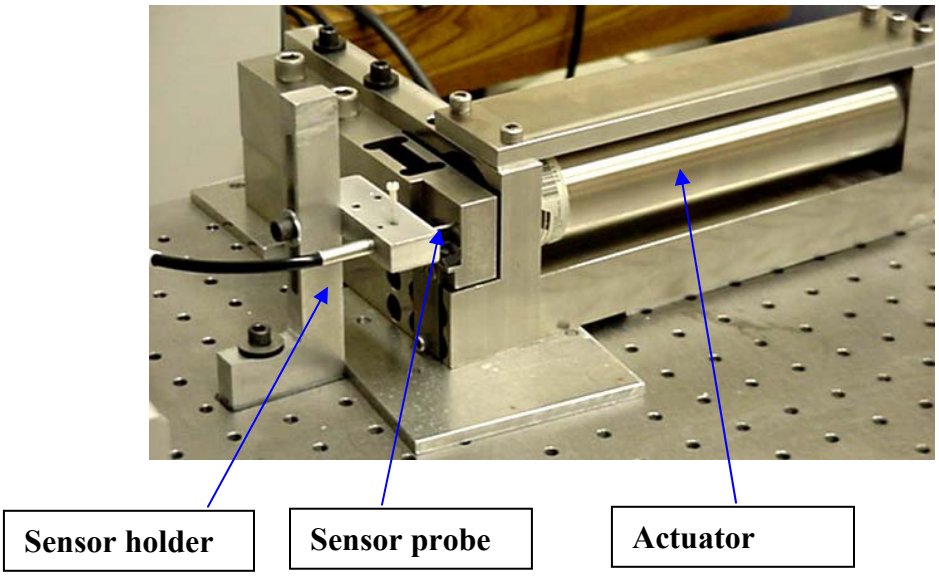

Figure 5.1: Optical Sensor and Magnetostrictive Actuator with Clamps

4. Sensitive direction

An optical fiber is predominantly sensitive to the effects of axial core motion and relatively insensitive to radial core motion. This is ideal for the measurement of the axial actuation displacement.

5.1.2 Sensor Calibration

Since the reflection rate of the optical sensor varies with the different surfaces being measured, prior to starting the measurement and experiments, it's necessary to calibrate the optical sensor on the surface of the magnetostrictive actuator. The set-up for the sensor calibration is shown in following picture:

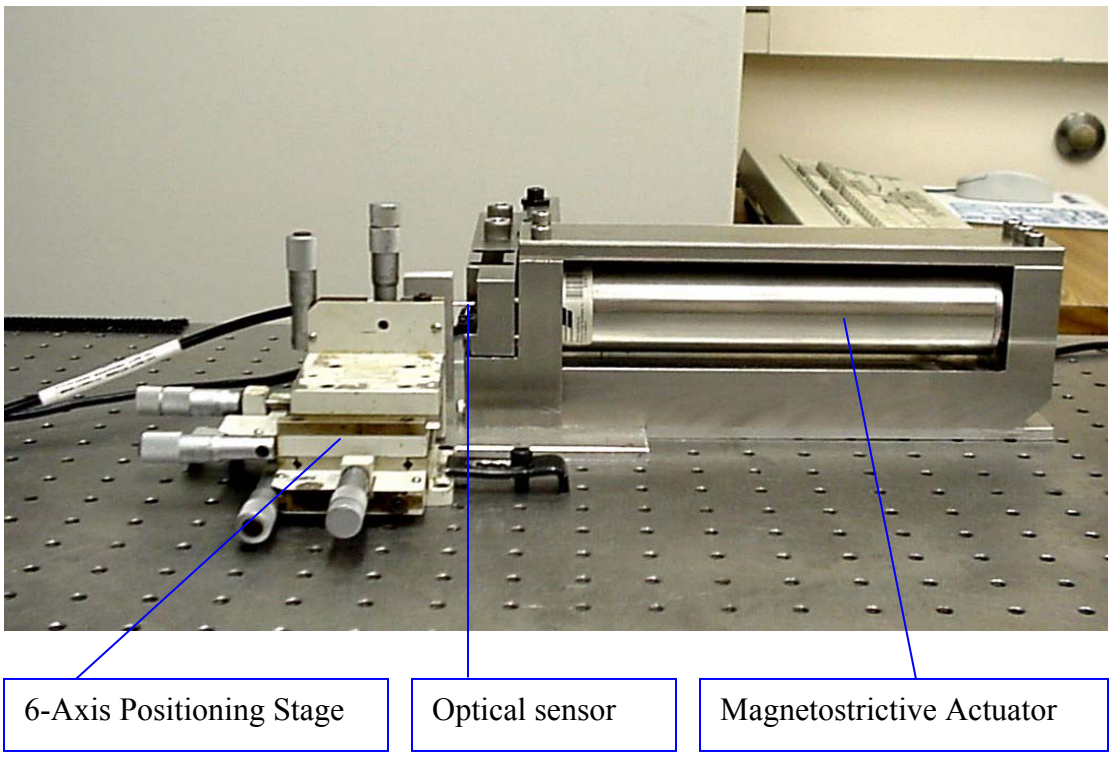

Figure 5.2: Sensor Calibration Experiment Setup

Using a 6-axis positioning stage as the fixture for the sensor, the surface of the tip of the sensor probe can be adjusted to parallel the surface of the actuator where it will be measured for displacement. For every step, the procedures are:

1. Turning the scale knob, moving the sensor 0.25 mill-inch one step along the axial direction of the actuator.
2. Reading the value (in voltage) on the LCD display from the Angstrom Resolver.

3. Repeating *Step1* through *Step 3* three times.

4. Averaging the three reading series as the final reading.

Thus, the sensor calibration ratio, or sensitivity gain of this optical sensor is obtained and the results are showed in *Figure 5.3*.

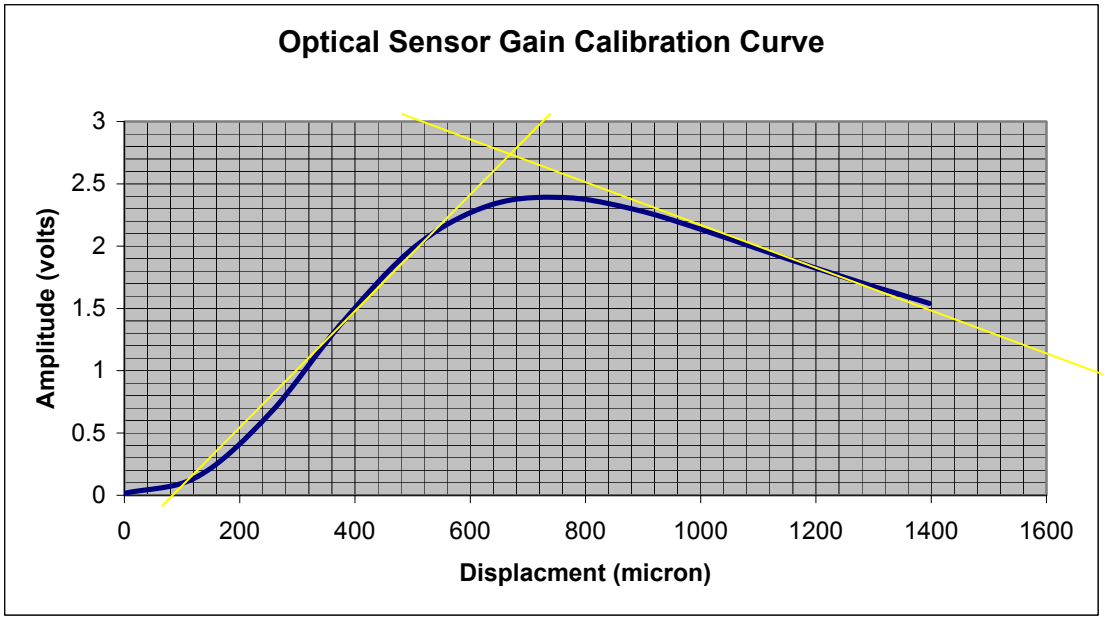

Figure 5.3: Angstrom Resolver Sensor Probe Calibration Curve

Note: 1. Sensitivity ratio for the front slope = 217.800 micron/mv
2. Sensitivity ratio for the back slope = 1434.074 micron/mv

As seen in *Figure 5.3*, there are two nearly linear sections on this optical sensor calibration curve. One section is on the front slope and the other is on the back slope. The ratio for the front and back slope is 217.800 micron/mv and 1434.074 micron /mv, respectively. Here, a smaller ratio means higher precision for the sensor gain, and the front slope amplitude range covers the actuation movement. The front slope is chosen as the sensor gain in all the experiments conducted.

5.2 Control Experiments Implementation

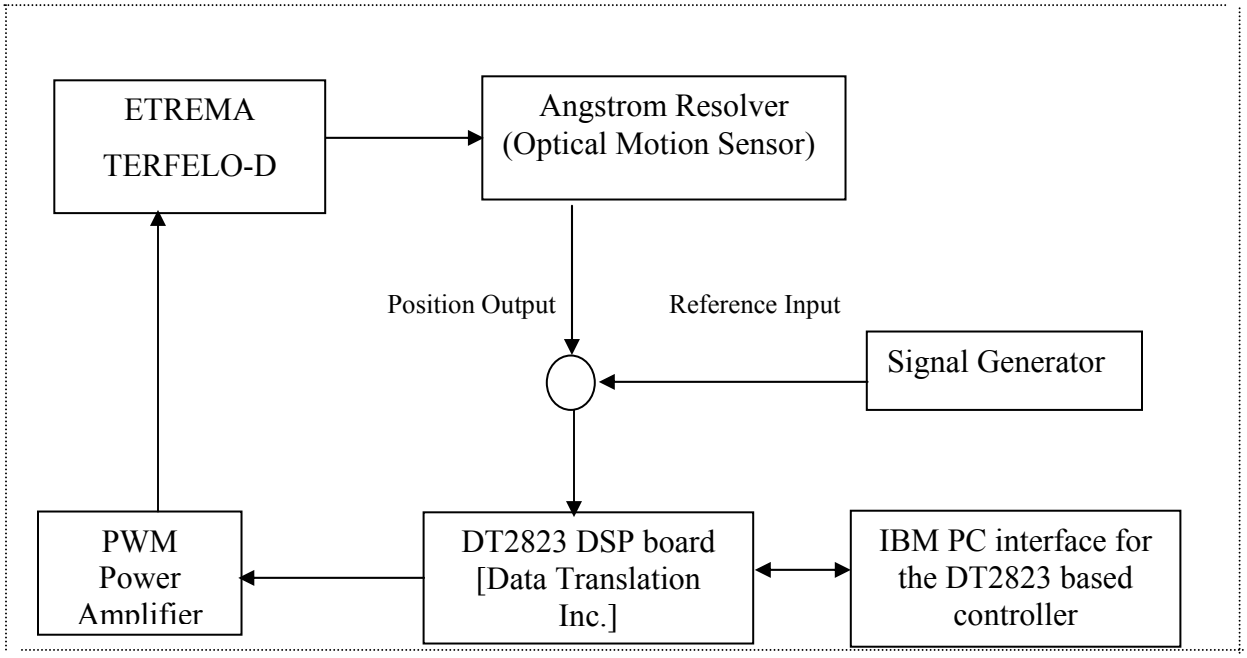

Figure 5.4: Schematic Diagram of the Experimental Setup

Figure 5.4 lists the schematic diagram for the implementation of the close-loop control. The optical sensor incorporated with the Angstrom Resolver observes the actuation displacement driven by the voltage signal from the PWM signal amplifier. Then the signal from the Angstrom Resolver is directed to the data acquisition board, which communicates with the computer. The DSP board converts the analog signal into a digital value. The computer then generates a digital control command obtained from the control algorithm to the DSP board. This command is directed to the PWM amplifier in analog form (voltage). Thus all these components in *Figure 4.1* form a close-loop control.

In order to reduce measuring errors and diminish the impact of temperature changes, during the experiments, a special time interval is set aside for two consecutive

experiments. This can cool off the actuator and keep it under room temperature. Because the actuator coil has a preload and bias condition, even without any input signal, the actuator will generate heat if it is kept at power on mode. A constant power off interval is a proven way to protect the actuator from damage or overheating.

5.3 Experiments and Results Analysis

5.3.1 PID control experiments

The open loop performance has been discussed in *Chapter II*. Under low drive level, the magnetostrictive actuator shows some near linear property. But at moderate or high drive levels the actuation displacement contains significant hyteresis and is very nonlinear [2]. Generally speaking, the open loop performance is not good and cannot be used directly in high precision actuation applications. Without introduction of an effective close-loop control algorithm, the behavior of the actuation system is very nonlinear. So, how will the actuator behave if a PID or sliding mode controller is introduced into the actuation system? *Figure 5.5* through *Figure 5.12* illustrate part of the experimental results.

Note: The desired output is in dashed line and the actual output is in solid line in all the figures in this chapter.

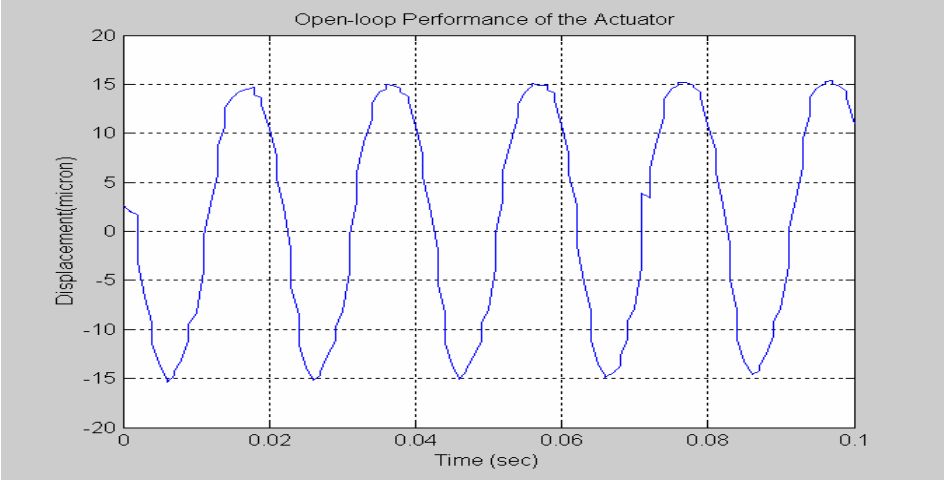

Figure 5.5: Open-loop Performance of the Actuator
Desired output: Sinusoid wave, Amplitude: 15 microns; Frequency: 50Hz

Figure 5.5 shows that the open loop actuation displacement trajectory is nonlinear. The maximum amplitude actually keeps around the same value. Then, a PID controller is introduced, making it a close-loop control system.

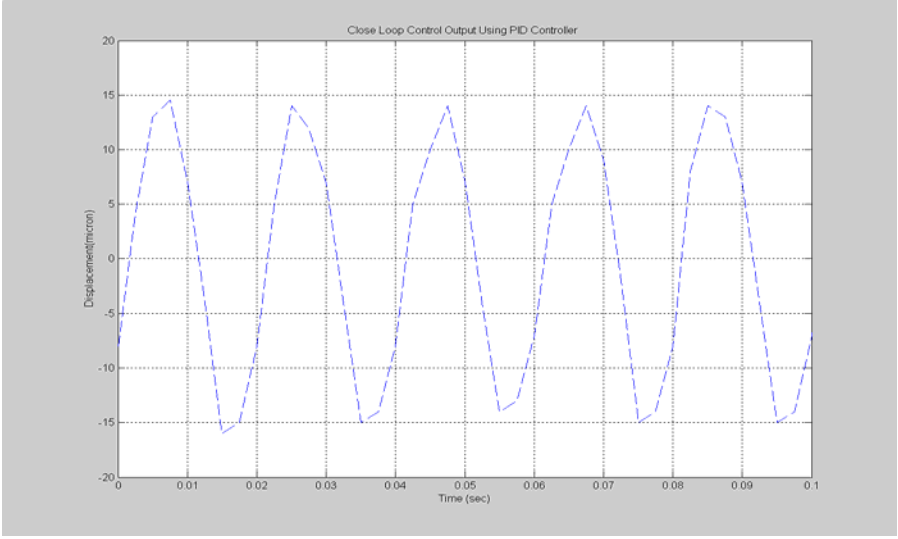

Figure 5.6: Close loop control using PID controller
Desired output: Amplitude: 15 microns; Frequency: 50Hz

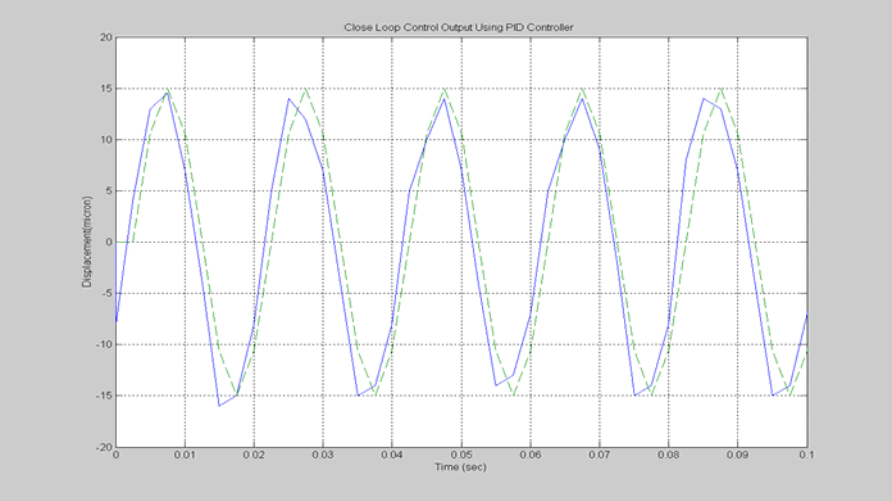

Figure 5.7: Close loop output vs. desired output
Desired output: Amplitude: 15 microns; Frequency: 50Hz
K*p* = 0.45, *Ki* = 0, D *Kd*= 0.00001

The result from close-loop control using the PID algorithm is shown in *Figure 5.6* and *Figure 5.7*. The actuation displacement trajectory using the PID controller stays closer to the desired output compared with those from the open loop control. But the amplitude of the output signal is not consistent. And there is a phase lag between the two.

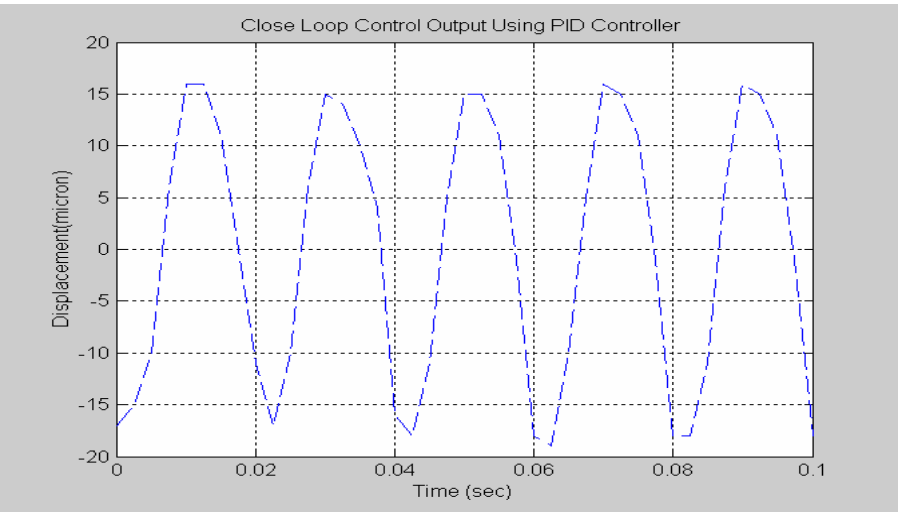

Figure 5.8: PID control output
Desired output: Amplitude: 15 microns; Frequency: 50Hz
Kp = 0.45; *Ki* = 0.0 ; *Kd* = 0.0

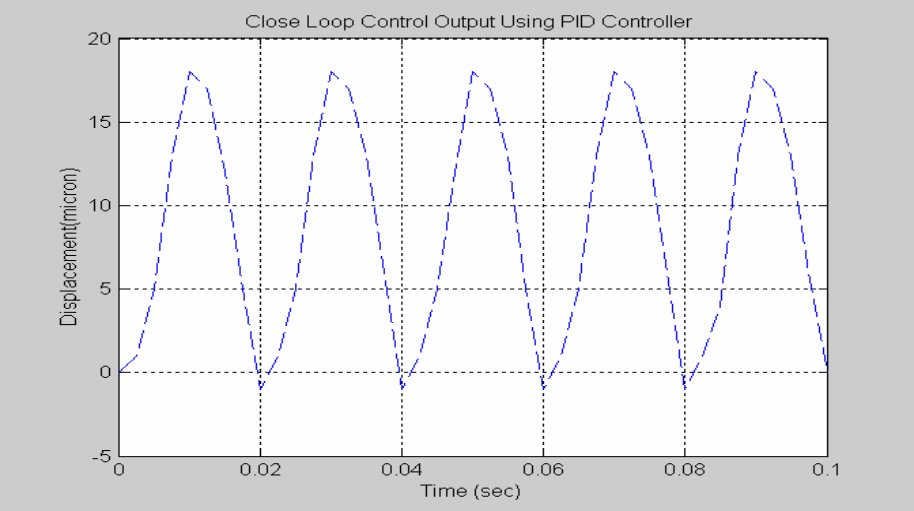

Figure 5.9: PID control output
Desired output: Amplitude: 15 microns; Frequency: 50Hz

In *Figure 5.9*, a deferential gain *Kd* is added and the trajectory outlook looks better.

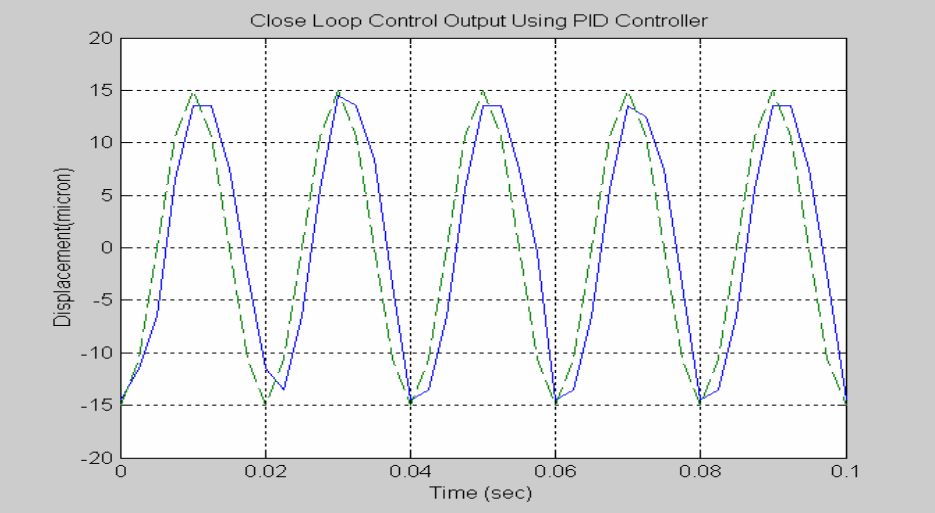

Figure 5.10: PID control output vs. Desired Trajectory
Desired output: Amplitude: 15 microns; Frequency: 50Hz
Kp = 0.4, *Ki* = 0, *Kd* =0.00001

In *Figure 5.10*, *Kp* is increased to get the desired amplitude. From *Figure 5.8* to *Figure 5.10*, some improvements are observed due to the adjustment of the PID parameters.

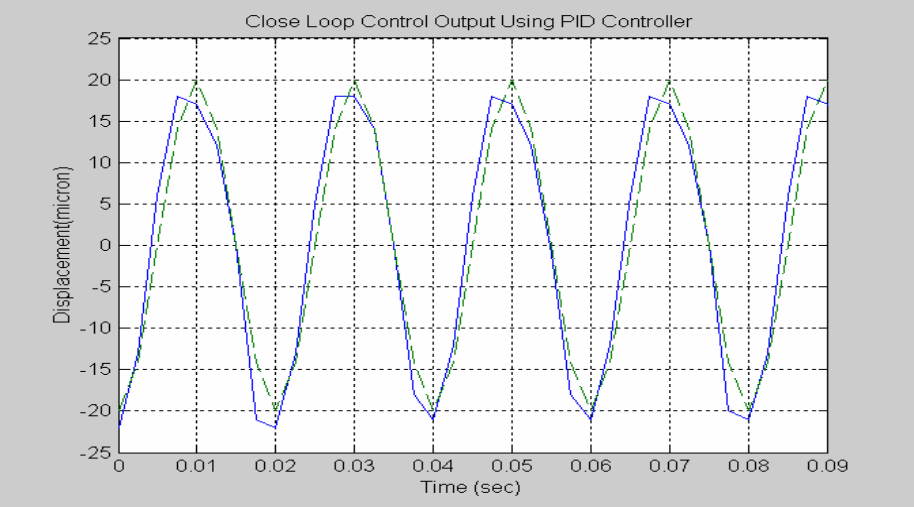

Figure 5.11: PID controlled output vs. Desired Trajectory
Desired output: Amplitude: 20 microns; Frequency: 50Hz
$Kp = 0.45$, $Ki = 0$, $Kd = 0.00001$

Figure 5.8 through *Figure 5.11* present the trial and error procedure for PID control. *Figure 5.9* shows result from a pure proportional control. Then *Figure 5.9* adds a differential gain. In *Figure 5.10* and *Figure 5.11*, further adjustment of the proportional gain is made to get a better controlled output. In *Figure 5.11*, the amplitude of the controlled output reaches the desired 20 microns and the tracking error is reduced.

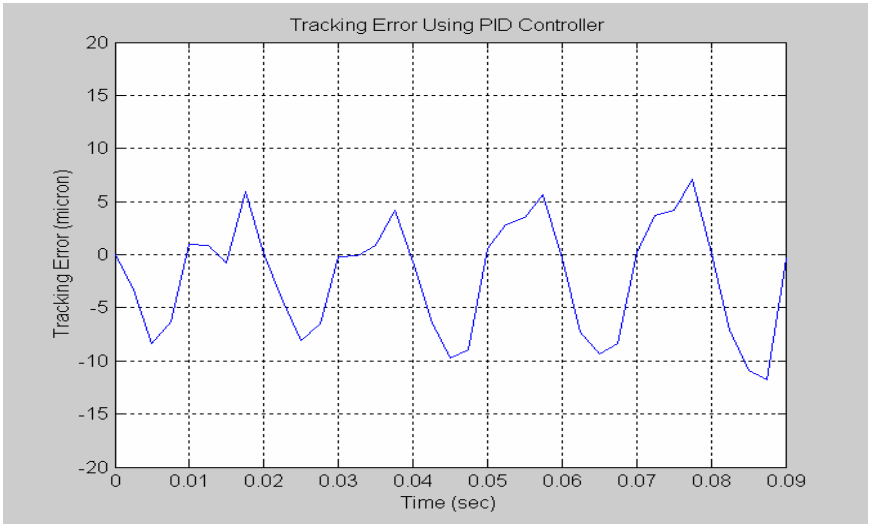

Figure 5.12: Tracking Error Using PID control

Overall, the frequency following performance is quite good using the PID controller. But the controlled output displacement does not match the desired displacement trajectory very well. This is not consistent with the results obtained from the simulation program in *Chapter IV*.

The results in the above figures also demonstrate that a linear dynamic model has its own inherent limitation in this highly nonlinear system. Certainly, modeling inaccuracy plays an important role in the tracking error. Other factors, including signal noise and phase lag, also have impact on the controlled results.

5.2.2 Sliding mode control experiments

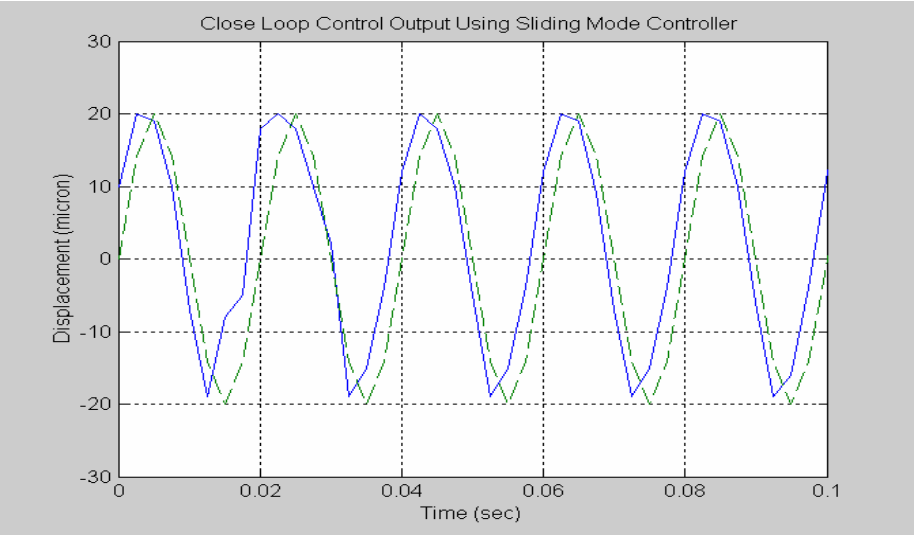

Figure 5.13: Sliding Mode Control Output
Desired output: Amplitude: 20 microns; Frequency: 50Hz
Lamda = 10, *Ks* =9.5

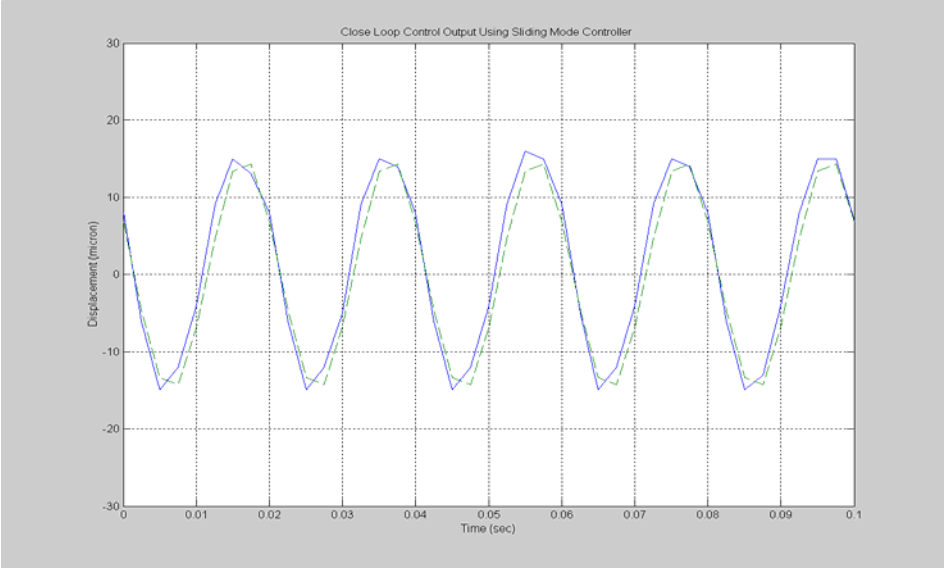

Figure 5.14: Experiments Result Using Sliding Mode Controller
Desired output :Amplitude: 15 microns; Frequency: 50Hz
Lamda = 8.0, *Ks* = 8.0

As seen in *Figure 5.6* through *Figure 5.12*, PID control yields larger tracking error. And, if the parameters *Kp* and *Kd* are changed, the amplitude of the output also changes. This also implies that the proposed model is not accurate enough.

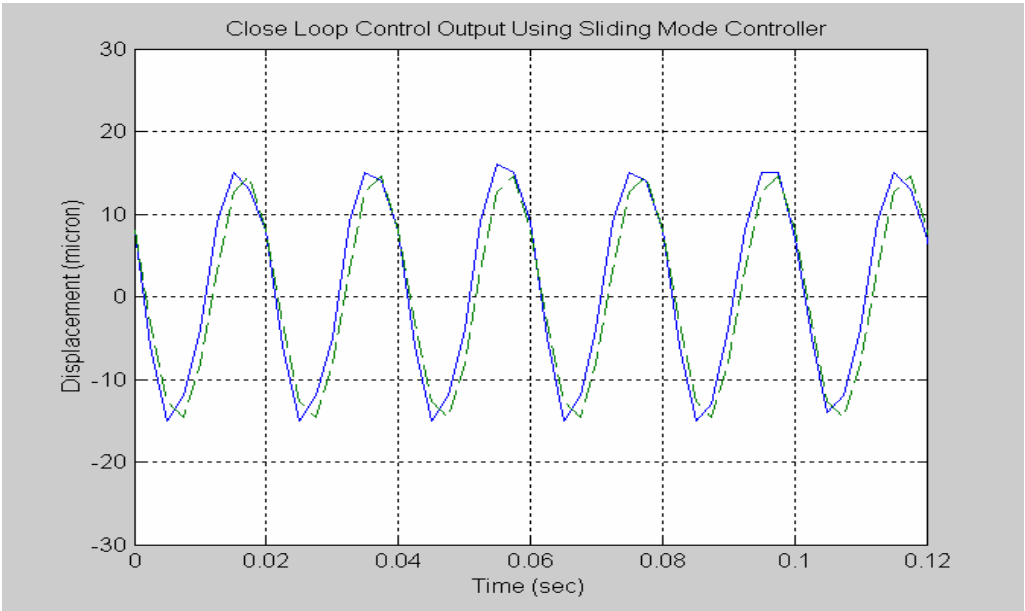

Figure 5.15: Sliding Mode Controller Response
Desired output: Amplitude: 15 microns; Frequency: 50Hz

In *Figure 5.15* and *Figure 5.16*, trajectories tracking for a sinusoid wave with the same frequency but different amplitudes are shown.

Generally, sliding mode control generates smoother outputs and the tracking error is reduced from that from the PID controller. But the tracking results are still not good enough. Sensor noise, finite sampling frequency, and the existence of phase lag are the main error factors.

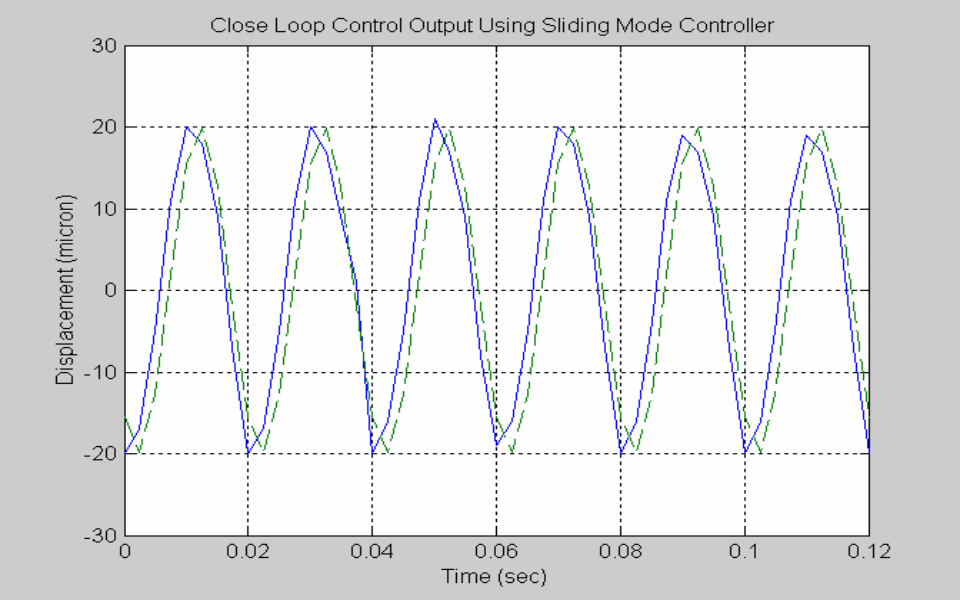

Figure 5.16: Desired Trajectory vs. Trajectory Using Sliding Mode Controller
Desired output: Amplitude: 20 microns; Frequency: 50Hz

Figure 5.16 lists both the desired and actual controlled trajectories while using sliding mode control. The tracking error between these two is represented in *Figure 5.17*. An obvious phase lag is shown in the beginning. Then the controlled trajectory follows the desired one quite well. But the tracking error never disappears here in *Figure 5.17*. Then phase lag happens again. The calculation in the states observer and sliding mode

control algorithm needs a relatively long time to get the final control command to the actuator. Thus, a time delay occurs inside the control loop. If the control strategy is too simple, its performance may be not good enough. But, if it's too complicated, then real time control can't be guaranteed. Therefore, real time control has to trade off among the performance, sampling frequency, and advanced control algorithm.

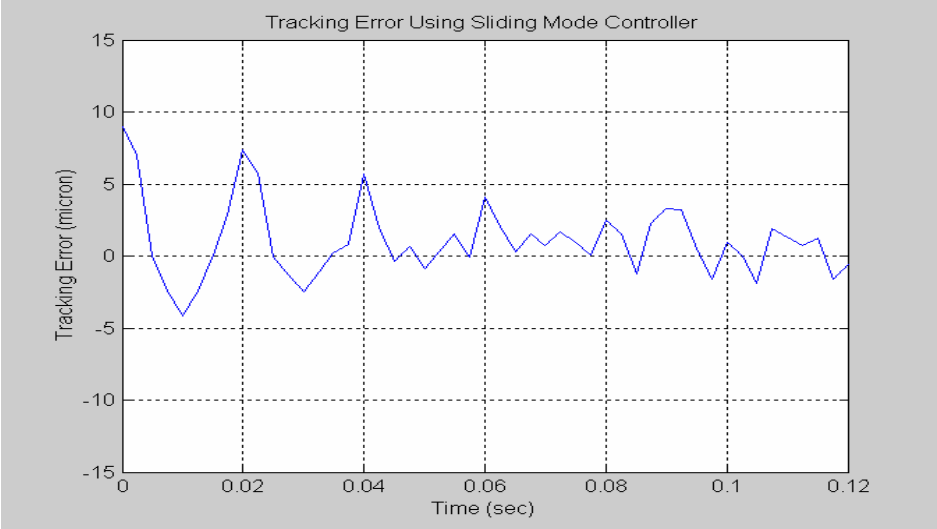

Figure 5.17: Tracking Error Using Sliding Mode Controller

As shown in *Figure 5.17*, the tracking error is decreased with time when sliding mode control is applied. But the tracking error remains large (2 micrometers range). It still accounts for about 5% of the whole actuation displacement, which is not an acceptable level. Sensor noise, disturbance, and phase delay—all may play their roles in the tracking error. Boundary layer method and the switching activity with a finite sampling rate (at most 4 KHz here) can't guarantee that the chattering error disappears.

As an approach often used in a nonlinear system, SMC shows some advantage over PID and open loop control at this particular frequency (50Hz). Although the modeling

technique is simple to implement, magnetostriction and the hysteresis phenomena cannot be neglected. A model without inclusion of these physics-based facts did not work very well even under lower drive level.

Further work will involve improvement on modeling utilizing the magnetostrictive theory by Jiles, etc. Modification for the sliding mode controller is under consideration.

References:

1. Reenough R.D., Jenner A. G., and Wikinson A. J., "Machine, Actuators & Control," pp67, ImechE. Seminar series, 1993.
2. W. Shim, and P. Ro, "Robust Friction Compensation of Submicron Positioning and Tracking for a Ball-screw Driven Slide System," Precision Engineering, J. Int. Soc. Precision Eng. and Nanotech., vol. 24, no. 2, pp.160-173, April 2000.

4. Gutierrez, H. M. and Ro, P. I., "Sliding-mode control of a nonlinear-input system: application to a magnetically levitated fast-tool servo," IEEE Trans. on Ind. Elec., vol.45, no.6, pp. 921-927, 1998.
5. Slotine, "Sliding Controller Design for Non-linear Systems," Int. J. Control, vol. 40, no. 2, pp.421-434, 1984.
6. J. Slotine, and L. Weiping, "Applied Nonlinear Control," Prentice Hall, 1991.
7. S. Mitra, "Digital Signal Processing A Computer-Based Approach," McGraw Hill Inc., 1998.
8. C.-L. Hwang, "Sliding mode control using time-varying switching gain and boundary layer for electrohydraulic position and differential control," IEEE Proc.-Control Theory Appl. Vol. 143, No. 4, July 1996.
9. Kuo-kai Shyu, et al., "A Modified Variable Structure Controller," Automatica, Vol. 28, No. 6 pp. 1209-1213, 1992.
10. S.S.GE, et al., "Adaptive Control of non-affine Nonlinear Systems Using Neural Networks," Proceedings of the 15th IEEE International Symposium on Intelligent Control (ISIC 2000), July 2000.

11. G. Monsees, et al., “Adaptive Switching Gain for a Discrete-Time Sliding Mode Controller,” Proceedings of the American Control Conference, Chicago, Illinois, June 2000.
12. Sarah Spurgeon and Raymond Davis, “A nonlinear Design Approach for Sliding Mode Control Systems,” Proceedings of the 32nd Conference on Decision and Control, San Antonio, Texas, December 1993.
13. Ralph C. Smith, “A Nonlinear Model-Based Control Method for Magnetostrictice Actuators,” Proceedings of the 36th Conference on Decision and Control, San Diego, California, USA, December 1997.
14. Ralph C. Smith, “Partial and Full Inverse Compensation for Hysteresis in Smart Material Systems,” Proceedings of the American Control Conference, Chicago, Illinois, June 2000.

Chapter VI

Discussion and Future Work

6.1 Discussion

In *Chapter* I through *Chapter V*, modeling and feedback control issues for the magnetostrictive actuator have been discussed. To simplify the modeling problem, a black box model was established by matching the input and output data series using Lease Sqaure Technique and SAS System V8. In order to further simplify the problem, the control issue was limited at 50Hz with different amplitudes. The proposed model provides an alternative and new tool for the qualitative analysis of magnetostrictive actuator behavior. This dynamic model was proved effective through the real time control experiments at the selected frequency (50Hz).

However, there are several shortcomings that will limit the application of this model. First, it is a linear model and the model does not provide a mechanism for the inherent nonlinearities and hysteresis properties of the actuator. In this sense, the model is not very accurate.

The proposed linear model works at a particular frequency range (around 50Hz), ignoring the nonlinear property in the high frequency range and under high driving

current or voltage inputs. This modeling approach could be extended to a broader frequency range, though modeling and controller design are involved at every frequency.

In addition, the model parameters strongly depend on operating conditions as described in *Chapter III*. If the application is broadened to any frequency range, then a cumbersome look-up table needs to be created to cover every frequency point before the close control implementation. This is neither practical nor efficient.

By observing the tracking error, results from the close-loop controllers were tested and compared with the open loop. Although the conventional sliding mode controller shows advantages and better performance over the PID controller or open-loop experiments with a fixed switching gain, it is not good enough to handle the magnetostrictive nonlinearities and hysteresis factors.

6.2 Future work

Given the very nonlinear open loop preformance and hysteresis, to linearize the nonlinearities using a simple feedback control scheme was proved not practical for the magnetostrictive actuation system.

A proper approach will require fully understanding the physical principle of the magnetostrictive actuator. The inclusion of nonlinearities and hysteresis is a necessity. Based upon this fact, a better and accurate model could be established.

Future work will include refining the model and designing new controllers. The development of a new model based on the physical properties of the magnetostictive materials will be considered. The new model should cover the hysteresis phonomena, and it should be subjected to rigorous mathmatical analysis. The controller should be designed for easy implementation.

Regarding the controller design, in order to improve the tracking performance, a more practical sliding model controller is considered. An SMC with a time-varying switching gain and boundary layer has been proven effective for a nonlinear system. Certainly, that is a right direction for future work [1]. An SMC with sliding sectors is a possible proper solution, too [2]. And, an approach that combines adaptive control and sliding mode control using Neutral Networks is a suitable nonlinear control technique, worth investigating further [3]. A model reference adaptive control (MRAC) proposed by J. M. Nealis and R. C. Smith [4] proved to be effective in simulation but could not be verified through experimental results.

Reference:

1. C.-L. Hwang, "Sliding mode control using time-varying switching gain and boundary layer for electrohydraulic position and differential control," IEEE Proc.-Control Theory Appl. Vol. 143, No. 4, July 1996.
2. Kuo-kai Shyu, et al., "A Modified Variable Structure Controller," Automatica, Vol. 28, No. 6 pp. 1209-1213, 1992.
3. S.S.GE, et al., "Adaptive Control of non-affine Nonlinear Systems Using Neural Networks," Proceedings of the 15th IEEE International Symposium on Intelligent Control (ISIC 2000), July 2000.
4. J. M. Nealis and R. C. Smith, "An Adaptive Control Method for Magnetostrictive Transducers with Hysteresis," pp. 4260-65, Proceedings of the 40th IEEE Conference on Decision and Control, Orlando, Florida USA, December 2001.

Appendix

1. Data Acquisition Program

```
/*********************************************/
/***** Open-loop measurement with DT2823 **********/
/***** Using DT2823 DSP board         ***************/
/***** For Magnetostrictive Actuator       *************/
/***** Date revised: 04/05/2002          ***************/
/****** File Name: sine.c                          *********/
/***************************** ****************/

#include <stdlib.h>
#include <stdio.h>
#include <conio.h>
#include <dos.h>
#include <math.h>


/* define programmable interval timer ports and constants  */
#define _PIT0   0x40          /* port 0 of timer */
#define _PIT3   0x43          /* command register of timer */


#define FSAMP   4000.0    /* sample frequency, Hz */
#define CLOCKRATE 1.19318e6           /* counter timer clock frequency*/
#define PI 3.14159265359
#define cpv (65536.0/20.0)


/*DT2823 register address */

#define adcsr     0x240        /*A/D control status register */
#define chancsr   0x242        /* channel gain control status */
#define addat     0x244        /* A/D data register */
#define supcsr    0x24C /* supervisory control/status register */
#define tmrctr    0x24E /*timer/counter register */

/* data recording definitions */
#define REC_LEN  5000          /* length of data recording array */


/* define interrupts */
void interrupt Gather_Data ();
void interrupt (far *oldisr)();      /* vector to original timer tick isr */
```

```
/* define global variables    */
unsigned char MSB;                    /* register values to set timer */
unsigned char LSB;
unsigned int count;
int x1,x2,y1,y2;              /* print location  */

static int data=0, inc=0;   /* DA output data incremental number */
int *data_array;
int i;

float displacement;
/*float volt_disp=1.0; */
float t;                      /* elapsed time */
float volt;
/* data recording variables */
float disp_array[REC_LEN];                    /* displacement array */
float time_array[REC_LEN];                    /* time index array  */
FILE *fp_out;                                 /* file pointer        */
unsigned int long index=0;                    /* index into arrays       */
int notdone=1;                        /* index to signal the end of measure.*/

/* declare functions    */

void InitGlobals();
void PrintScr();
void Wait_For_Cue();
void SetADC();
void SetISR();
void ClearISR();
void WriteFile();
void WriteDisp();
void DoUser();


void main()
{
     data_array =(int *)malloc(REC_LEN*sizeof(int));
     for(i=0; i< REC_LEN;i++){
               data_array[i]= 2.5*cpv* sin(2*PI*50*i/FSAMP);
     }
InitGlobals();
/*Wait_For_Cue(); */
PrintScr();
SetADC();
```

```
SetISR();

while(!kbhit() && notdone)
  DoUser();
ClearISR();


WriteFile();

WriteDisp();
return;
}



/************************************/
/**** initialize global variables ***********/
/************************************/

void InitGlobals()
{
unsigned int tcount;                    /* timer count    */

/* computer interrupt  timer count */

tcount=CLOCKRATE/FSAMP;         /* divide clock rate by sample frequency */
MSB = tcount/256;               /* most significant byte  */
LSB = tcount%256;               /* least significant byte */

return;
}

/************************************/
/**** print screen        ***********/
/************************************/

void PrintScr()
{
clrscr();                       /* clear screen   */
gotoxy(2,5);
printf("Elapsed time(sec):   ");
x1=wherex();
y1=wherey();
gotoxy(2,6);
printf("Displacement(mm):   ");
x2=wherex();
```

```
y2=wherey();
return;
}

/*****************************************/
/* Ready until synthesizer is turned on **/
/*****************************************/

 void Wait_For_Cue()
{
int flag=1,i_volt,x1,y1;
float dummy;
printf("index voltage:");
x1=wherex();
y1=wherey();


/* set up A/D input on channel 2    */
outport (tmrctr, 0xF0D7);       /* set pacer clock to 100 kHz  */
outport (supcsr, 0x2240);       /* initialize  A/D        */
outport (chancsr,0x8000);       /* disable channel gain list  */
outport (adcsr,  0x0202);       /* enable clock,ch 2*/
outport (chancsr,0x0000);       /* specify single channel    */
outport (supcsr, 0x0010);       /* set board parameter   */

/* wait for muliplexer to settle      */
     while((inport(adcsr)  & 0x100 )==0x100);

/* wait for cue from synthesizer*/
while(flag)
{
outport(supcsr, 0x08);          /* trigger A/D conversion */
/* wait for A/D conversions to finish   */
while (0x80 & inport(adcsr) !=0x80);    /* wait */
dummy=(float)(inport(addat)/3276.7);  /* read converted values in mm */
 gotoxy(x1,y1);
 printf("%6.3f",dummy);
if(fabs(dummy-2.8) < 0.01)
 flag=0;

}
return;
}

/*****************************************/
/* set A/D parameters for the DT2823 board ***********/
```

```
/*****************************************/

 void SetADC()
{
/* set up A/D input on channel 1    */
outport (tmrctr, 0xF0D7);       /* set pacer clock to 100 kHz  */
outport (supcsr, 0x2240);       /* initialize  A/D        */
outport (chancsr,0x8000);       /* disable channel gain list  */
outport (adcsr,  0x0201);       /* enable clock,ch 1*/
outport (chancsr,0x0000);       /* specify single channel    */
outport (supcsr, 0x0010);       /* set board parameter   */

/* wait for muliplexer to settle      */
     while((inport(adcsr)  & 0x100 )==0x100);
return;
}

/*********************************************/
/****  set the control program to be an interrupt service routine **/
/*********************************************/

void SetISR()
{
/* change the count on the programmable interval timer   */
outportb(_PIT3, 0x34);  /* command byte to counter  */
outportb(_PIT0, LSB);           /* couter LSByte     */
outportb(_PIT0, MSB);   /* couter LSByte   */

/* install new interrupt service routine   */
oldisr=getvect(0x1c);           /* get vector to timer tick isr   */
disable();                      /* disable interrupts     */
setvect(0x1c, Gather_Data);     /* replace isr with control function */
enable();                       /* enable interrupt again    */
return;
}

/*********************************************/
/****  restore the old  interrupt service routine   ************/
/*********************************************/

void ClearISR()
{
/* restore  the count on the programmable interval timer  */
outportb(_PIT3, 0x34);
outportb(_PIT0, 0xDE);
outportb(_PIT0, 0xFF);
```

```
disable();
setvect (0x1C,oldisr);          /* restore oldisr   */
enable();
return;
}

/*********************************************/
/****  the  control interrupt  service routine   **************/
/*********************************************/
void interrupt Gather_Data()

{

/* DA output */
/*data[i++]; */
outport(adcsr+6, 0x123);  /* DA Control Register Set Up */
/*outport(adcsr+8,  data);   DA Output */
outport(adcsr+8,  data_array[inc++]);  /* DA Output */
/*printf("data= %d \n", data); */

/* read infrared sensor  */
outport(supcsr, 0x08);          /* trigger A/D conversion */

/* wait for A/D conversions to finish   */
while (0x80 & inport(adcsr) !=0x80);    /* wait */
count = (( 0x1<<15) ^ inport(addat));  /* read converted values in mm */
volt = (float) (20.0/65536.0*count) -10.0;

/*  record data */
if (index < REC_LEN)
{

     disp_array[index]= volt*217.8;  /* in um */
     t=(float) (index/FSAMP);
     time_array[index]=t;        /* time index array  */
     index++;
     }

if (index >= REC_LEN)
{
     notdone=0;
     }
return;

}              /* end of control routine */
```

```
/*********************************************/
/**** write  data  into  a file  ********** **********/
/*********************************************/

void WriteFile()
{
int i;
fp_out = fopen(".\\disp.txt", "w");
for (i=0;i<index;i++)
     fprintf(fp_out,"%6.3f\t%d\n",time_array[i*10], data_array[i*10]);
fclose(fp_out);

return;
}

void WriteDisp()
{
int i;
fp_out = fopen(".\\disp1.txt","w");
for (i=0;i<index;i++)
     fprintf(fp_out,"%6.3f\t%f\n",time_array[i*10],disp_array[i*10]);
     fclose(fp_out);
     return;
     }

/*********************************************/
/****  screen  display  ********** **********/
/*********************************************/

void DoUser()
{
gotoxy(x1,y1);
printf("%6.3f", t);
gotoxy(x2,y2);
printf("%10.3f", displacement);        /* displacement */
return;
}
```

2. Close Loop Control Program

```
/*********************************************************/
/* PID and Sliding Mode Control program                  */
/* Using DT2823 DSP board                                */
/* For Magnetostrictive Actuator                         */
/* Date revised: 04/05/2002                              */
/* File Name: msmc.c                                     */
/*********************************************************/

#include <stdlib.h>
#include <stdio.h>
#include <conio.h>
#include <dos.h>
#include <math.h>
#include <alloc.h>            /* for memory allocation only*/


/* define programmable interval timer ports and constants    */

#define _PIT0   0x40          /* port 0 of timer */
#define _PIT3   0x43          /* command register of timer */
#define FSAMP   4000.0        /* sampling frequency in Hz, sampling time = 1/FSAMP
second */
#define delta_t (1.0/FSAMP)
#define CLOCKRATE 1.19318e6     /* counter timer clock frequency*/
#define bias 0                /* A/D Bias in counts          */
#define true 1
#define false 0
#define PI 3.14159265359

#define vpc (20.0 / 65536.0)   /* volts per count       */
#define cpv (65536.0 /20.0 )   /* counts per volt       */

#define v_max 4.0*cpv         /* max voltage magnitude */

/*DT2823 register address */

#define adcsr     0x240       /* A/D control status register */
#define chancsr   0x242       /* channel gain control status */
#define addat     0x244       /* A/D data register           */
#define dacsr     0x246       /* D/A control status register */
#define dadat     0x248       /* D/A data register           */
#define diodat    0x24A       /* Digtal I/O data register    */
#define supcsr    0x24C       /* supervisory control/status register */
```

```
#define tmrctr    0x24E        /* timer/counter register      */

/* data recording definitions   */
#define fp_format  "%11.51e %17.81e %17.81e %17.81e\n"
#define REC_LEN  20000          /* length of data recording arrays */


/* define global variables      */

int *cmd_array;               /* real voltage control input array                    */
int *sensor_array;            /* volatage measured by snesor  array                  */
int *dmicrons;               /* Desired Displacement path in Microns                 */
double volt;                 /* voltage measured through A/D channel from Anstrom
Resolver */
double displ;               /* Displacement values stored in array                  */

void   interrupt (*oldisr)();    /* vector to original timer tick isr              */
int  cmd[3];                 /* voltage control input to actuator in counts      */
double error[3];             /* diff between the actual displacement and desired */

unsigned int angstrom;         /* Angstrom Resolver Feedback in micron           */
unsigned char MSB;             /* register values to set timer                   */
unsigned char LSB;

void interrupt Control(void);    /* Declare new ISR                              */
void WriteFile();
void WriteDisp();
void PrintScr();

int x1,x2,y1,y2;              /* On Screen Display Postion                       */
int index;                  /* index into arrays                                */
int record;                 /* flag to tell if recording                        */
int notdone=1;

float t;
float dummy;
float delta_PID;
float displacement;
float distance;

double state_x1[2];          /* virtual state x1  from observer   */
double state_x2[2];          /* virtual state x2  from observer   */
double dot_state_x1[2];
double dot_state_x2[2];

long h;                     /* time scale to synchronize        */
```

```
FILE *fp_out;


/* PID control gains in continuous and discrete time domains     */
double  Kp;                     /* poportional  gain       */
double  Ki;                     /* integral    gain        */
double  Kd;                     /* derivative  gain        */
double  K0, K1, K2;                 /* discrete control gains  */

/* Sliding Mode Controller Parameters */
double dot_error;                   /* differencial error      */
double int_error;                   /* integral error          */

float lamda = 10.0;                     /* lamda---positive number           */
float Ks = 9.5;                     /* Switching gain                    */
float S;                        /* Switching surface                 */
float Ueq;                      /* Equivalent Control input          */



/* Subroutines */

void InitGlobals()
{
   unsigned int tcount;
   int i;

/* computer interrupt  timer count */
tcount = CLOCKRATE/FSAMP;               /* divide clock rate by sample frequency */
MSB = (char) (tcount/256);              /* most significant byte  */
LSB = (char) (tcount%256);              /* least significant byte */


/* Allocate arrays in memory        */

    cmd_array    = (int*)malloc(REC_LEN*sizeof(int));
    sensor_array = (int*)malloc(REC_LEN*sizeof(int));
    dmicrons     = (int*)malloc(REC_LEN*sizeof(int));

if ((cmd_array == NULL) ||( sensor_array == NULL)||(dmicrons == NULL))
{
   printf(" Cound not allocate arrays!");

   exit(1);                             /* exit program */
}
```

```
record = 0;
for (i=0; i<3; i++)
   state_x1[i] = 0;
   state_x2[i] = 0;
   dot_state_x1[i] = 0;
   dot_state_x2[i] = 0;

for ( i=0; i<3; i++)
    error[i] = 0;

for ( i=0; i<4; i++)
    cmd[i] = 0;

for (i=0; i<REC_LEN; i++)
{
   sensor_array[i] = 0;
   cmd_array   [i] = 0;

   dmicrons[i] = 30.0 * sin(2.0*PI*50.0*i/FSAMP);
/* input a squre wave to actuator  in 2 volts*/

/*    dummy = sin(2*PI*50.0*i/FSAMP);
   if (dummy>=0) {
   dmicrons [i] = 1.5*cpv;}
   else {
   dmicrons [i] = -1.5*cpv;}  */


}

/************************************/
/**** initialize PID paramters ******/
/**** initialize Gain values   ******/
/************************************/

Kp=1.0;
Ki=0.0;
Kd=0.0;

/* calculating discrete PID gains */
K0 = ( Kp + Ki/FSAMP/2 +  Kd*FSAMP);
K1 = (-Kp + Ki/FSAMP/2 -2*Kd*FSAMP);
K2 = (                  Kd*FSAMP);

/*initial h =0*/
```

```
h=0;

/* return; */
}

/*****************************************************/
/***  set A/D parameters for the DT2823 board    *****/
/*****************************************************/

void SetADC()
{
/* set up A/D input on channel 1 --Angstrom Resolver Feedback  */

outport (tmrctr, 0xF0D7);       /* set pacer clock to 100 kHz  */
outport (supcsr, 0x2240);       /* initialize  A/D        */
outport (chancsr,0x8000);       /* disable channel gain list  */
outport (adcsr,  0x0201);       /* enable clock,ch 1*/
outport (chancsr,0x0000);       /* specify single channel    */
outport (supcsr, 0x0010);       /* set board parameter   */

/* wait for multiplexer to settle      */
   while((inport(adcsr) & 0x100)== 0x100);
}

void SetDAC()
{
/* set up D/A input on channel 1--control input signal to the Actuator  */
outport (tmrctr, 0xF0D7);       /* set pacer clock to 100 kHz          */
outport (supcsr, 0x0020);       /* initialize  DAC Buffer              */
outport (dacsr,  0x0100);       /* Choose single channel D/A           */
}

/*****Set the D/A output to zero     **********************/
void ZeroOutput()
{
outport(dadat, 0x0);        /* Load D/A data register          */
outport(supcsr, 0x80);      /* Execute D/A conversion          */

/* check for D/A conversion done */
while ((inport(dacsr)& 0x80 )!= 0x80);

}
/* end of ZeroOutput   */

void PrintScr()
{
```

```
clrscr();
gotoxy(2,5);
printf("Elaspsed time(sec):  ");
x1=wherex();
y1=wherey();
gotoxy(2,6);
printf("Displacement(um):  ");
x2=wherex();
y2=wherey();
return;
}


/*****************************************************************/
/****  set the control program to be an interrupt service routine **/
/*****************************************************************/

void SetISR()
{
/* change the count on the programmable interval timer      */

outportb(_PIT3, 0x34);          /* command byte to counter  */
outportb(_PIT0, LSB);           /* couter LSByte            */
outportb(_PIT0, MSB);           /* couter MSByte            */

/* install new interrupt service routine   */

oldisr = getvect(0x1C);         /* get vector to timer tick ISR      */
disable();                      /* disable interrupts                */
setvect(0x1C, Control);         /* replace ISR with control function */
enable();                       /* enable interrupt again            */
return;
}


/*****************************************************************/
/****  Restore the old  interrupt service routine   *************/
/*****************************************************************/

void ClearISR()
{
/* restore  the count on the programmable interval timer  */
outportb(_PIT3, 0x34);
outportb(_PIT0, 0xDE);
outportb(_PIT0, 0xFF);
```

```
disable();
setvect (0x1C,oldisr);          /* restore oldisr   */
enable();
return;
}

/* Sign function for Sliding Mode Controller        */

sign(float S)
{
  int result;
  if ( S > 0 ) result = 1;
  else
  {  if ( S < 0 )
    result = -1;
    else
    result = 0;
    }
    return result;
    }


/*** Main Interface to Run the Magnetostrictive Actuator   *****/
/*************************************************************/
/****  The  Control Interrupt  Service Routine     ************/
/*************************************************************/
void interrupt Control(void)
{
int i;

/* read Angstrom Resolver */

outport(supcsr, 0x08);              /* Triger A/D conversion     */

/* shift displacement errors */

error[1] = error[0];
  cmd[1] = cmd [0];                 /* shift control input       */

dot_state_x1[1] = dot_state_x1[0];
dot_state_x2[1] = dot_state_x2[0];

state_x1[1] = state_x1[0];
state_x2[1] = state_x2[0];

/* Now wait for A/D conversions to finish   */
```

```
while ((0x80 & inport(adcsr)) != 0x80);
angstrom = ((0x1<<15) ^ inport(addat));

volt = (double) ((inport(addat) - bias)/cpv-10.0);
/* read converted value in counts */

distance =  (float) (vpc * angstrom)-10.0;
/* in volt  */

/* converting counts into volts  */
/* sensor_array[h] = (int)angstrom;  */

displ =(double) volt*217.8;

/* Filter the measured displacement signal using IIF Filter */
/* y[h] = A1*y[max(0,(h-1))]+A2*y[max(0,(h-2))]+A3*y[max(0,(h-3))]+
   A4*y[max(0,(h-4))]+A5*y[max(0,(h-5))]+A6*y[max(0,(h-6))]+
   B0*displsave[(h)]+B1*displsave[max(0,(index-1))]+
   B2* displsave[max(0,(h-2))] +B3*displsave[max(0,(h-3))]+
   B4*displsave[max(0,(h-4))]+B5*displsave[max(0,(h-5))]+
   B6*displsave[max(0,(h-6))];        */
/* Desired or reference displacement path   */

error[0]  = (float) (dmicrons[h] - displ);       /* displacement error in um                    */
dot_error =  (error[0] - error[1])/delta_t;     /* differential (error1-error0)/(sampling time)
*/
int_error = int_error + (error[0] + error[1])/2*delta_t;

if( h<REC_LEN )
  h++;
else
  return;

/* Now Start Calculation for the controller  */


/* delta_PID = (int) ((K0 * error[0] +K1 *error[1] + K2 * error[2])*cpv/8.0); */

/* S---Sliding switching surface in 2nd order   */

S = (2*lamda*error[0]+ dot_error + lamda*lamda*int_error);

/* States Observer         */
/* virtual states        */
```

```
dot_state_x1[0] = (- 777.018 * state_x1[1] + 713.1923 * state_x2[1] +359.86*displ)
+cmd[1]/cpv;
dot_state_x2[0] = (- 835.70 * state_x1[1]+ 767.027 * state_x2[1] + 386.86 * displ);

state_x1[0] = (double) ((state_x1[0] + dot_state_x1[1] + dot_state_x1[0])/2.0*delta_t);
state_x2[0] = (double) ((state_x2[0] + dot_state_x2[1] + dot_state_x2[0])/2.0*delta_t);


/* Ueq---Equivalent control term  */

Ueq = (dmicrons[h] - 2.1628* state_x1[0] - 1.9827 * state_x2[0])/7.5615;

cmd[0] = (int) (( Ueq + Ks * sign(S))/2.0*cpv);

if (cmd[0] > v_max) {cmd[0] = v_max; }
else if (cmd[0] < -v_max) {cmd[0] = -v_max;}
else {cmd[0] = cmd[0]; }


/* check if previous D/A conversion is done   */

while ((inport(dacsr) & 0x80) != 0x80);

/* Now, output the current command through Channel 0   */

outport(dadat, (cmd[0]));    /* Load D/A data register   */
outport(supcsr, 0x80);      /*  Execute D/A conversion */

/*record data  */
if (index <REC_LEN)
{
    cmd_array[index]    = (int) (cmd[0]);
    sensor_array[index] = distance*217.8;   /* in um */
    t = (float) (index/FSAMP);
    displacement = displ;
    index++;

}

return;
}


/*************************************************************/
/****  write input  data/voltage  into  a file       **********/
/*************************************************************/
```

```
void WriteFile()
{
int i;
fp_out = fopen("disp.txt", "w");

for (i=0;i<index;i++)
   fprintf(fp_out,"%7.4f\t%d\n",(float) (i/FSAMP*10), cmd_array[i*10]);

fclose(fp_out);

return;
}


/*************************************************************/
/****  write Output/Displacement data  into  a file  *******/
/*************************************************************/


void WriteDisp()
{
int i;
fp_out = fopen("disp1.txt", "w");

for (i=0;i<index;i++)
   fprintf(fp_out,"%8.5f\t%d\n",(float) (i/FSAMP*10), sensor_array[i*10]);

fclose(fp_out);

return;
}


/*********************************************/
/********  On Screen  Display  ***************/
/*********************************************/

void DoUser()
{
gotoxy(x1,y1);
printf("%6.3f", t);
gotoxy(x2,y2);
printf("%10.3f", displacement);
return;
}
```

```
/*** Main SubRoutine  ***/

main()
{
delay(0);
InitGlobals();

   SetADC();

   SetDAC();

   ZeroOutput();

   PrintScr();

   SetISR();
   x1=wherex();
   y1=wherey();
   x2=x1;
   y2=y1+1;

   while (!kbhit())
   DoUser();

   ClearISR();

   ZeroOutput();

   WriteFile();

   WriteDisp();

   clrscr();

}
→
```